NUMERICAL STUDY ON A PARTIALLY FILLED CHANNEL

WITH OPEN-CELL METAL FOAM

SATISHWARA RAO S/O NARASIMMANAIDU

UNIVERSITI TEKNIKAL MALAYSIA MELAKA

NUMERICAL STUDY ON A PARTIALLY FILLED CHANNEL WITH OPEN-CELL METAL FOAM

SATISHWARA RAO S/O NARASIMMANAIDU

A report submitted in fulfilment of the requirements for the Degree of Bachelor of Mechanical Engineering (Thermal Fluids)

Faculty of Mechanical Engineering

UNIVERSITI TEKNIKAL MALAYSIA MELAKA

2020

DECLARATION

I declare that this project entitled “Numerical study on a Partially Filled Channel with Open-cell Metal Foam” is the result of my own work except as cited in the references.

Signature : ....

Name : SATISHWARA RAO A/L NARASIMMANAIDU

Date : 24 JUNE 2020

`

APPROVAL

I hereby declare that I have read this project report and in my opinion this report is sufficient in terms of scope and quality for the award of the degree of Bachelor of Mechanical Engineering (Thermal Fluids).

Signature : ....

Name of Supervisor : DR. FADHILAH BINTI SHIKH ANUAR

Date : 24 JUNE 2020

`

DEDICATION

To my beloved father, mother and siblings for the endless support

`

ABSTRACT

A metal foam is widely used in automotive, furniture, and construction industry. Metal foam has excellent fire penetration, thermal insulation and sound absorption properties. In this study, partially filled channel with metal foam is investigated as a replacement to a fully filled channel that causes a massive pressure drop effects. The interface of the porous medium has to be identified and remodelled to simulate the exact airflow in metal foam because of the metal foam complex interior. The objectives of this project are to model a partially filled channel with a porous medium and also to investigate the fluid flow behaviour and pressure drop in a partially filled channel. Different pore density of the open-cell aluminium foam block, 5, 10 and 30 pores per inch (PPI) foam is considered, including various foam thickness and inlet velocity. The Computational Fluid Dynamics (CFD) is conducted to extend the results of past literature to obtain accurate data. The Ergun-Forcheimmer's equation is used to define the viscous and inertial resistance in the porous medium domain while the Navier-Stokes equation was used for the clear region. Two-dimensional (2D) channel configuration is developed because of its symmetrical model. A validation with 20 PPI porous medium from other literature was made. The results are acceptable. From the simulations, the velocity distribution in the channel was examined particularly at the fluid flow behaviour at upstream, partially filled and downstream sections. The pressure drop was discussed in detail by observing the contours. Comparison of velocity and pressure gradient between experimental and simulation data are also shown in the form of a graph including the in agreement results of past literature. Thus, the flows behaviour at the upstream and downstream region were also explained which are relevant to this project.

`

ABSTRAK

Busa logam banyak digunakan dalam industri automotif, perabot, dan pembinaan. Logam berliang ini mempunyai sifat penembusan api, penebat haba dan penyerapan bunyi yang sangat baik. Dalam kajian ini, saluran yang diisi sebahagiannya dengan busa logam telah dipertimbangkan sebagai pengganti saluran penuh busa logam yang menyebabkan kesan penurunan tekanan yang besar. Muka medium berliang yang seusai harus dikenal pasti dan diubah suai untuk simulasi aliran udara dengan tepat dalam busa logam kerana strukturnya yang rumit.Objektif projek ini adalah untuk membuat model saluran yang diisi sebahagiannya dengan medium berliang serta menganalisis tingkah laku aliran bendalir dan penurunan tekanan pada saluran yang telah diisi sebahagian dengan blok berliang aluminium sel terbuka. Busa aluminium sel terbuka dengan ketumpatan berlainan, 5, 10 dan 30 liang per inci PPI telah dipertimbangkan, termasuk ketebalan busa dan halaju masuk. Perkomputeran Dinamik Bendalir (CFD) dijalankan berdasarkan eksperimen yang dibuat oleh kajian sebelumnya untuk mendapatkan data yang lebih tepat. Formula Ergun-Forcheimmer telah digunakan untuk menentukan kelikatan dan inersia dalam domain medium berliang manakala persamaan Navier-Stokes telah digunakan untuk kawasan yang jelas.Konfigurasi saluran dua dimensi (2D) dibentuk kerana ukurannya yang simetri. Pengesahan dengan busa logam 20 PPI daripada literatur lain telah dibuat.Keputusan yang diperoleh dari simulasi CFD boleh diterima. Melalui simulasi yang dilakukan, pengedaran halaju dalam saluran diperiksa terutamanya pada tingkah laku aliran bendalir di bahagian hulu, tengah, dan hilir saluran.Penurunan tekanan juga diperiksa dengan memerhatikan konturnya. Selain itu, perbandingan kelajuan dan tekanan antara data eksperimen dan simulasi juga ditunjukkan dalam bentuk carta termasuk kajian sebelumnya. Oleh itu, tingkah laku aliran di kawasan hulu dan hilir yang berkaitan dengan projek ini juga telah dijelaskan.

`

ACKNOWLEDGEMENTS

First and foremost, I would like to express my sincere gratitude and the deepest appreciation to my supervisor Dr. Fadhilah binti Shikh Anuar for the guidance and endless support towards the completion of this final year project with smoothness.

I would also like to show gratitude to Dr. Nazri bin Md Daud and Dr. Mohamad Firdaus bin Sukri as my examiners for giving me useful advices and suggestions upon the completion of this project. Their co-operation is highly appreciated. Million thanks to Universiti Teknikal Malaysia Melaka (UTeM) for giving me a chance to participate and to gain experience in handling a final year project. Furthermore, I would like to thank all my friends for helping and giving me pieces of advices throughout the completion of this final year project.

Last but not least, not to forget to express my deepest sense of gratitude to my beloved parents and siblings for their never endless encouragement. They gave me a lot of persistence in not giving up to do my best in the project.

`

TABLE OF CONTENTS

`

LIST OF FIGURES

`

`

`

LIST OF TABLES

`

LIST OF ABBREVIATIONS

PIV	Particle Image Velocimetry

`

LIST OF SYMBOLS

d_p	=	pore diameter (m)
h	=	foam height (m)
H	=	channel height (m)
H_f	=	free stream region height (m)
h/H	=	blockage ratio
K	=	permeability (m^2)
L_c	=	length of channel (m)
PPI	=	pore per linear inch
U_o	=	inlet velocity (m/s)
U_s	=	upstream velocity (m/s)
U_p	=	average pore velocity (m/s)
∇p^*	=	pressure gradient of flow direction ($\Delta p/\Delta x$)
u^*	=	flux per unit area of the porous medium (Φ/m^2)
ε	=	porosity (-)
μ	=	dynamic viscosity (kg/(m.s))
v	=	kinematic viscosity (kg/(m.s))
ρ	=	density (kg/m^3)
β	=	inertial resistance coefficient (-)

`

CHAPTER 1

INTRODUCTION

1.1 BACKGROUND

Generally, configurations of having a part of the passageway filled with the metal foam or any type of material are called a partially filled channel. The partially filled channel can be divided into three sections which are upstream, free stream, and downstream region. The upstream is a region where the input of fluid and downstream is a region where low-velocity air merges with high-velocity air. The free stream region is a non-porous region on the metal foam [1]. The partially filled channel is used to minimise the pressure drop in the fluid flow compared to fully-filled channel [2]. The high-pressure drop of a fully-filled channel reduces the performance of the system and consumes a large amount of energy. Other than that, fully filled channel reduces the velocity of fluid flow compared to the partially filled channel [3].

One of the main properties of metal foam is permeability. Permeability (K) measures the capability to transmit fluids through a porous medium. The permeability can be divided into three categories; absolute permeability relative permeability and affective permeability [9]. It shows the ability to transmit fluids across the porous medium. The critical pore size gives an impact on the permeability of porous media [10]. The examples of permeable media in nature are the sand beds and limestone [11]. Other important properties of the metal foam are porosity (ε), which is defined as the ratio of the volume of pore space divided by the total volume [5].

`

There are many types of metal foams in the market. Some of the examples are copper foam, aluminium foam, silicon carbide foam and zirconium oxide foam. It can be either closed-cell foam or open-cell foam. The open-cell metal foam is a cellular structure made up of solid metal with a large volume fraction of gas-filled pores. Each of the metal foam has its properties and applications. For example, the open-cell metal foams used as the replacement of conventional fins used in aerospace as this metal foam could provide higher surface area to volume ratio with marginally increased in pressure drops values [4]. The expensive honeycomb structure can be replaced by metal foam sheets or sandwich panels in the aerospace industry. It can reduce cost and retain the integrity of the structure from any case of fire. Other than that, metal foam preferred for their lightweight properties.

In the automotive industry, metal foams reduce the number of parts in the car frame thus reduces the cost and increases the performance [5]. The good relation between stiffness and weight support of metal foam makes it suitable for large-area light parts with increased requirements on stability. Examples are engine hoods and trunk lids. The metal foam is used to strengthen the protection inside of the trucks. In rear and front car bumpers, it is used as energy-absorbing structures. While in furniture and household industry, metal foams can be used in lamps and tables. Its combination with the wood surface can give new effects in the room. Lightweight furniture can be a great advantage in fairs or exhibitions to be moved from one place to another. For the construction and building industry, the metal foam has excellent fire penetration resistance and thermal insulation properties. Due to their thermal insulation properties, it can be used as energy-saving elements. They are being used beneath highway bridges, building interior and railway tunnel for their sound-absorbing properties. It is also perfect for ceilings and roofs due to their lightweight and easy to be installed without any mechanical lifting equipment. The other application of open-cell metal foams is for filtration [6], sound absorption [7] and medical devices [8].

`

Commonly, the metal foams properties are classified based on their pores densities (PPI) e.g. 5, 10 and 30 PPI. A proper selection of pore density is important to ensure a suitable amount of fluid or air flows into porous region instead of the non-porous region. This is because the pore density affects metal foam performance and functionality such as heat exchangers. Many studies [11] agreed that metal foam efficiency also depends on the porosity in addition to the PPIs. Metal foam is defined as porous media in numerical studies. The interface of the porous medium has to be assumed and remodelled to improve the airflow in metal foam because the metal foam multi-struts interconnected to each other. However, the interface condition of the metal foam remains debated due to complex interface condition and flow behaviour at those regions [12].

To describe the flow of fluid through a porous medium, the Darcy equation can be used. However, there are four conditions for Darcy Equation to be applicable; (1) laminar flow in the porous medium, (2) porous media should not interact with fluid, (3) no accumulation and (4) creeping flow [4]. Darcy law has a low Reynolds number. However, with higher porosity configurations, range from 0.90 - 0.97 and also high permeability, Darcy model cannot give precise answers [13].

This Brinkman term in momentum gives a more precise mathematical model when the inertial term is significant. The Brinkman equation used to justify the flow by considering different parameters such as fluid velocity, pressure and gravitational potential. Meanwhile, the Navier-Stokes equation is used to explain fluid flows in clear domains. This equation is used when the viscosity is crucial. While the Forchheimer equation can be used for flow with higher Reynold number specifically for this condition; (1) turbulent flow in a porous medium and (2) viscous and inertial effect are more crucial [14]. The Reynolds number for fluid flow in porous medium are $Re < 1$ (Creeping flow), $1 < Re < 10$ (Inertial flow regime), $150 < Re < 300$ (Laminar flow) and $Re > 300$ (Turbulent flow) [15].

`

1.2 PROBLEM STATEMENT

Metal foam is designed as a porous medium in numerical studies using ANSYS Fluent. The common pore density of open-cell metal foam used in experiments is 5, 10, 20, and 30 PPI. Pore density stands for the number of pores per one inch in a metal foam. Note that, low PPI foam has larger size pores compared to high PPI foam. It was concluded in [1] that for the low PPI foams with higher blockage ratio, the momentum of airflow maintains its consistency until the end of the foam.

On the other hand, for high PPI foam, the airflow tends to search a way out by entering the nearer pores which causes the momentum of the airflow to drop and the air flows towards the interface [12]. There are three main reasons for variation of pressure drop due to high blockage ratio; (1) different metal foams pore density and sizes used, (2) flow separation in the channel due to the existence of porous medium block and (3) formation of wakes at the downstream of the foam block.

For the 5 and 10 PPI metal foam which blocks that partially filled channel, the airflow passes through the open-cell aluminium foam from the entrance toward the foam end without entering non-porous region but with 30 PPI the air flows into the non-porous region on the top of the foam block before reaching the foam end. The formation of the recirculating zone at downstream region was caused by the increase of free stream velocity with the blockage ratio. Interestingly, this situation occurs with the high PPI foam and solid block but not with the low PPI foam [1]. Unfortunately, past numerical studies [16] could not capture such flow behaviours. This is because the fluid flow in porous media does not have a constant movement that can be measured.

`

Suitable parameters have to be identified for the partially filled channel; eg: pore density, foam length and blockage ratio to make sure the unique structure of the porous foam can be fully utilized. The interface of the porous medium has to be identified and remodelled to simulate the exact airflow in metal foam because the metal foam multi-struts interconnected to each other and the interface condition of the porous media remains a debated issue.

1.3 OBJECTIVE

The objectives of this project are as follows:

1. To model a partially filled channel with a porous medium.
2. To investigate the fluid flow behaviour and pressure drop in a partially filled channel with different properties of the porous medium.

1.4 SCOPE OF PROJECT

This project studied inertial resistance and other properties by modelling a porous medium in a partially filled channel. Only results of the simulation are presented in this report using the dimensions of the wind tunnel and aluminium foam with the pore densities are obtained from other literature [1]. The Finite Volume-based Software ANSYS Fluent is used to simulate the porous media in the partially filled channel. Limited parameters are introduced in the simulation such as the pore densities (5, 10, and 30 PPI), blockage ratio (the difference between channel and porous block height) and inlet velocity (3.9, 5.5, 6.2, 6.5, 9.5 and 12.5 m/s).

`

CHAPTER 2

LITERATURE REVIEW

2.1 INTRODUCTION

This chapter has four main sections which explain the fluid flow and pressure drop of air in a partially filled channel with porous medium. The metal foam physical properties are shown in section 2.2. The equations for flow in porous media are discussed in section 2.3. Additionally, previous studies on the metal foam will be discussed in section 2.4 and 2.5, including both experimental and numerical studies which are related to this project.

2.2 METAL FOAM AND PHYSICAL PROPERTIES

Metal foam can be either closed-cell foam or open-cell foam. Each of the metal foam has its properties and applications. There are different types of materials manufactured for metal foam such as aluminium, copper and titanium. The open-cell metal foam is a cellular structure made up of solid metal with a large volume fraction of gas-filled pores. Open-cell metal foam has good permeability, high strength and high specific surface. Moreover, the foam can be used for medical purposes such as bone replacement [17].

`

On the other hand, closed-cell metal foam is stiff at low weight and effective in structural damping with electromagnetic shielding. These metal foams also are being used for engineering applications such as filtration [6] and sound absorption [7]. There are few ways for metal foam manufacturing including casting, metallic deposition and powder metallurgy. No matter which method is used to form the metal foam, they are still differentiated by labelling either poor quality or high cost [18].

Table 2.1: Open-cell aluminium metal foam properties [19]

Parameters	**Values**
Foam topology	Open, interconnected
Standard cell size, d_p (cm)	2 to 16 pores
Relative density (%)	4 to 10
Melting point (°C)	660
Compression/tensile/shear strength (MPa)	2.53 /1.24 / 1.31
Specific heat, C_p (J/g-C)	0.895

The physical properties of open-cell aluminium foam other than **Table 2.1** are such as permeability (K) porosity (ε), and pore diameter (d_p) depends on pore density (PPI) of the foam. When the pore size increases, the permeability also increases together with the porosity (ε) [20].

2.3 EQUATIONS FOR FLOW IN POROUS MEDIA

2.3.1 Pressure drop

Pressure drop, ΔP is one of the parameters used to understand the fluid flow through a porous medium of different pore densities (PPI). For laminar flow, the pressure drop is calculated as [21]:

`

$$\Delta P = P_1 - P_2 = \frac{32\mu L V_{avg}}{D^2} \quad (2.1)$$

Equation 2.2 is convenient for laminar and turbulent flow for any types or shapes of the pipes such as rough, circular and square. The equation is expressed as [21]:

$$\Delta P_L = f \frac{L}{D} \frac{\rho V_{avg}^2}{2} \quad (2.2)$$

where;

ρ : Density of fluid (kg/m^3)

f : Darcy friction factor

D : Diameter of pipe (m)

V_{avg} : Average velocity of fluid flow (m/s)

L : Overall length of pipe (m)

μ : Dynamic viscosity (kg/ms)

2.3.2 Reynolds number

Generally, the Reynolds number is used to determine the ratio of inertial forces to viscous forces. It is used to categorize the fluid into laminar, transitional or turbulent flows [21]. The types of internal flow are laminar ($Re_D \leq$ 2300), transition (2300< Re_D<4000) and turbulent ($Re_D \geq$ 4000). The internal flow in a circular pipe can be expressed as:

$$Re = \frac{V_{avg} D}{v} = \frac{\rho V_{avg} D}{\mu} \quad (2.3)$$

`

The Reynolds number for fluid flow in porous medium are $Re < 1$ (Creeping flow), $1 < Re < 10$ (Inertial flow regime), $150 < Re < 300$ (Laminar flow) and $Re > 300$ (Turbulent flow) [15].

where;

ν : Kinematic viscosity of the fluid (m^2/s)

μ : Dynamic viscosity of fluid (kg/ms)

V_{avg} : Average velocity of the fluid (m/s)

D : Diameter of pipe (m)

A : Cross-sectional area of pipe (m^2)

2.3. Darcy Law

Darcy Law is used for laminar flow through a porous medium as shown in **Equation 2.4** [22].

$$-\nabla p^* = \frac{\mu}{\alpha} u^* \tag{2.4}$$

where ∇p^* = pressure gradient of flow direction (Pa/m), α = porous medium permeability (m^2), μ = dynamic viscosity of fluid (kg/ms) and u^* = flux per unit area of the porous medium (m/s). This law is an approach for single-phase fluid flow for homogenous porous medium [23] and does not determine the inertial effects..

`

2.3.4 Forchheimer Law

Forchheimer law is used for turbulent flow through a porous medium where both inertial and viscous effects are considered. This equation is an extension of Darcy's equation specifically for high flow rates. The Forchheimer equation shown in **Equation 2.5** [24]:

$$-\nabla p^* = \frac{\mu}{\alpha} u^* + \beta \rho u^{*2} \tag{2.5}$$

where *1/α* is the viscous coefficient resistance ($1/m^2$) and β is the inertial resistance coefficient (1/m). These two parameters will be used as the inputs in the ANSYS simulation of the present study.

2.3.5 Ergun Law

For ANSYS Fluent setup of fluid flow in a porous medium, viscous coefficient resistance (*1/α*) and inertial resistance coefficient (β) have to be determined. Some parameters have to be known first such as porosity and pore size. Ergun's equation used to show the pressure drops of fluid flow through packed beds which are made of cylinders, rough sands or other sphere-shaped particles [25]. It is also commonly used in metal foam studies. The Ergun's equation is as shown in **Equation 2.6** [26]:

$$-\nabla p^* = \frac{150\mu(1-\varepsilon)^2 u^*}{d_p^2 \varepsilon^3} u^* + 1.75 \frac{(1-\varepsilon)}{\varepsilon^3} \frac{\rho u^{*2}}{d_p} \tag{2.6}$$

where d_p represents the pore diameter of the porous medium. The correlations of *1/α*, viscous coefficient resistance and β, inertial resistance coefficient can be obtained when

`

Equation 2.5 and **Equation 2.6** are combined as shown in **Equation 2.7** and **Equation 2.8** [14]:

$$\alpha = \frac{d_p^2}{150} \cdot \frac{\varepsilon^3}{(1-\varepsilon)^2} \tag{2.7}$$

$$\beta = \frac{3.5}{d_p} \cdot \frac{(1-\varepsilon)}{\varepsilon^3} \tag{2.8}$$

2.4. Experimental studies

One of the recent studies on a partially filled channel with metal foam has been conducted in a small wind tunnel. They used 2D image post-processing to obtain more accurate ligament and pore diameter of the metal foam. The pore density (PPI) of 5, 10 and 30 PPI with different heights were used to investigate the fluid flow experimentally. Three different velocity profile used which was 3.9 m/s, 6.2 m/s and 12.5 m/s. Two different channels used; height and length were constant but the width differs according to the foam width used. The flow of the study is turbulent. The turbulence intensity of the fluid flow is 1.7% and the Reynold number was 22,000 ~ 36,000. The experiment set up and measurement locations are shown in **Figure 2.1**. The study found that the pressure drop is insignificant when smaller blockage ratio, 0.05 used on 10 PPI and 30 PPI but once higher blockage ratio, 0.39 was used, the 30 PPI show a significant difference compared to 10 PPI.

The study concluded that higher pore density caused a higher pressure drop in the airflow. Metal foam with larger pore size maintains the momentum of airflow until the end of the foam but higher pore density foam has smaller pore size left with enough momentum to choose shortcut into free stream region which is less-restricted flow area. This causes the airflow moves from the porous region to the non-porous region and forms a circulation zone at the back of the metal foam [1][12].

`

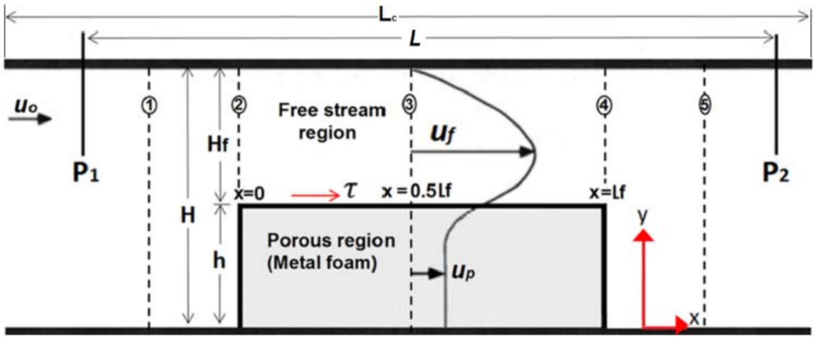

Figure 2.1: Schematic of the experimental setup [12]

In other experimental studies, Mehmet et. al [27] had done an experiment on Forchheimer forced convection in a rectangular partially filled channel with aluminium foam. The schematic view of the experiment is shown in **Figure 2.2**. The aluminium foam was placed inside the channel in four different types; (1) completely full, (2) convex, (3) concave and (4) triangular against the flow. The foam used for this experiment was 10 to 20 PPI studying both laminar and turbulent channel flow regimes. The pressure drop experiments were conducted with 22 different airflow rates for laminar flow and 8 different airflows rated for turbulent flow. When the surface curvature parameter, k=0, the pressure gradient increased 8 times from the minimum Darcy velocity of 0.25 m/s. For k = 0.5, the pressure gradient increased 3.5 times from maximum Darcy velocity of 15.5 m/s. It was concluded that 10 PPI (low pore density) caused only a low-pressure drop effect. The pore density is proportional to pressure drop and the Reynolds number inversely proportional to *k* parameter.

`

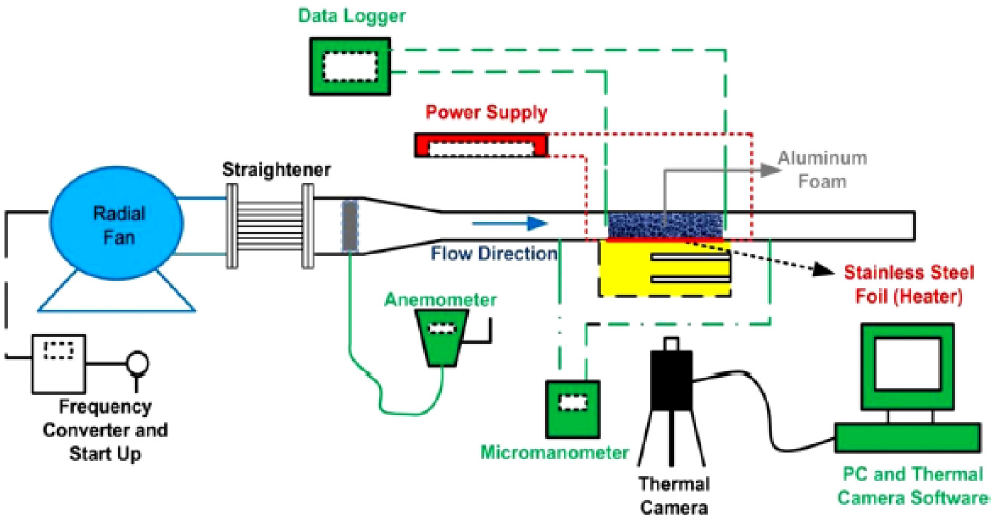

Figure 2.2:Schematic of the experimental setup [27]

2.5 Numerical studies on porous media

The numerical simulation on developing fluid flow in a square partially filled channel with a porous medium was developed by Yan et.al [10]. This was developed by a single-domain CFD simulation. This caused the interface of porous media coupled. The model as in **Figure 2.3**. The vorticity-velocity with the power-law scheme used to solve axial velocity flow. The fluid flow was tested by flowing it into the channel in the axial direction. The Reynolds number was set to 100. When the axial velocity of z = 0.0008 and Darcy number, 10^{-5} with porosity 0.67, the axial in fluid velocity is higher compared to the porous medium. The difference can be seen when axial y- velocity profile, z = 0.05, Darcy number, 2.5 x 10^{-4} with the porosity of 0.75, maximum velocity increases to 5.5 m/s. For the secondary flow pattern, there were two large vortices at the porous medium interface and one vortex in the porous media layer. This was generated due to instability blowing effect in the porous medium.

The blowing velocity created due to low pressure in the fluid layer, high-pressure porous layer side pushed out towards the fluid layer. The secondary flow pattern reduces as the porous layer ratio 0.75 changed to 0.33, and the velocity magnitude is lower in the porous medium compared to the fluid layer. The results obtained from the factors of the velocity profile, Darcy number and porosity shows that the maximum velocity increases with porosity.

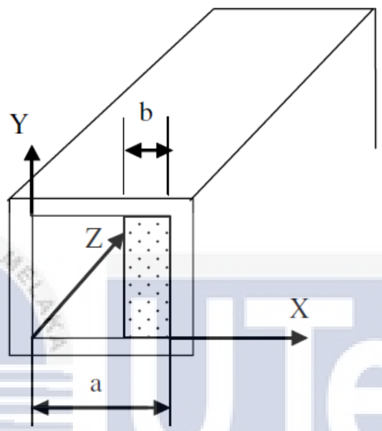

Figure 2.3: Schematic diagram of the numerical study [10]

Hriberkk et.al [13] had developed a simulation on fluid flow in a partially filled channel with the porous medium by using a boundary-domain integral method (BDIM). Configuration of the model is shown in **Figure 2.4**. The flow is this study was prescribed as laminar flow. Darcy number used was based on the porous height (H/2). The Reynolds number used was 100. The computational mesh at x-direction had 20 subdomains and y-direction had 8 subdomains which total up to 160 subdomains. Two different Darcy number which was 0.01 and 0.1 used was for the same heights porous medium in this numerical study. Based on the results obtained, the method used is capable of dealing with the fluid flow in different porous domains.

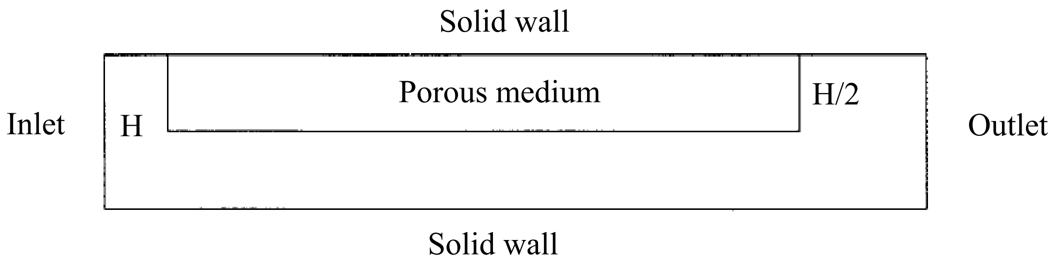

Figure 2.4: Geometry of the layout [13]

Another numerical study was made by Diani et. al [28] which uses four different types of pore sizes (5, 10, 20 and 40 PPI) copper foams. The copper foams have the same relative density (6.4 – 6.8%) with the size of 100mm (L), 100mm (W) and 40 mm (H). The sample metal foams were scanned by using microcomputer tomography where the structure of the foam was re-build and meshed subsequently using Simpleware software. Simpleware software is commercial software which can design and simulate workflows. The meshed product then exported into Ansys FLUENT to run the fluid flow simulation. The length of the sample in the flow direction was 100mm which leads to the fully developed flow. The equation of Darcy-Forchheimer and continuity equation were used in this numerical study. In Ansys Fluent, the velocity-inlet boundary condition is set at inlet the fluid domain, the pressure-outlet boundary is set as outlet and symmetry boundary condition on the lateral side of the domain. The boundary conditions are as shown in **Figure 2.5**. The six velocities are ranging between 2.5 m/s to 5 m/s. The results are compared to the experiments [29]. It was concluded that the pressure gradient increases as the number of PPI increases.

`

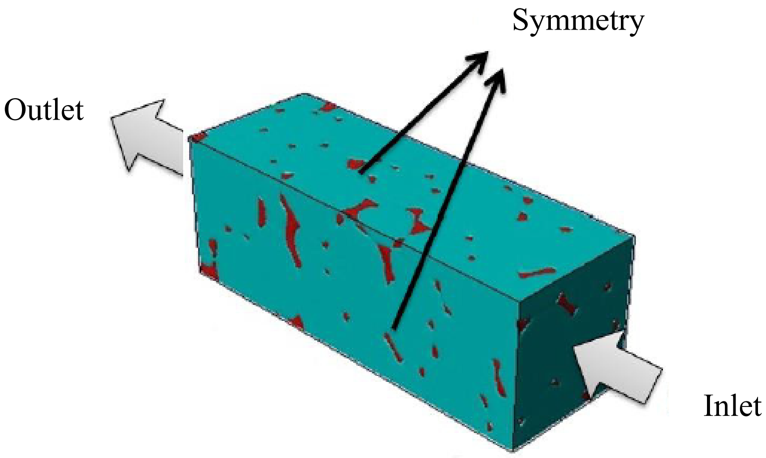

Figure 2.5: Boundary conditions of the numerical study [28]

A numerical study [30] investigates velocity profile of metal foam with various inlet velocities, foam heights and pore densities (PPI). The two-dimensional computational domain is established in FLUENT software. The foam samples are 20 and 40 with two different heights of 3 mm and 4 mm with an inlet velocity of 6 m/s, 10 m/s and 30 m/s. The computational grid had 23,348 nodes with a minimum face size of 0.3 mm and a maximum sizing face of 0.5 mm. The interface was refined at the grid between the non-porous region and the porous region. The growth rate was set at 1.2. The non-porous region used standard k-ε turbulence model. The pressure drop results from the simulation were compared to experimental data from their previous study [27]. When the air velocity 10 m/s, results of pressure drop simulation in porous channel show 0.85 meanwhile the experiment data [15] was 0.53. On the other hand, the air velocity of 30 m/s shows the results of the pressure drop simulation was 5.3 while the experimental data [15] was 5.5. There was a large difference in results at low inlet velocity compared to higher inlet velocity. These discrepancies were attributed to the interface region. Nevertheless, the study concluded that the increase in PPI leads to higher pressure drop in all inlet velocities.

`

Figure 2.6: Velocity contour for 20 PPI – 4mm at 30 m/s [30]

Kotresha et.al [31] conducted a numerical study on forced convection in a partially filled channel with two different PPIs; 20 and 40. The dimension of the channel is 0.235m (L), 0.008m (H) and 0.03m (W) and the metal foam height, H_f is half of the channel as **Figure 2.7**. Copper and aluminium metal foams were considered with the porosity of 0.937. Two different velocities of 10 and 30 m/s were used in their study. The non-porous region used standard k-ε turbulence model. The solution method used in ANSYS Fluent was SIMPLE coupling scheme. Three different grids were used for the numerical domain; 9200, 18400 and 23000. When the velocity is 10 m/s, the pressure drop in the porous channel is 0.53 KPa meanwhile the experiment data [15] was 0.572 KPa. On the other hand, the air velocity of 30 m/s shows simulation data was 4.38 KPa and the experimental data [15] was 5.5 KPa. When the velocities increase together with the pore density, the pressure drop also increases.

`

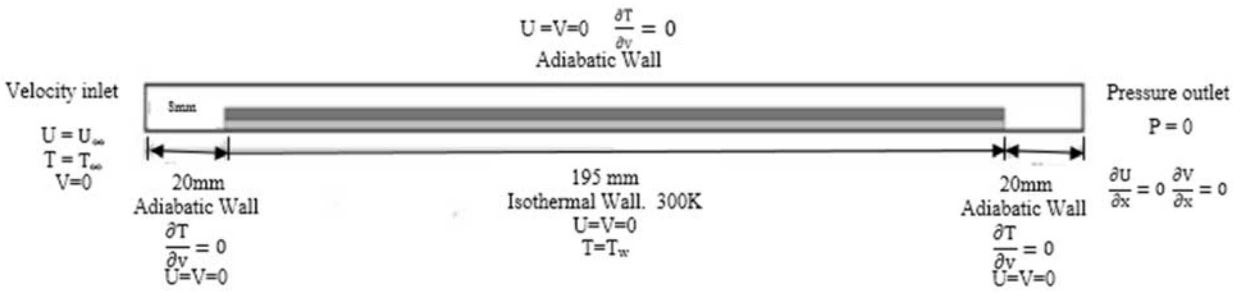

Figure 2.7: Computational domain with boundary conditions [31]

Shuja et. al [32] made research on fluid flow over rectangular porous medium with the fixed-width channel by using different parameters of porosity and blockage ratio. The aspect ratio used was in the range of 0.25 to 4 with air as the working fluid at the inlet velocity of 0.085 m/s. The governing equations of mass continuity, momentum and energy were used to formulate flow over the porous block. Two different porosities were used 0.9726 and 0.8991. Domain and boundary conditions were being shown in **Figure 2.8**. A grid size of 192 x 341 selected to reduce computation time.

A SIMPLE algorithm was chosen as it provides pressure connection between through continuity equation. The dimension of the partially filled channel metal foam was 63 x 45 x 114 mm. When the blockage ratio of 4 with 0.9726 porosity was applied, the fluid flow at the back of the porous medium changes due to blockage effect. A circulation cell formed behind the porous medium because of fluid acceleration between the channel and the porous medium. This happens due to low-velocity flow merges with the high-velocity flow at the back of the porous block. The cell formation does not occur in the porous block due to air penetration through the block. The results obtained are compared with the previous experiment [33] used to validate the simulation data. The study concluded that the blockage ratio has more effect on fluid flow compared to porosity.

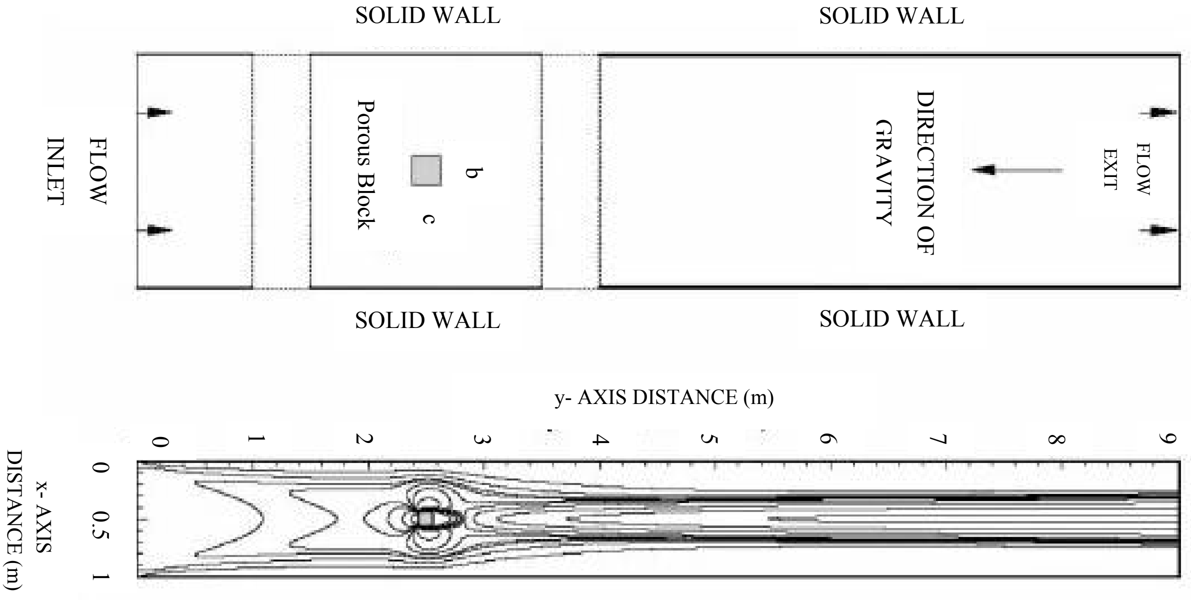

Figure 2.8 : Domain and boundary conditions [32]

CHAPTER 3

METHODOLOGY

3.1 INTRODUCTION

This chapter is divided into three main subtopics which describes in details on the methods used to study the fluid flow in a partially filled channel with open-cell metal foam. This present study extended the previous experiment results [1][12] conducted an experimental study of flow visualization of a partially filled channel with open-cell aluminium foam block by using thermal imaging method and Particle Image Velocimetry (PIV) method. This present study simulates the flow behaviour in the partially filled channel by using ANSYS Fluent software. In this study, the k-ε turbulence model is used for the non-porous region. Two-dimensional geometry is considered due to its symmetry design. The geometry development is explained in Section 3.2 while Section 3.3 discusses the setup procedure in ANSYS FLUENT software. From this simulation, the results that are expected to be obtained are the fluid flow behaviour and pressure drop through a partially filled channel with a porous medium. The methodology of this project is summarized in the flow chart as shown in **Figure 3.1**.

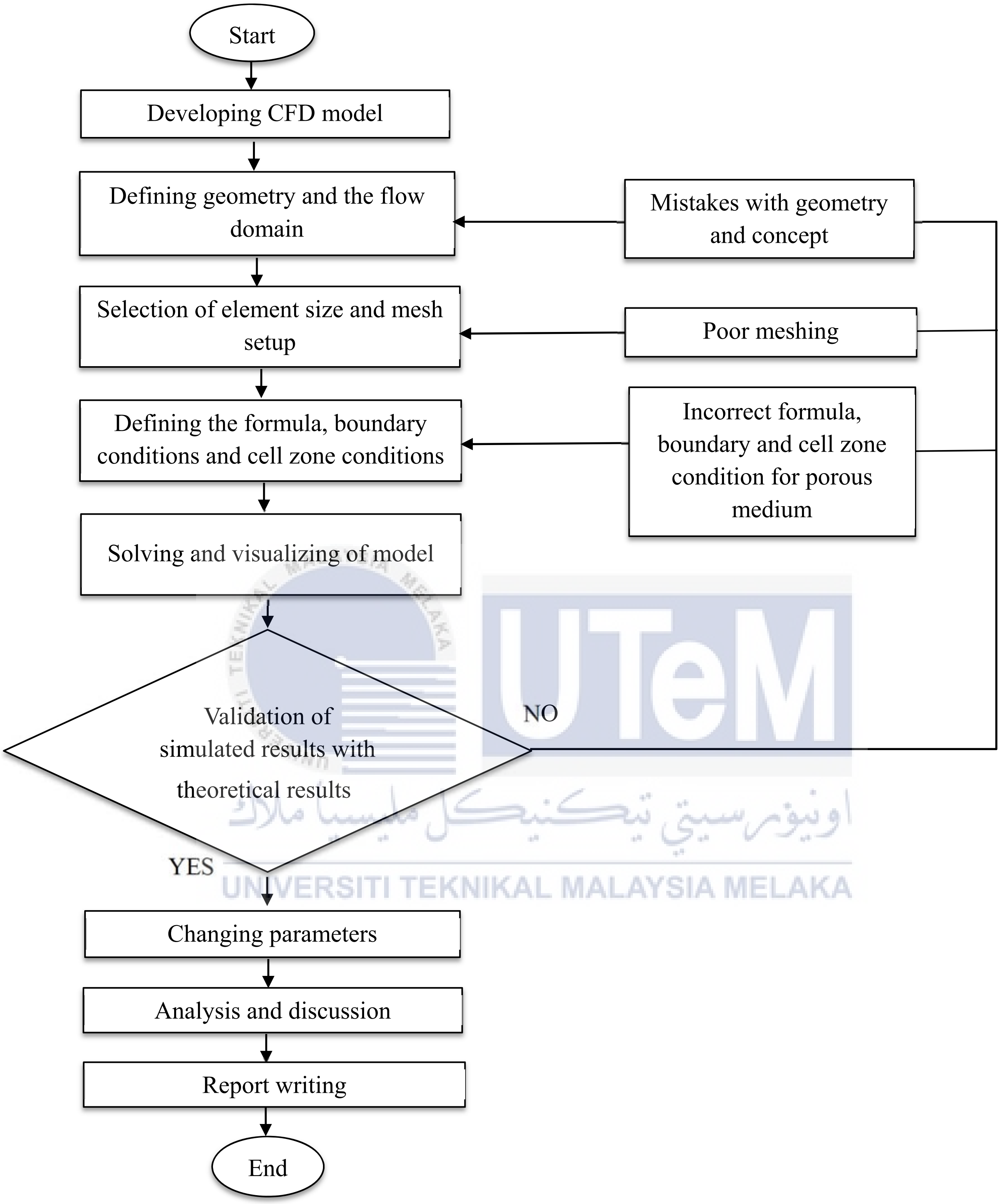

Figure 3.1: Methodology Flow Chart

3.1.1 Numerical method validation

To validate the simulation conducted using the ANSYS Fluent software, a previous numerical study by Sauret et.al [30] and Kotresha et.al [31] is used. This is mainly done to validate the procedure used. They used 20 and 40 PPI are used with two different velocities which are 10 and 30 m/s. The dimensions of the channel are 0.008m (H) x 0.195m (L). Meanwhile, the porous medium is placed half of the total height of the channel. The k- ε is used for the non-porous region. In the meshing section, the interface between the porous and non-porous region is refined. The walls are also refined to obtain a better reading of velocity profile near the wall. The computational grid has 23,348 nodes with a max face size of 0.5 mm and a minimum face size of 0.3 mm. The comparison between the current simulation and previous simulation is done by using 20 PPI foam configurations with velocity speed of 30 m/s. The comparison can be observed in **Figure 3.2**.

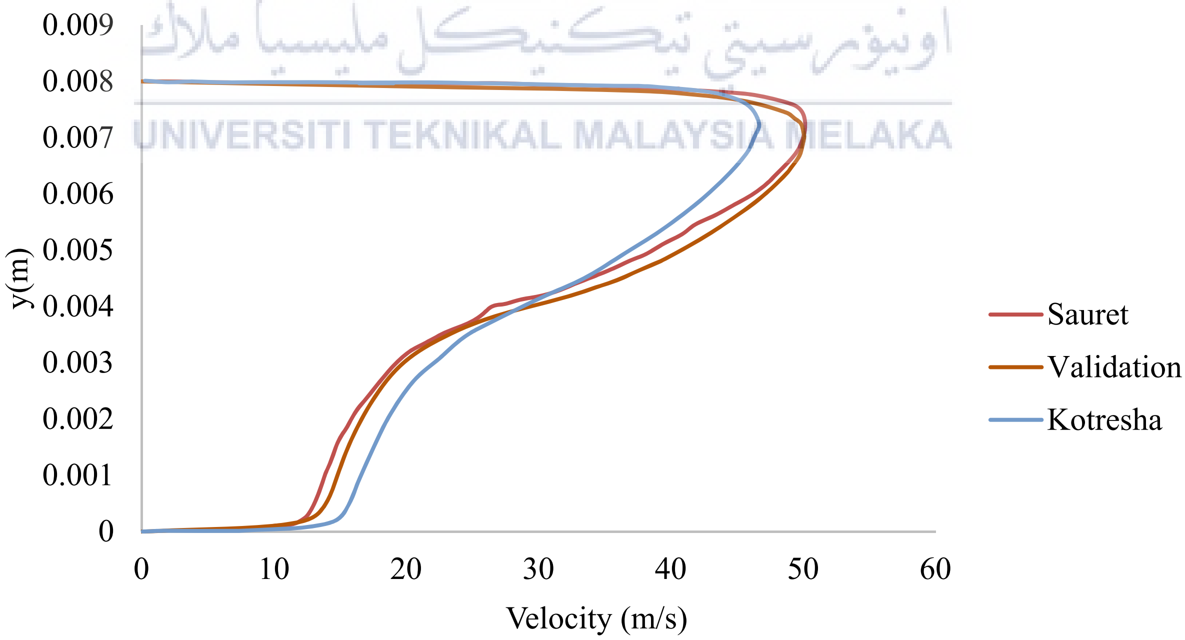

Figure 3.2: Comparison between previous literatures [30] [31] and validation simulation using present ANSYS setup

The comparison in term of velocity contours is also shown in **Figure 3.3** and **Figure 3.4**. There is a difference slightly different in the freestream region of the validation simulation.

Figure 3.3: Velocity contour of 20 PPI – 4mm at 30 m/s from previous literatures [30]

Figure 3.4: Velocity contour of 20 PPI – 4mm at 30 m/s by present study simulation using present ANSYS setup

The pressure drop in the channel is calculated by the difference of channel with and without foam. The pressure drop is used to validate the simulation of pressure drop results. **Figure 3.5** shows the pressure contour of the channel with foam and **Figure 3.6** shows the pressure contour without foam.

Figure 3.5: Pressure contour with foam

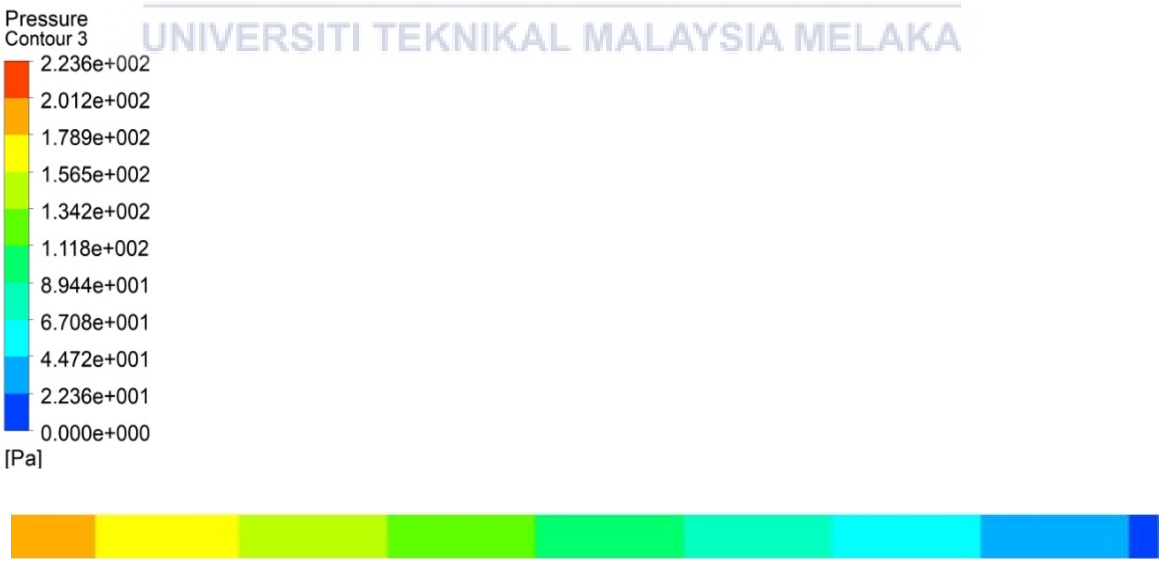

Figure 3.6: Pressure contour without foam

`

In the present simulation, the pressure drop value obtained from the difference [(Pressure $drop_{foam}$) – (Pressure $drop_{no\text{-}foam}$)] between the two channels is 4.5 KPa. The pressure drop value from a previous study [30] was 5.3 KPa. Overall, the results from validation simulation are in good agreement with previous literature [30] [31]. The fluid velocity in the channel without foam is lower compared to the channel with foam which the channel with foam increases the velocity of about 58%. As the velocity increases, the pressure drop also increases.

3.1.2 PARAMETERS AND DESIGN OF GEOMETRY

The parameters to be set are as shown in **Table 3.1** and **Table 3.2**:

Table 3.1: The dimensions of the channel and porous medium

Pore density (PPI)	Channel dimension (m)	Porous medium height, h_f (m)	Porous medium length, L_f (m)
5PPI	0.32(W) × 0.32 (H) × 2 (L)	0.01,0.02,0.05(h_f)	0.27
10PPI 30PPI	0.1(W) × 0.078 (H) × 0.35(L)	0.004, 0.01, 0.03 (h_f)	0.09

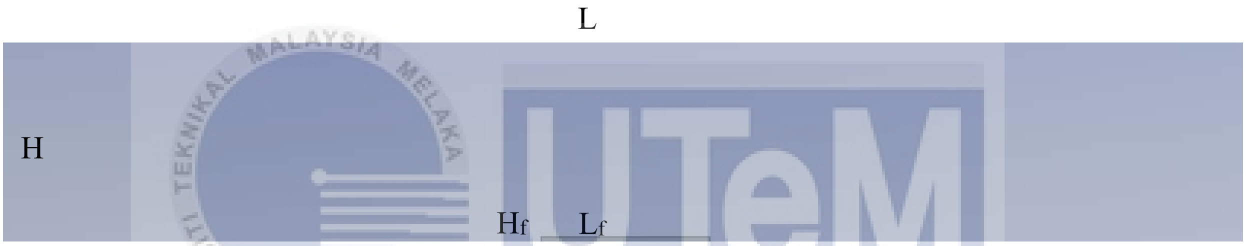

Figure 3.7: Channel configurations of 5 PPI with porous height of 0.01m

Figure 3.8: Channel configurations of 5 PPI with porous height of 0.02m

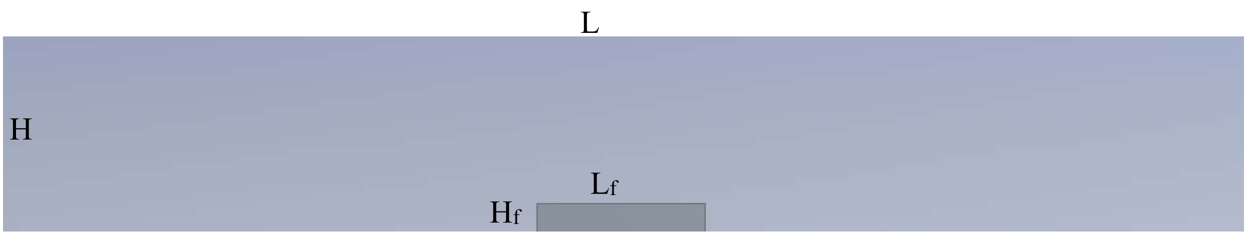

Figure 3.9: Channel configurations of 5 PPI with porous height of 0.05m

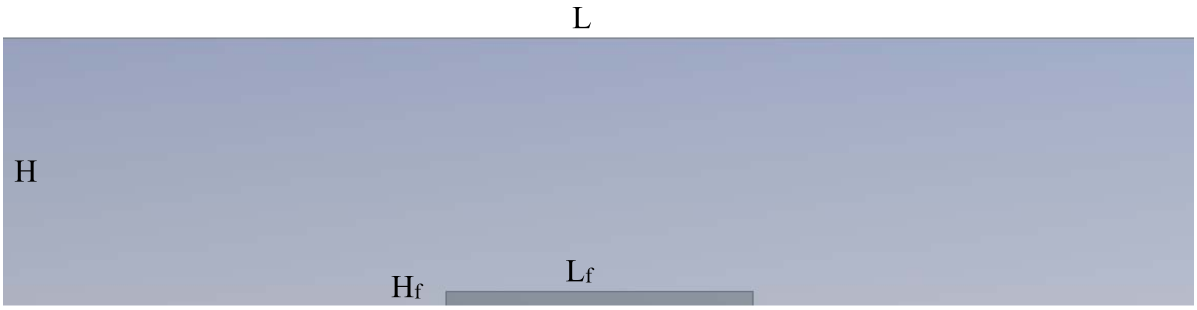

Figure 3.10: Channel configurations of 10 & 30 PPI with porous height of 0.004m

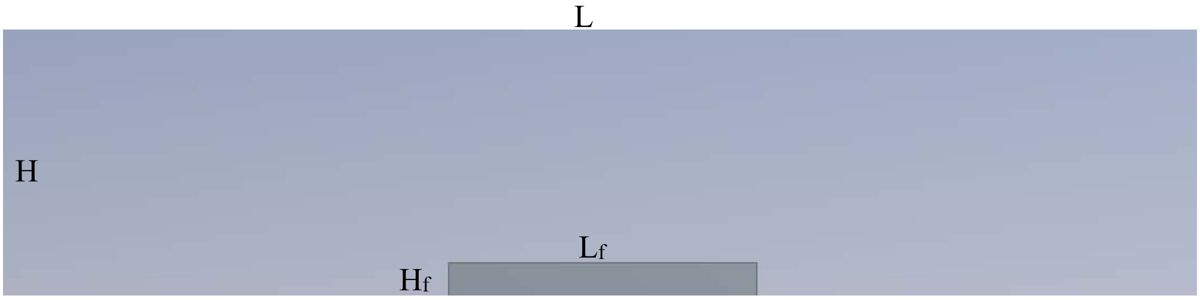

Figure 3.11: Channel configurations of 10 & 30 PPI with porous height of 0.01m

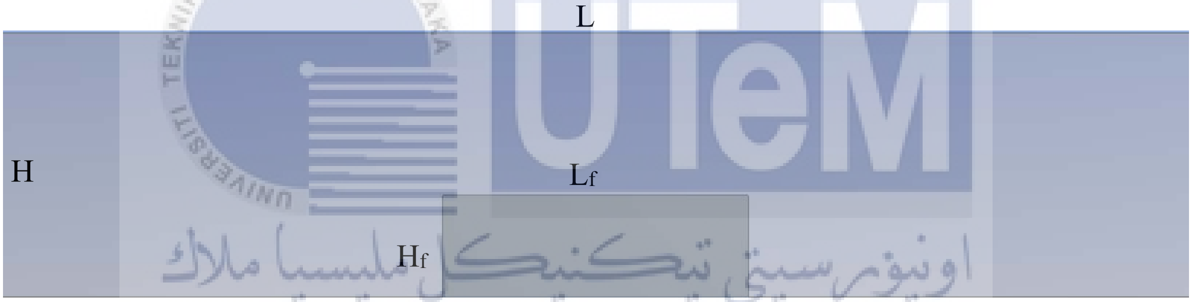

Figure 3.12: Channel configurations of 10 & 30 PPI with porous height of 0.03m

Table 3.2: The parameter and boundary conditions for channel and porous medium

Parameters \ Pore density	5 PPI	10 PPI	30 PPI
Velocity (m/s)	6.5, 9.5, 12.5	3.9, 5.5, 6.2	
Porosity, ε (-)	0.92	0.82-0.91	0.88-0.94
Pore diameter (m)	0.0058	0.0026	0.00087

3.2 SET UP PROCEDURE

In the geometry section, these steps are taken to create a two-dimensional partially filled channel with porous medium:

1. The geometry is done in Workbench 15.0
2. The two-dimensional geometry is designed according to the same measurements from the experimental study [1].
3. The channel dimensions for 5 PPI is set up differently compared to 10 and 30 PPI as shown in **Table 3.1**.
4. Channel is drawn on 'Sketch 1' and the porous zone is drawn in 'Sketch 2'. Once done, click 'Generate' after each sketch done.
5. Channel is chosen as a frozen and porous medium is chosen as material under 'Surface from sketches' from 'Concept' tab. The add-frozen is used to create a separate body.
6. Channel is defined as a frozen and porous medium is defined as material.
7. Then, '2 part, 2 bodies' are merged to become '1 part, 2 bodies' by highlight both sketches. This method used to avoid the contact region between the bodies created. The geometry is as shown in **Figure 3.7 - 3.12**.
8. The geometry is saved to be viewed in the meshing section.

In meshing section, these following steps are taken;

1. The two-dimensional geometry relevance centre is set to 'Fine' and smoothing set to 'Hard'
2. Then, Map Face Meshing and Refinement are set to '3' on the 2 faces of the 2D model. The growth rate defined to the wall is the default which is 1.2 are mainly used to observe the fluid physics.

`

3. Once 'Generate Mesh' is clicked, the two-dimensional computational grid is generated and halving cell size is acceptable based on the validation data [30]. This is proven in **Table 3.6 - 3.8**.
4. In 'Named Selection', 'Inlet', 'Outlet' and 'Wall' are defined as shown in **Figure 3.5** to set up their parameters in the next section.

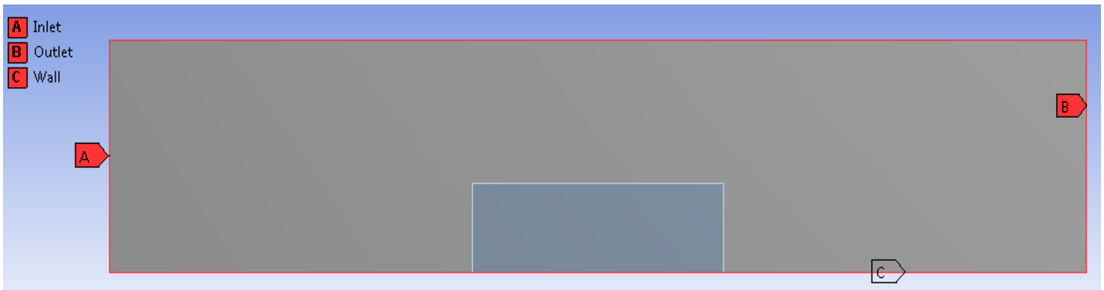

Figure 3.13: Named Selection Setup

In the setup section,

1. For FLUENT launcher, before click 'OK' double precision is ticked.
2. For these configurations, the k-ε turbulence model is used because the fluid flow in this numerical simulation is in turbulent condition.
3. The working fluid used is air. At the materials tab, the porous medium is set as aluminium with default parameters.

Table 3.3: The parameters of viscous resistance and internal resistance coefficient.

Pore Density (PPI)	5 PPI		10 PPI		30 PPI	
Direction	X	Y	X	Y	X	Y
Viscous resistance coefficient	3.66×10^{4}	3.66×10^{4}	7.403×10^{4}	7.403×10^{4}	1.917×10^{5}	1.917×10^{5}
Inertial resistance coefficient	62	62	265.75	265.75	480.47	480.47

4. The properties of the porous zone can be set in two different methods which are (1) cell zone condition and (2) boundary conditions. There will be 2 parts available which are ‘Channel’ and ‘Porous’ in cell zone condition. The ‘Porous’ is double-clicked. Then, the ‘porous zone’ is ticked. In ‘Porous Zone’ tab, the Equation 2.7 and Equation 2.8 are used to calculate viscous and inertial resistance. The X and Y direction have the same value because the domain is defined as homogenous isotropic. The input values are shown in **Table 3.3**.
5. The laminar zone is unticked because the flow in the porous medium is turbulent. This is proven through calculation from the data from the previous study [1]. The calculation is done by using the equations below at average room temperature of 23°C:

$$U_p = \frac{U_{us}H - U_f H_f}{\varepsilon h} \tag{3.1}$$

$$Re = \frac{\rho V_p D_p}{\mu} \tag{3.2}$$

`

where;

Re_p : Pore Reynold number

U_p : Average pore velocity (m/s)

U_{us} : Upstream velocity (m/s)

U_f : Freestream velocity (m/s)

H : Channel height (m)

H_f : Porous medium height (m)

h : Free stream region height (m)

ε : Porosity

Table 3.4: The Reynolds number for the porous medium of 5 PPI

Porous height, h_f (m) / Velocity, v_o (m/s)	0.01	0.02	0.05
	5 PPI		
6.5 m/s	921	774	477
9.5 m/s	1402	1097	635
12.5 m/s	1939	1466	827

Table 3.5: The Reynolds number for the porous medium of 10 and 30 PPI

Porous height, h_f (m) / Velocity, v_o (m/s)	0.004		0.01		0.03	
	10 PPI	30 PPI	10 PPI	30 PPI	10 PPI	30 PPI
3.9 m/s	760	332	750	320	609	303
5.5 m/s	1126	351	1107	345	942	305
6.2 m/s	1292	403	1274	397	1054	307

6. At boundary conditions, ‘Inlet’ is double-clicked to be set according to the velocity parameter by the previous experiment which 3.9, 6.2 and 12.5 m/s. The simulation under ‘Hydraulic diameter and turbulent viscosity’ will be used.
7. Once finish, click ‘OK’ and save the project before proceeding to the solution method.

In the solution section,

1. The SIMPLE algorithm method is chosen because this method uses the relationship between velocity and pressure to enforce mass conservation and obtain pressure field which links to the objective of this numerical study.
2. Hybrid initialization is used under ‘solution initialization’ tab because it is mainly used to determine velocity and pressure parameters by solving Laplace’s Equations.
3. Then under ‘run calculation’ tab, the number of iterations is set, the best results can be obtained when iterations stop automatically showing that ‘solution is converged’.

In the results section,

1. The velocity will be computed at specific areas as shown in **Figure 3.14** and **3.15**. The airflow distribution will be observed based on contour, streamline and vector. The lines represent:
    a. Line 1: Upstream
    b. Line 2: x = 0
    c. Line 3: x = 0.5Lf
    d. Line 4: x = Lf
    e. Line 5: Downstream

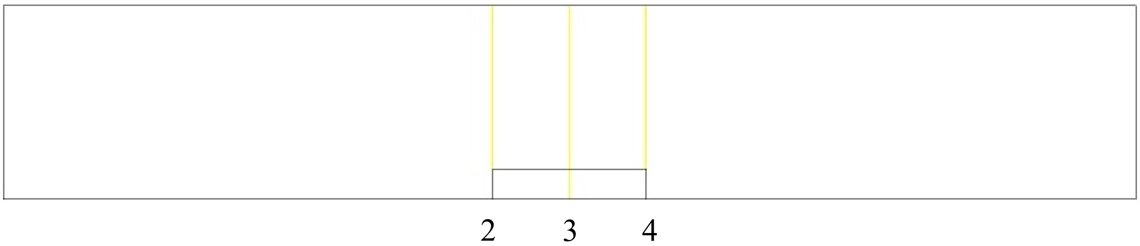

Figure 3.14: Area of observation for 5 PPI channel

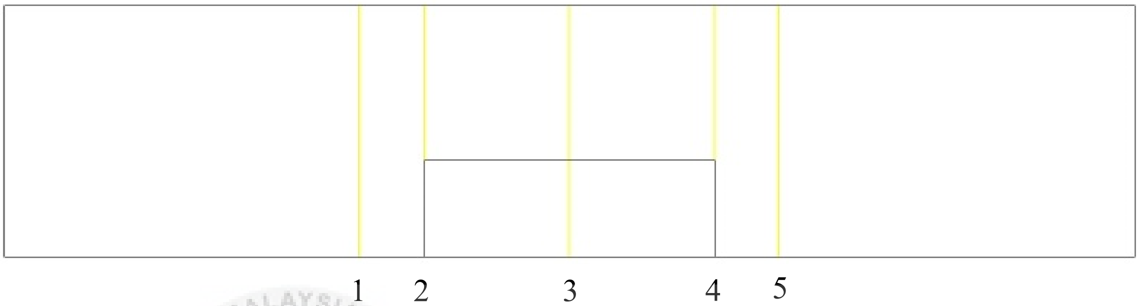

Figure 3.15: Area of observation for 10 and 30 PPI channel

2. The pressure drop is computed differently between 5 PPI with 10 and 30 PPI as shown in **Figure 3.16** and **3.17**. The pressure taps for 5 PPI are 0.4 m and 10, 30 PPI are 0.25 m.

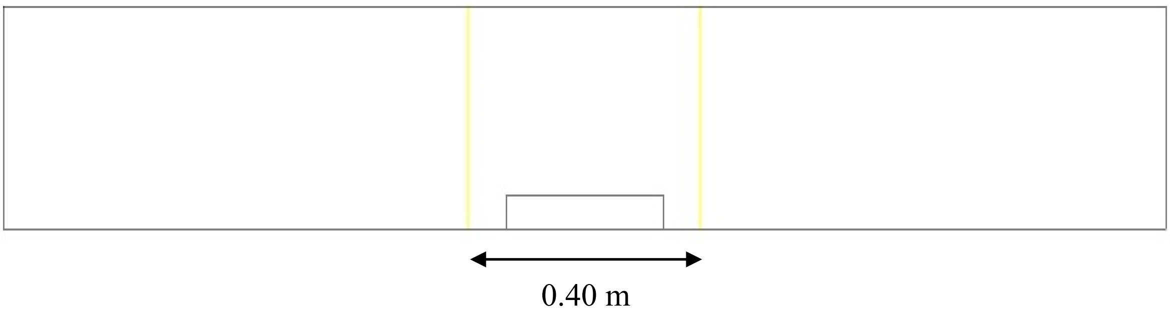

Figure 3.16: Pressure tap measurements for 5 PPI channel

`

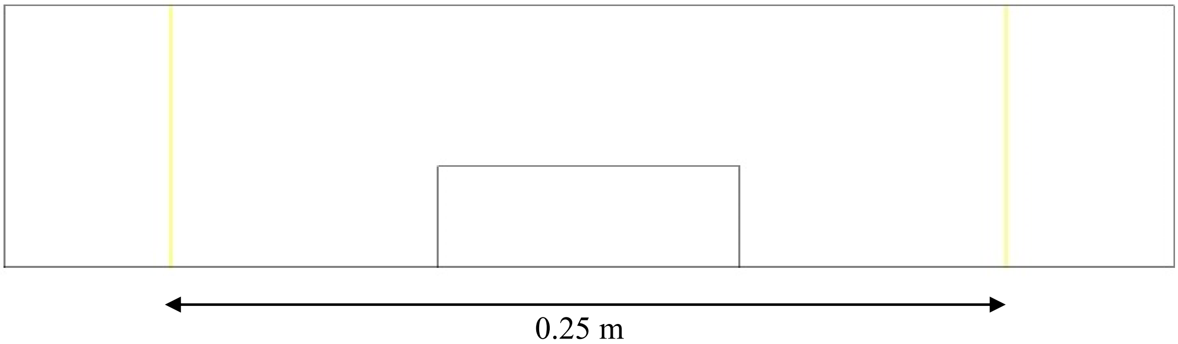

Figure 3.17: Pressure tap measurement for 10 and 30 PPI channel

3.3 GRID INDEPENDENCE TEST FOR THE CHANNEL AND POROUS MEDIUM

Some parameters affect the solver performance and accuracy such as mesh too coarse and high skewness, large aspect ratios and also inappropriate boundary layer mesh. Thus, a grid independence test is conducted to refine the mesh further. The purpose is to identify the optimum point for a more accurate solution results by using smaller cell sizes and finer grids.

`

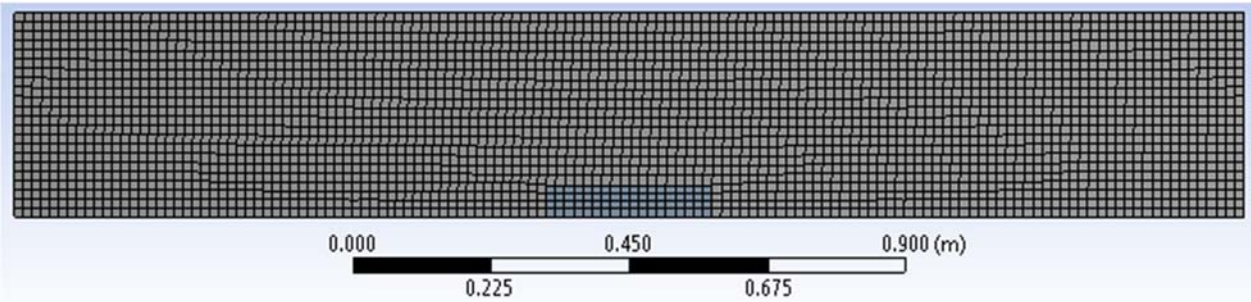

Figure 3.18: Meshing of 5 PPI with foam height of 0.05 m for Grid Independence Test 1

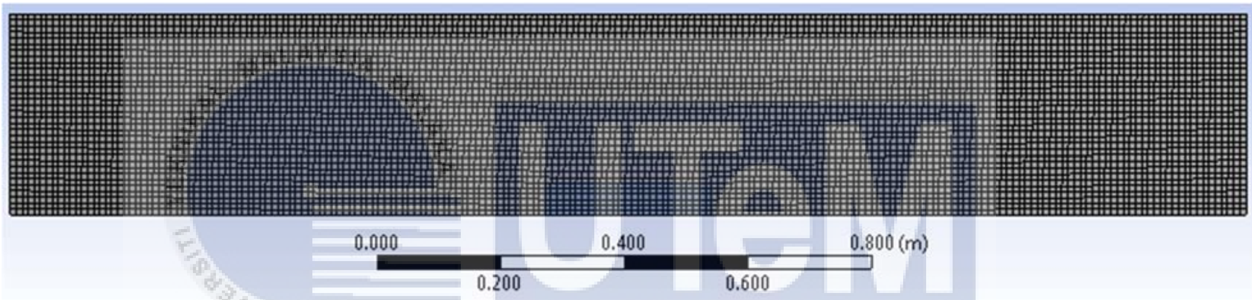

Figure 3.19: Meshing of 5 PPI with foam height of 0.05 m for Grid Independence Test 2

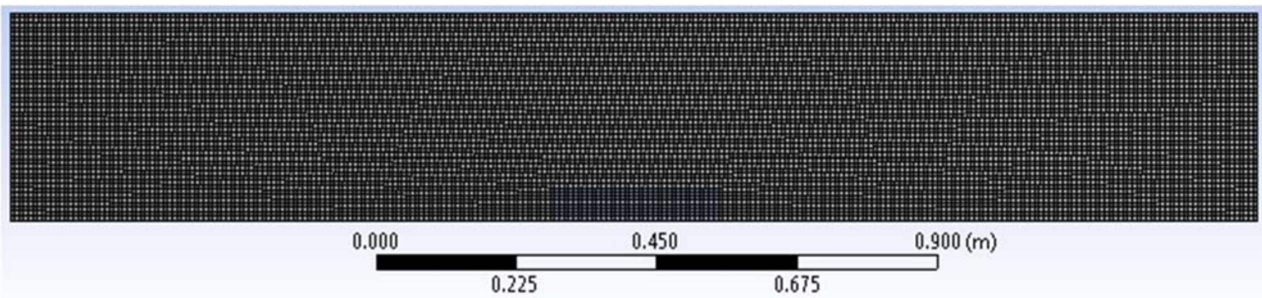

Figure 3.20: Meshing of 5 PPI with foam height of 0.05 m for Grid Independence Test 3

`

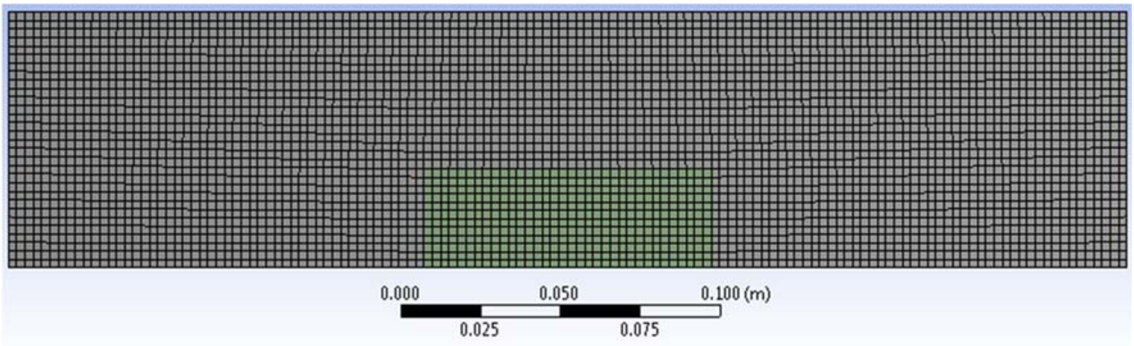

Figure 3.21: Meshing of 10 & 30 PPI with foam height of 0.03 m for Grid Independence Test 1

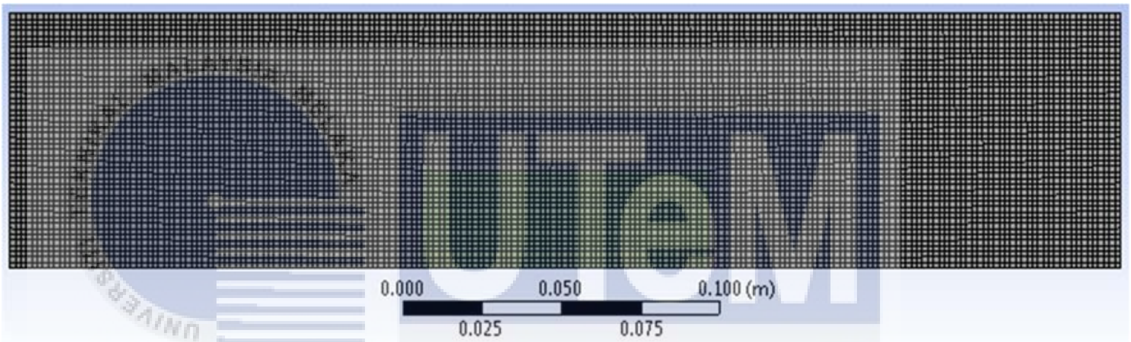

Figure 3.22: Meshing of 10 & 30 PPI with foam height of 0.03 m for Grid Independence Test 2

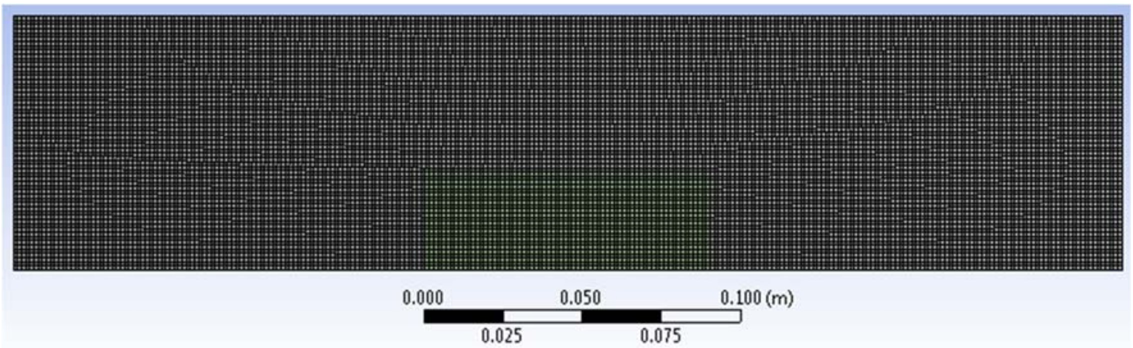

Figure 3.23: Meshing of 10 & 30 PPI with foam height of 0.03 m for Grid Independence Test 3

`

Table 3.6: Parameters of Grid Independence Test for 5 PPI and foam height of 0.05 m with velocity speed – 12.5 m/s

Parameters	Grid Independence Test 1	Grid Independence Test 2	Grid Independence Test 3
Refinement	1	2	3
Relevance centre	Fine	Fine	Fine
Nodes	3151	6970	12285
Element	2992	6732	11968
Velocity (m/s)	15.24	15.32	15.38

Table 3.7: Parameters of Grid Independence Test for 10 PPI and foam height of 0.03 m with velocity speed – 6.2 m/s

Parameters	Grid Independence Test 1	Grid Independence Test 2	Grid Independence Test 3
Refinement	1	2	3
Relevance centre	Fine	Fine	Fine
Nodes	4185	9292	16409
Element	4020	9045	16080
Velocity (m/s)	11.32	11.34	11.35

Table 3.8: Parameters of Grid Independence Test for 30 PPI and foam height of 0.03 m with velocity speed – 6.2 m/s

Parameters	Grid Independence Test 1	Grid Independence Test 2	Grid Independence Test 3
Refinement	1	2	3
Relevance centre	Fine	Fine	Fine
Nodes	4185	9292	16409
Element	4020	9045	16080
Velocity (m/s)	11.47	11.50	11.51

`

Therefore, the refinement of '3' is chosen for the 5, 10 and 30 PPI channel for meshing. Refinement'3' was chosen because there were no obvious effects caused by the meshing. In the grid independence test, test 3 for 5, 10 and 30 PPI channel can produce an optimum number of nodes and elements with a smaller cell element size without adding unnecessary burden to the ANSYS Fluent software.

`

CHAPTER 4

RESULTS AND ANALYSIS

4.1 INTRODUCTION

This project conducted CFD simulation using ANSYS Fluent to investigate the airflow behaviour and the pressure drop across a partially filled channel with metal foam. The inlet velocities in a channel with 10 and 30 PPI foams was set at 3.9, 5.5 and 6.2 m/s, meanwhile for 5 PPI channel, the velocities were 6.5, 9.5 and 12.5 m/s. The flows in both channels are assumed fully developed (turbulent). In the simulations, the results of velocity distribution in the channel were examined particularly at the fluid flow behaviour at upstream, partially filled and downstream sections. The pressure drop across the partially filled channel was also determined by using the result of pressure contours and presenting in the form of graph and discussed in detail in this chapter. In this chapter, comparisons of velocity and pressure gradient between experimental and simulation data are also shown, considering the results of past literature that are relevant to this project.

`

4.2 VELOCITY DISTRIBUTION CONTOUR

4.2.1 Velocity contour

In ANSYS Fluent, the contours are used to illustrate the magnitude of a variable on the surfaces on which it is plotted. These contours can help the researcher to understand the flow path or any other complex flow that results in parameters of interest, for example, the velocity. The high and low-pressure regions in the partially filled channel with the porous medium can be observed. Various colours are being used to understand the flow of interests. In this project, red indicates the highest velocity and blue indicates the lowest velocity and a linear variation in between these two colours is used to represent the range of velocities in between.

4.2.2 5 PPI foam with various thickness & air velocities

(a)

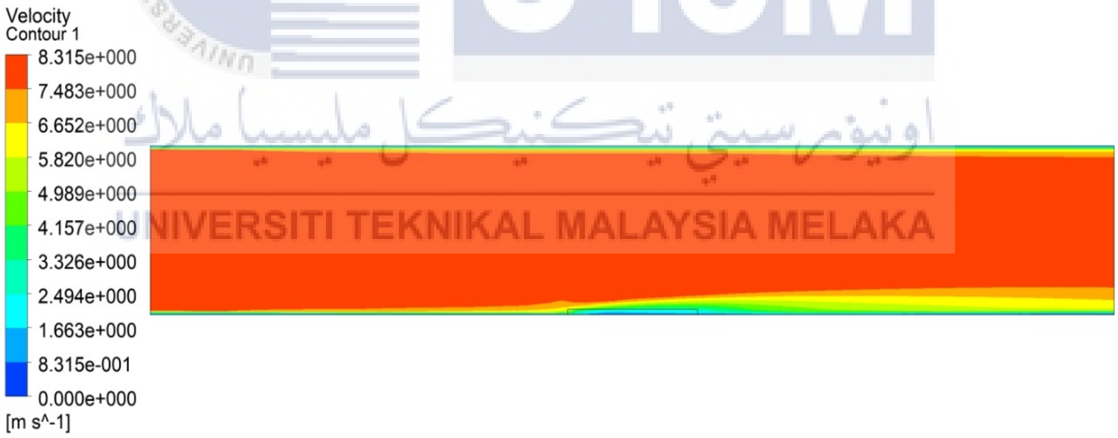

(b)

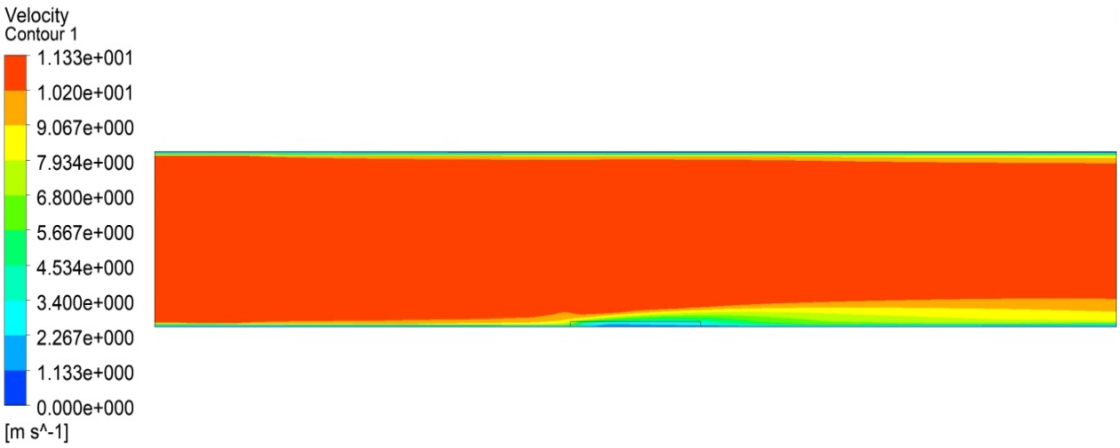

(c)

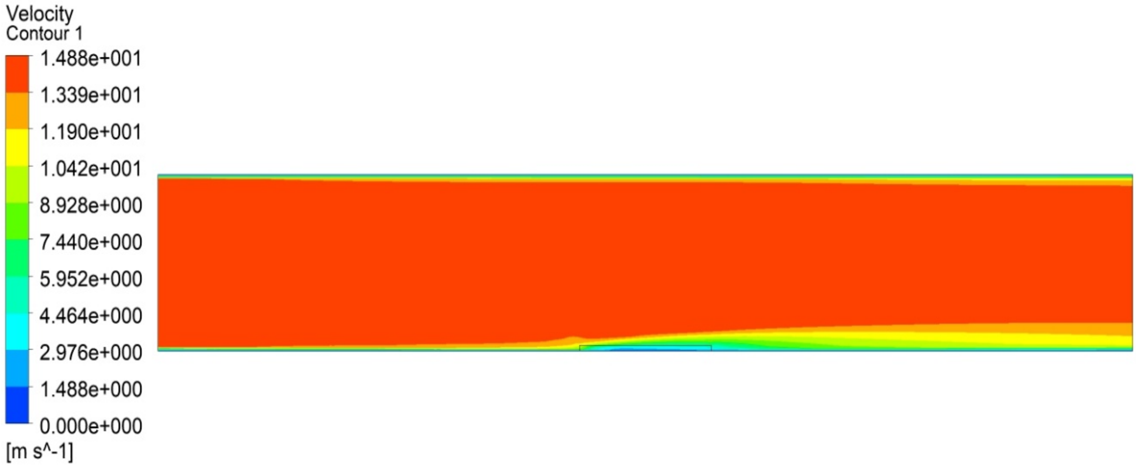

Figure 4.1: Velocity contour of 5 PPI with h/H = 0.03 at different velocities (a) u_{inlet} = 6.5 m/s, (b) u_{inlet} = 9.5 m/s, and (c) u_{inlet} = 12.5 m/s

The 5 PPI porous medium has a larger pore size compared to 10 and 30 PPI porous medium. The porous medium is positioned at the middle of the channel to prevent data losses during simulation [1] [30]. Based on **Figure 4.1**, the configuration with the lowest blockage ratio of 0.03 has no significant effect on the velocity distribution. The flow starts to develop at the entrance region of the channel. The fluid flow in the partial section (free-stream region) is fully developed as the velocity distribution remains unchanged throughout the channel as the velocity contour colour remains red. The free stream region is a non-porous region at the top of the porous medium and where the fluid flow is fully developed [1]. The upstream, free-stream and downstream of the channel are monitored. The upstream is also no-filled region (without porous medium), at the beginning of the flow stream and the downstream is also no-filled region right at the end of the flow block. For the larger channel with a height of 0.32 m, a porous medium with a height of 0.01 m does not affect the fully-developed flow across the larger channel.

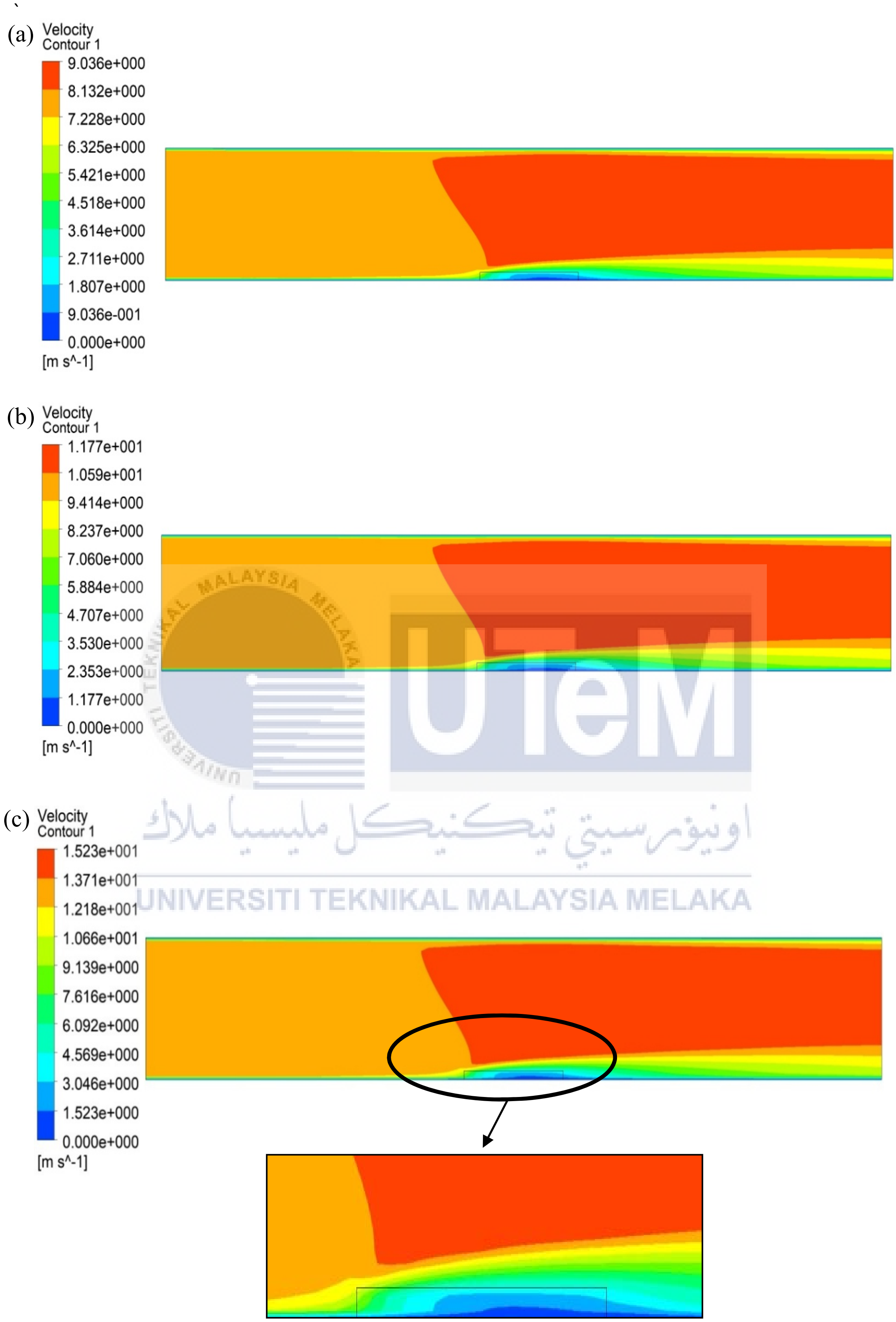

Figure 4.2: Velocity contour of 5 PPI with h/H = 0.06 at different velocities (a) u_{inlet} = 6.5 m/s, (b) u_{inlet} = 9.5 m/s, and (c) u_{inlet} = 12.5 m/s

Figure 4.2 shows that at the upstream region, the velocity starts to develop and is in orange colour showing lower velocity as compared to Figure 4.1 and the increment of porous block thickness starts to affect the flow behaviour. Once the velocity contour reaches the free-stream region, it becomes red colour which is higher than inlet velocity, where **Figure 4.2 (a)**, v = 9.36 m/s **(b)**, v = 11.77 m/s and **(c)** v = 15.23 m/s. However, the velocity contours are in the same colour despite a slightly different velocity distribution, it shows that the blockage ratio, 0.06 are insufficient to cause flow disturbance in the channel. At the boundary layer of the porous medium, the velocity is starting from zero to a value close to the free-stream velocity, changing in the normal direction to the boundary. The velocity above the boundary layer is constant and equal to the freestream velocity. In the porous medium, there is a small blue colour region (v = 0 m/s) formed at its bottom. Also, it shows the lowest velocity region exits in the porous medium.

(a)

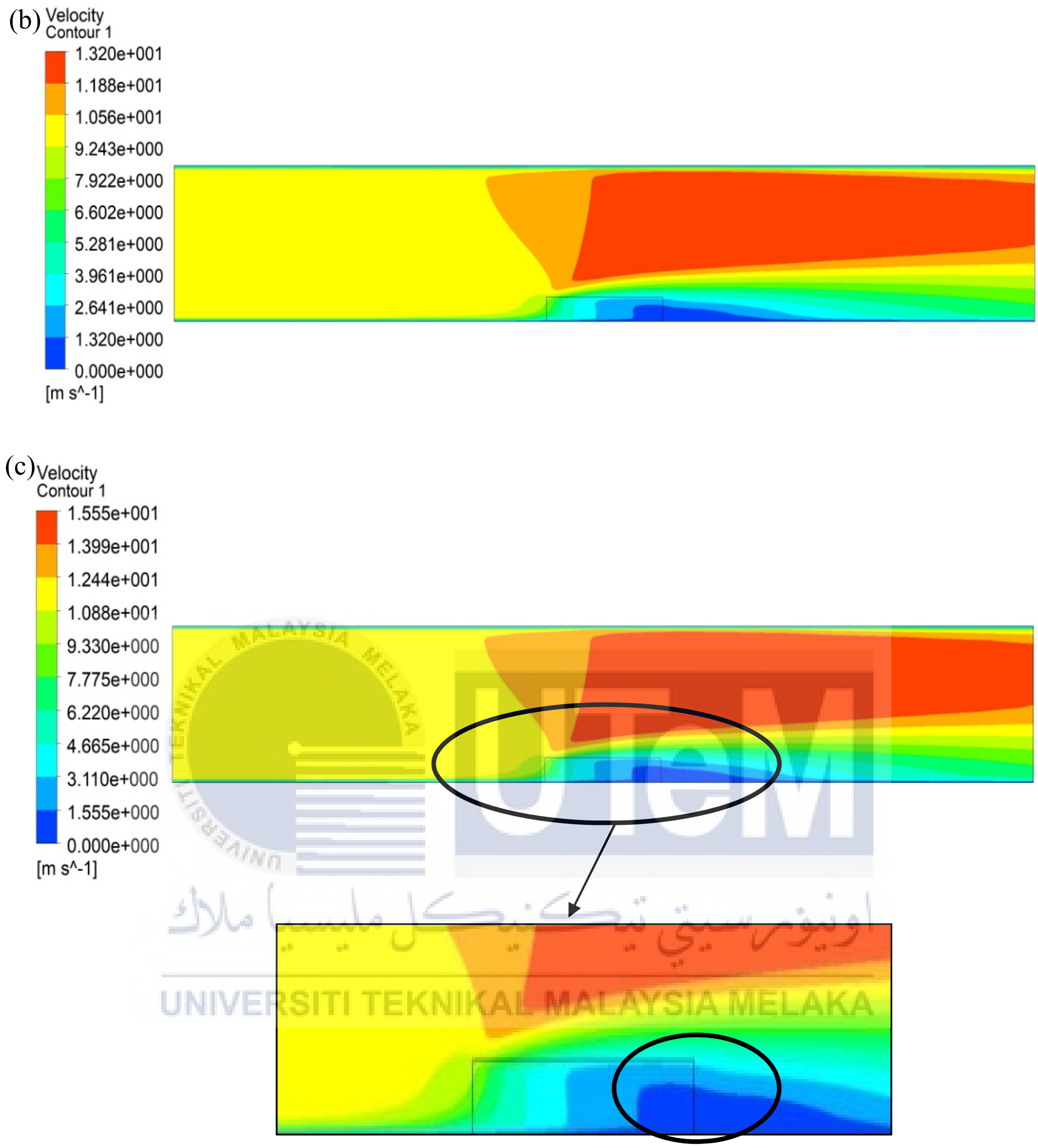

Separation point

Figure 4.3: Velocity contour of 5 PPI with h/H = 0.16 at different velocities (a) u_{inlet} = 6.5 m/s, (b) u_{inlet} = 9.5 m/s, and (c) u_{inlet} = 12.5 m/s

Figure 4.3 shows the highest blockage ratio configuration of 0.16 has a significant effect on the velocity distribution across the channel. For example in **Figure 4.3 (c),** the contour is in yellow (v = 12.44 m/s) at the entrance region up to almost half of the channel, where the contour turns orange colour, showing a higher velocity (v = 14 m/s). About half of the partially filled section, the velocity contour reaches its highest velocity as the contour is in red (v = 15.55 m/s). In the porous medium, the contour colour changes from light blue to dark blue representing a decrease in pore velocity from v = 4.65 m/s to v = 0 m/s. This probably due to a significant foam height and resistance in the porous medium, there exists a flow separation at the back of the porous medium block. The flow separation is in the form of a vortex which occurs when the fluid in close proximity to the wall surface reverses its flow direction. However, the shear stress is considered to be zero at a point of forward and backward flow which is called a separation point as shown in the enlarged image of **Figure 4.3 (c)**.

4.2.3 10 PPI foam with various thickness & air velocities

(a)

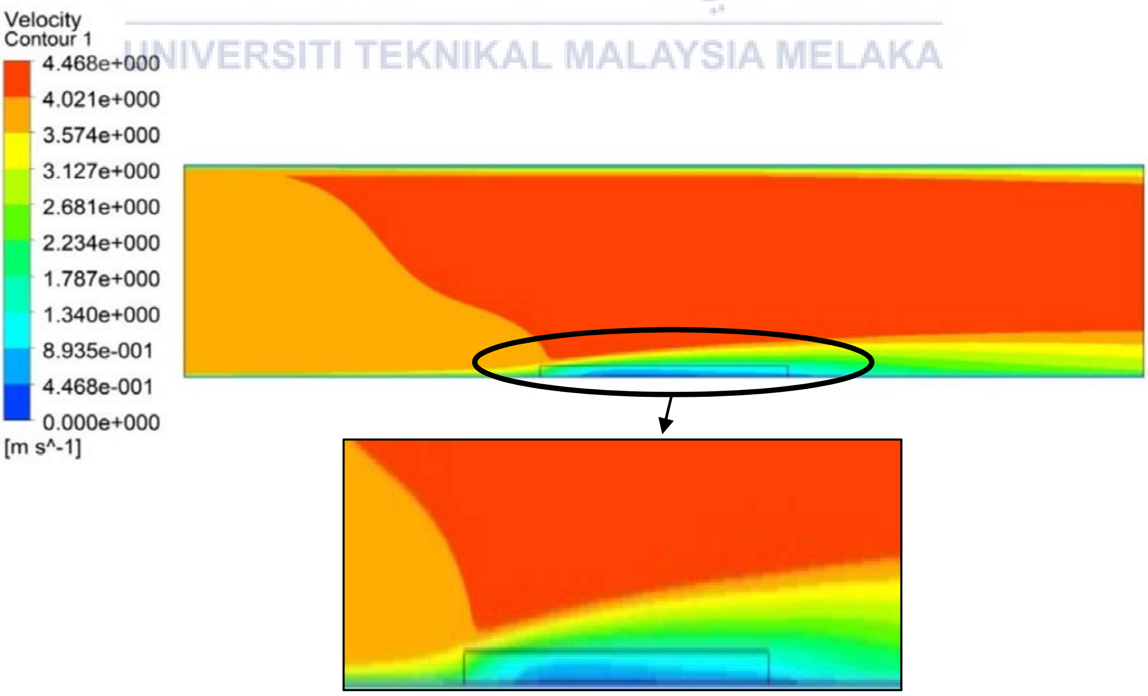

`

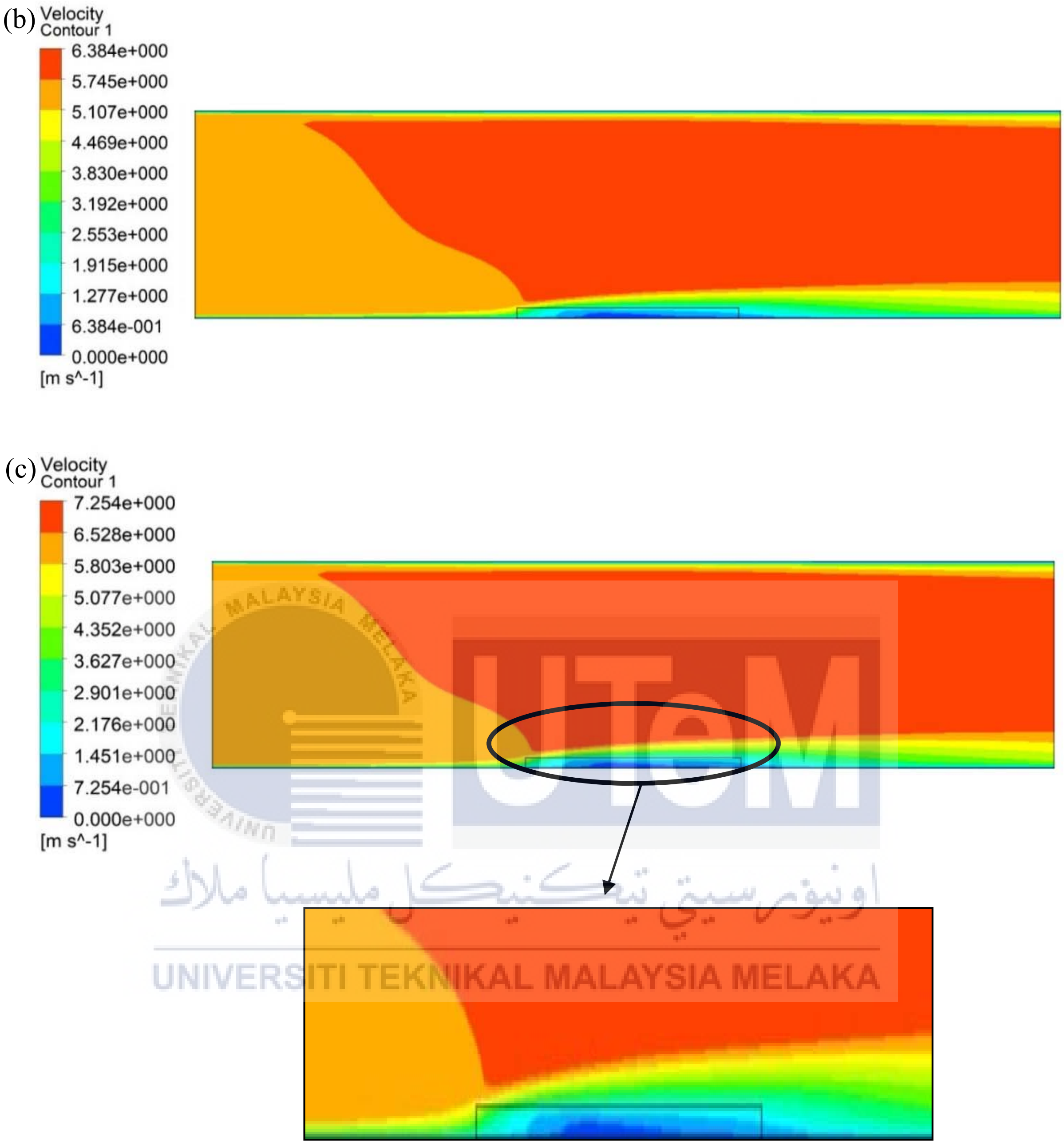

Figure 4.4: Velocity contour of 10 PPI with h/H = 0.05 at different velocities (a) u_{inlet} = 3.9 m/s, (b) u_{inlet} = 5.5 m/s, and (c) u_{inlet} = 6.2 m/s

`

The 10 PPI porous medium have higher inertial and viscous resistance as shown in **Table 3.3** compared to 5 PPI porous medium. Based on **Figure 4.4** shows that the blockage ratio of 0.05 is meaningless, as no significant effects on the velocity distribution throughout the partially filled channel. **Figure 4.4 (c)** shows the velocity contour is in orange colour (v = 6.52 m/s) before it changes to red colour (v = 7.25 m/s) at x = 0.08 m of the partially filled channel. Since the porous block height is 0.004 m which too small for this channel configuration, there is no disturbance in the channel at the downstream region as shown in the enlarged **Figure 4.4 (c)**. Within the porous region **Figure 4.4 (a)**, there is smaller blue (v = 0 m/s) region in the porous medium compared to **Figure 4.4(b)** and **4.4 (c)**. There is also very low velocity or almost zero velocity formed at the back of the porous medium in the downstream region. However, the region is small, probably due to a very thin block is introduced.

(a)

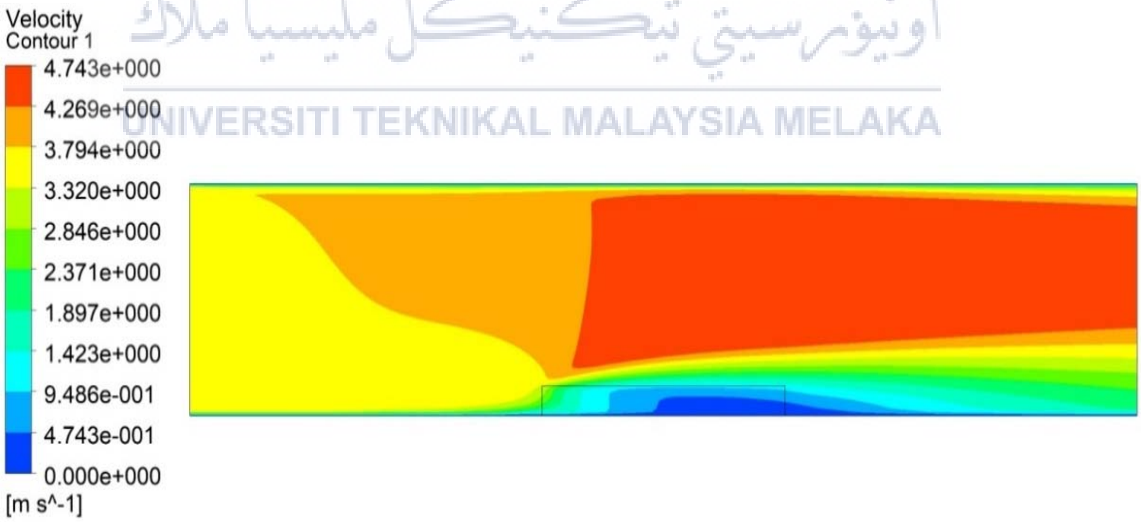

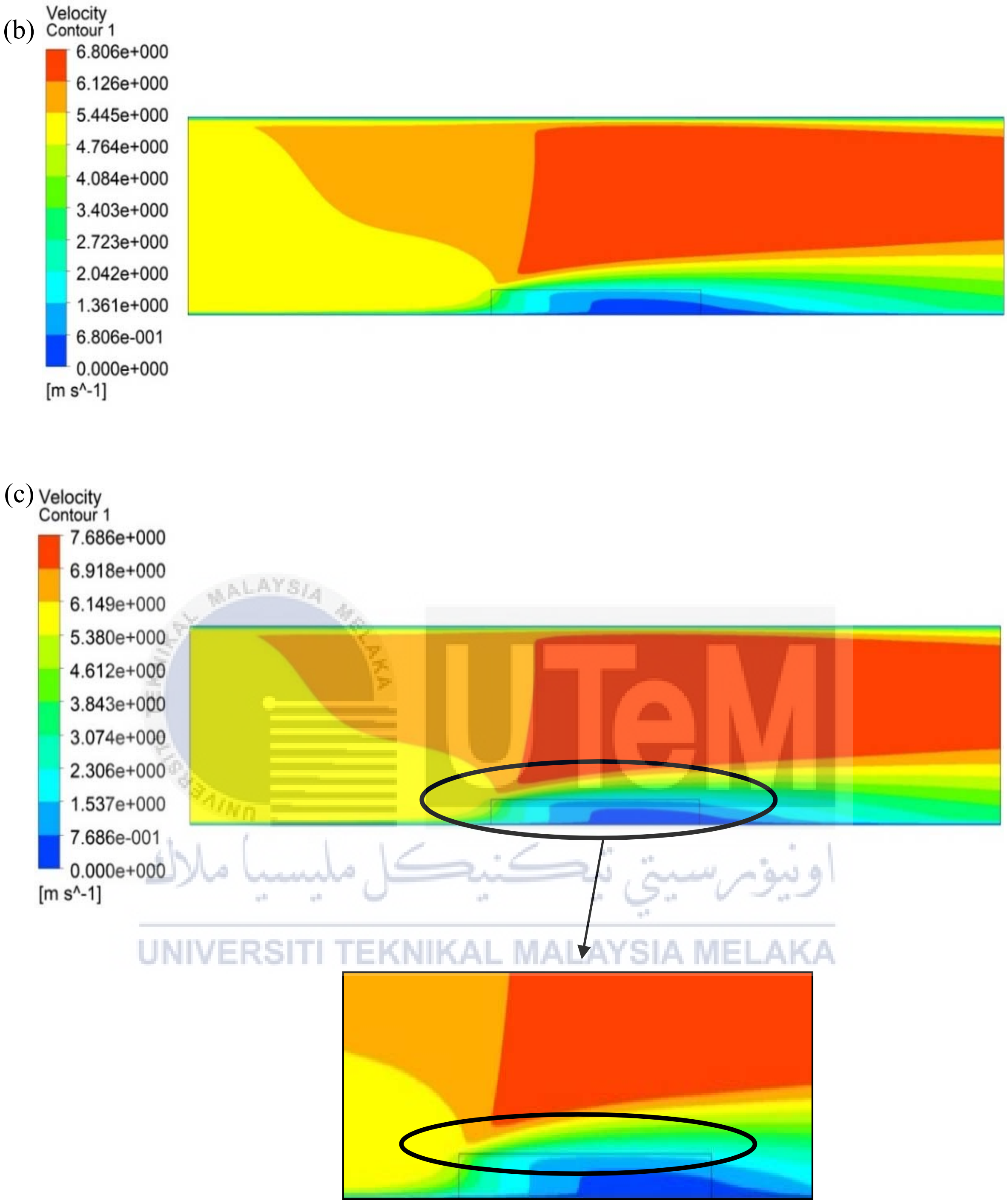

Figure 4.5: Velocity contour of 10 PPI with h/H = 0.13 at different velocities (a) u_{inlet} = 3.9 m/s, (b) u_{inlet} = 5.5 m/s, and (c) u_{inlet} = 6.2 m/s

This channel applied a blockage ratio, h/H = 0.13 are as shown in **Figure 4.5 (a), (b),** and **(c)**. This configuration also has a limited effect on the velocity distribution across the channel. As shown above in **Figure 4.5 (c)**, the contour is in yellow (v = 6.15 m/s) at the entrance region and changes to orange colour (v = 6.92 m/s) at x = 0.04 m of the channel. Once it reaches the freestream region, a higher velocity can be observed as the contour turns red (v = 7.69 m/s) specifically at the location, x = 0.15 m. At the interface of the porous and non-porous region, the fluid flows from the upper porous medium merge with the flow in the freestream region. In the porous region, velocity contour changes from light blue to dark blue colour (v = 0 m/s) for all different velocities. There is a possibility of a small recirculation zone formed behind the porous medium due to dark blue colour in the region.

(a)


(b)
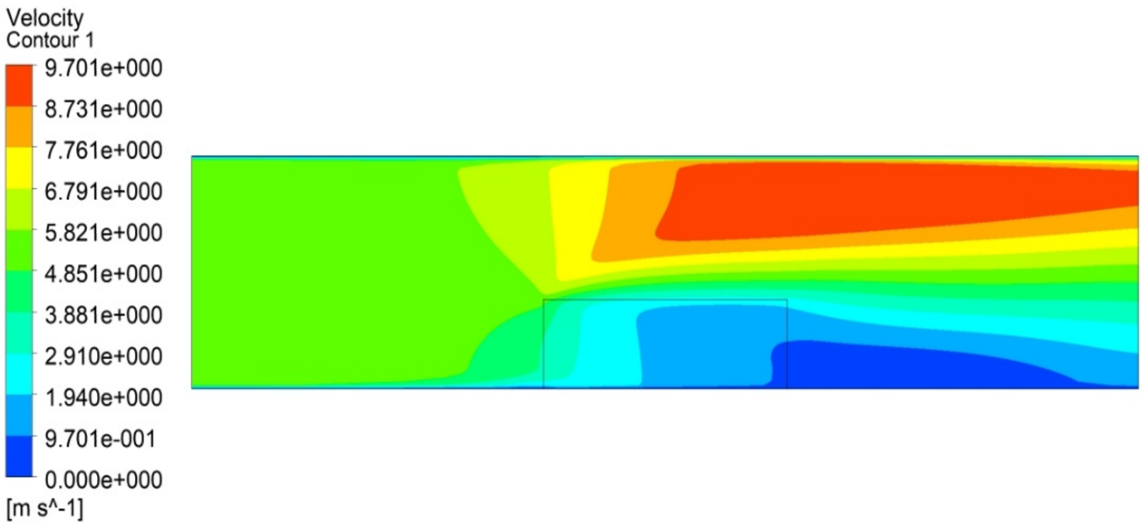

`

(c)

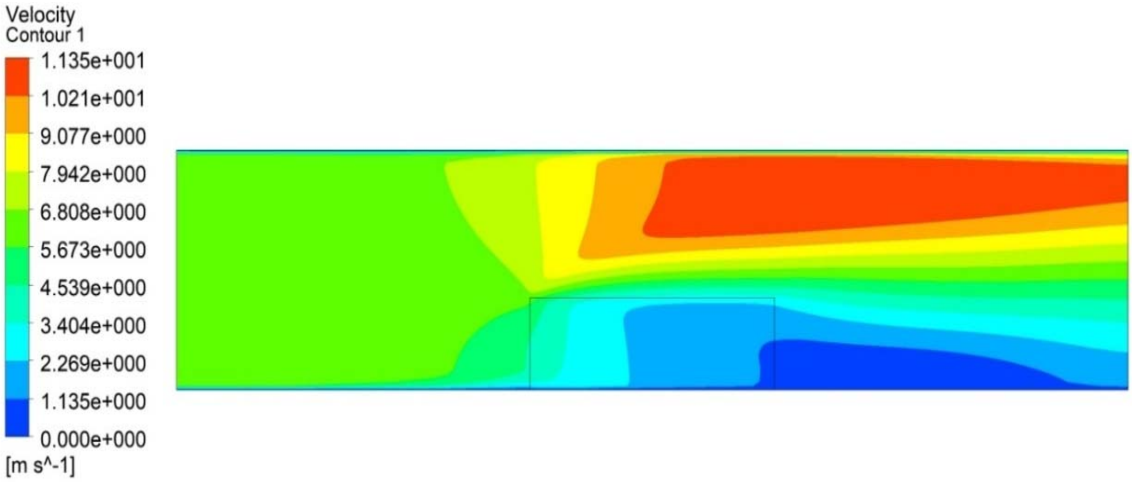

Figure 4.6: Velocity contour of 10 PPI with h/H = 0.39 at different velocities (a) u_{inlet} = 3.9 m/s, (b) u_{inlet} = 5.5 m/s, and (c) u_{inlet} = 6.2 m/s

For 10 PPI porous medium with h/H = 0.39, the colour variation existed in the freestream regions shown in **Figure 4.6. Figure 4.6 (c)** shows the entrance region of the channel is green (v = 6.81 m/s) until the velocity profile reaches the freestream region with a higher blockage ratio, smaller velocity can be seen right before the partially filled section. Then, in the free-stream region, the boundary layer existed and becomes light green colour (v = 7.94 m/s). In vertical direction, the colour changes to yellow (v = 9.08 m/s), orange (v = 10.21 m/s) and red (v = 11.35 m/s) out of the boundary layer region. The colour transitions from yellow to red, all occurred in the freestream region. In the porous region, the light blue (v = 3.4 m/s) becomes dark blue at the very end of the porous block as shown in **Figure 4.6**, not as the previous case with the blockage ratio, 0.16 where the velocity 0 m/s in the entire porous medium. In this case, the flow in the porous region has the same value, showing the existence of fluid flow in the 10 PPI foam, unlike the 5 PPI foam.

4.2.4 30 PPI foam with various thickness & air velocities

(a)
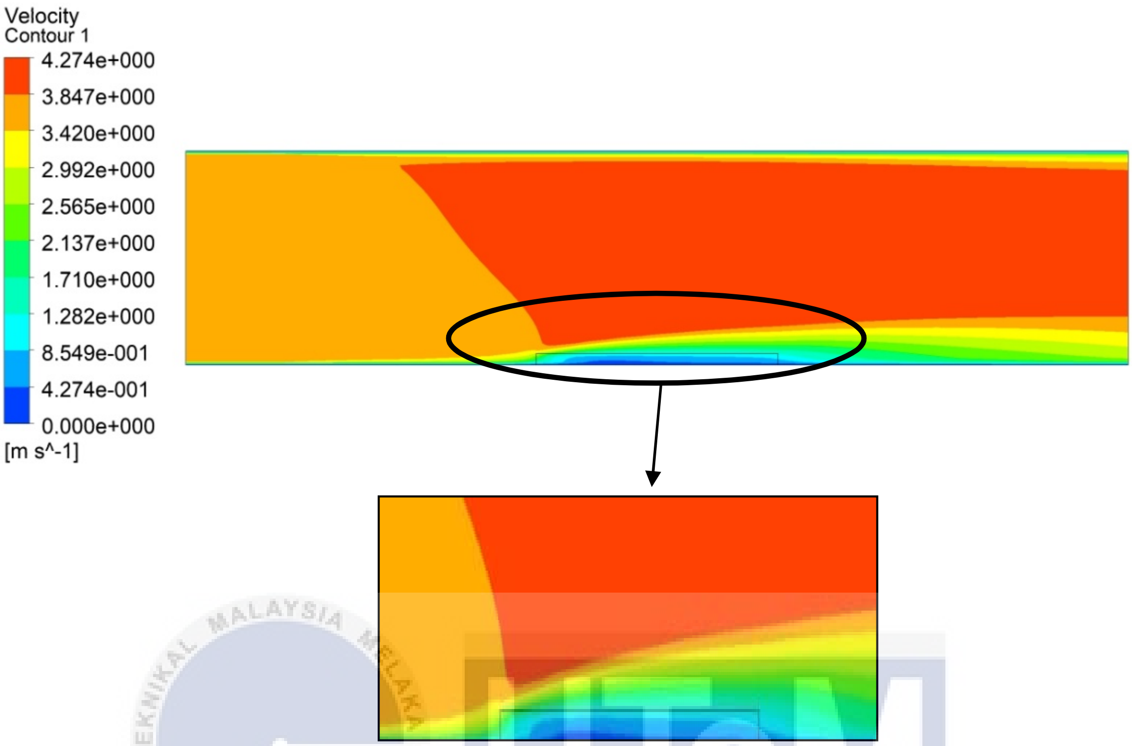

(b)
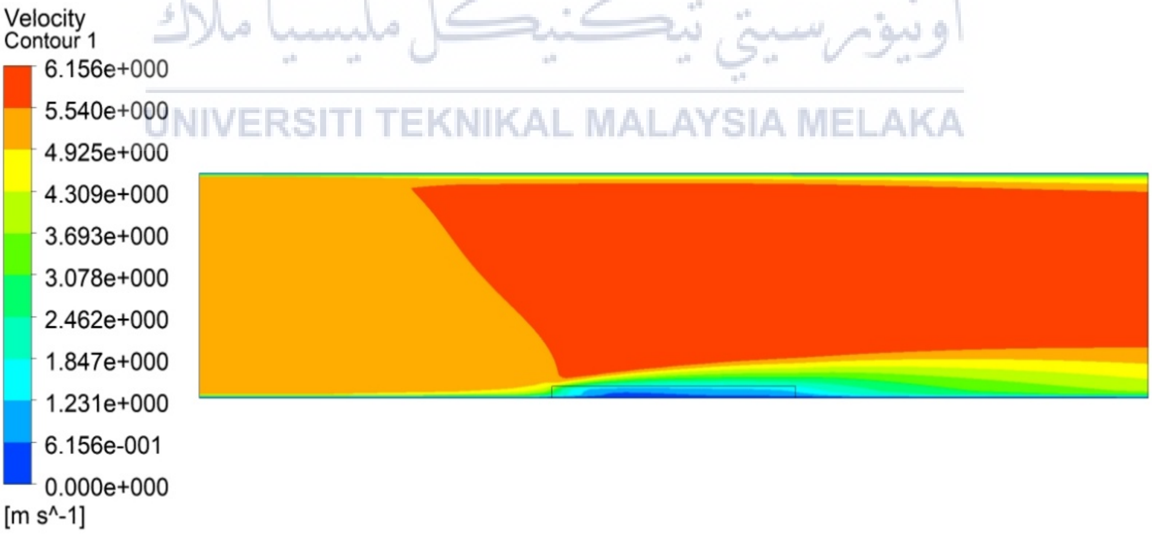

`

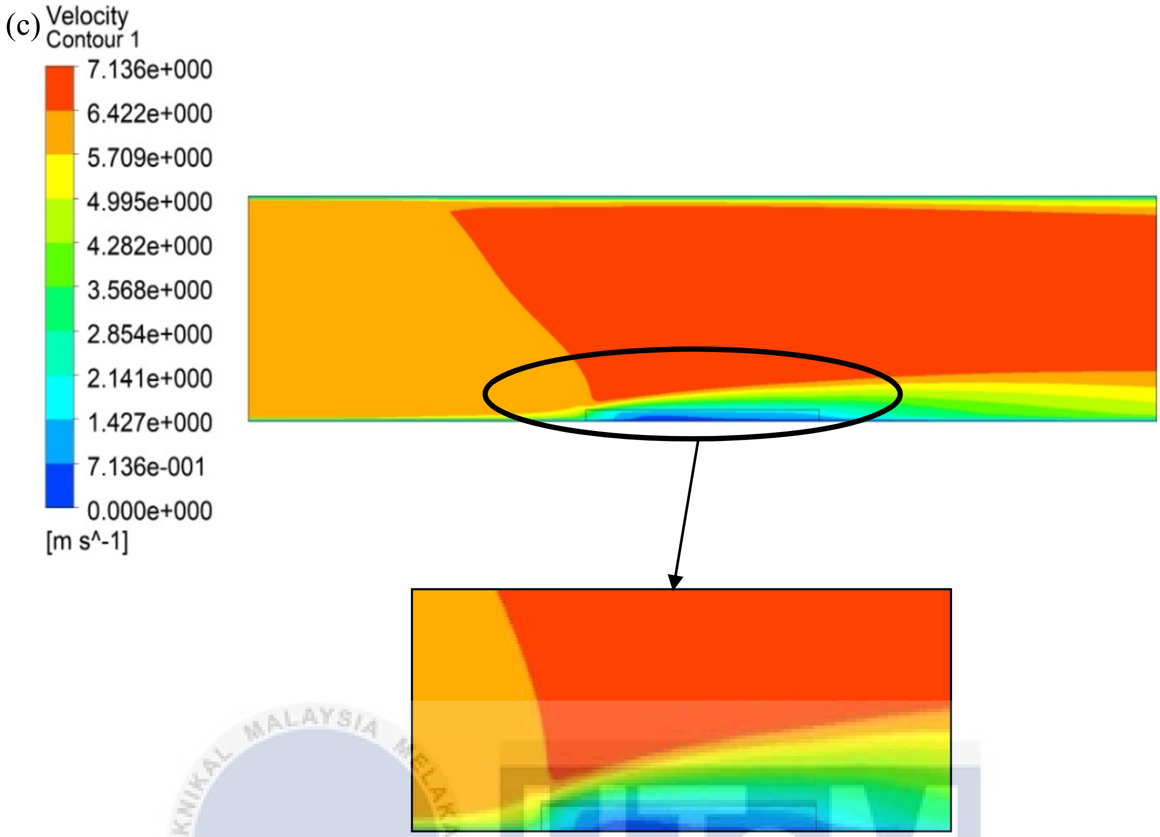

Figure 4.7: Velocity contour of 30 PPI with h/H = 0.05 at different velocities (a) u_{inlet} = 3.9 m/s, (b) u_{inlet} = 5.5 m/s, and (c) u_{inlet} = 6.2 m/s

Similarly, with the 10 PPI, the use of 30 PPI with h/H =0.05 shows no effect on the velocity distribution across the channel and porous medium based on flow contours in **Figure 4.7**. The velocity profile at the entrance region is in orange (v = 6.42 m/s) and it becomes fully-developed at x = 0.09 m of the channel turning into red colour (v = 7.14 m/s) throughout the channel. In the porous medium, contour changes from light blue (v = 2.14 m/s) to dark blue (v = 0 m/s) until the lower half-height of the porous medium as shown in enlarged **Figure 4.7 (c)**. There is also no disturbance for the fluid flow in the downstream region as the height of the porous medium, 0.004 m is small for the 0.078 m channel. Other than that, there is no recirculation. Overall, the simulation results of 30 PPI are almost similar to 10 PPI porous medium with the same blockage ratio and flow conditions.

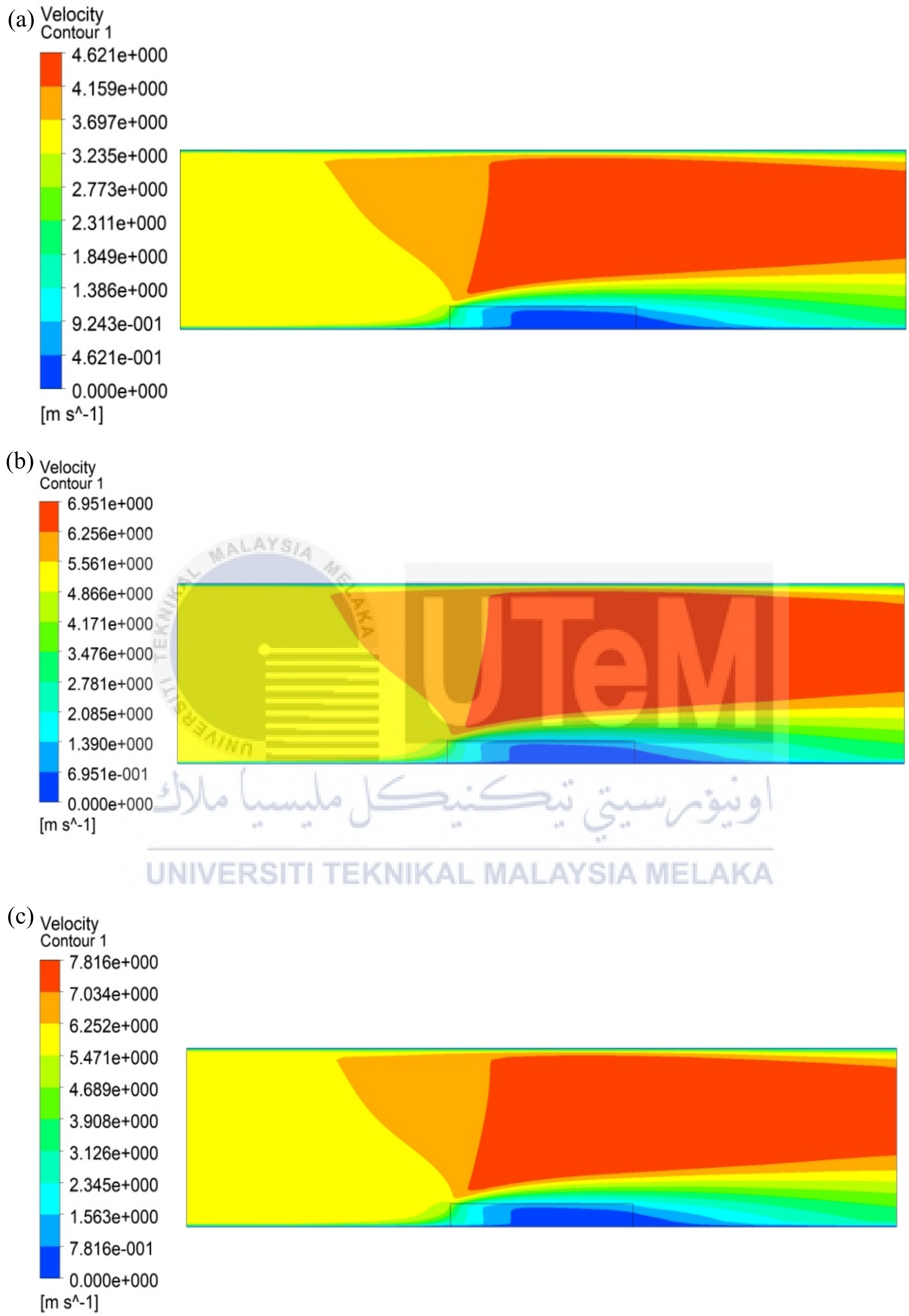

Figure 4.8: Velocity contour of 30 PPI with h/H = 0.13 at different velocities
(a) u_{inlet} = 3.9 m/s, (b) u_{inlet} = 5.5 m/s, and (c) u_{inlet} = 6.2 m/s

Based on **Figure 4.8**, 30 PPI porous medium with a height of 0.01m has a noticeable effect on the velocity distribution across the channel. The flow contour is in yellow colour (v = 6.25 m/s) at the entrance region until quarter (x = 0.07 m) of the channel. Then, it becomes orange (7.03 m/s) after a quarter of the channel. It becomes red as the air merged with the air outside of the boundary layer of the interface of the porous medium. From **Figure 4.8 (a), (b),** and **(c)**, before the entrance, the velocity contour is in light green before turning into green and then light blue showing a decrease in velocity as the flow enters the porous region. The ligaments restriction could be the reason for these changes. Once the airflow reaches half of the porous, it achieves its lowest velocity it in until the end of the porous medium.

(a)


(b)
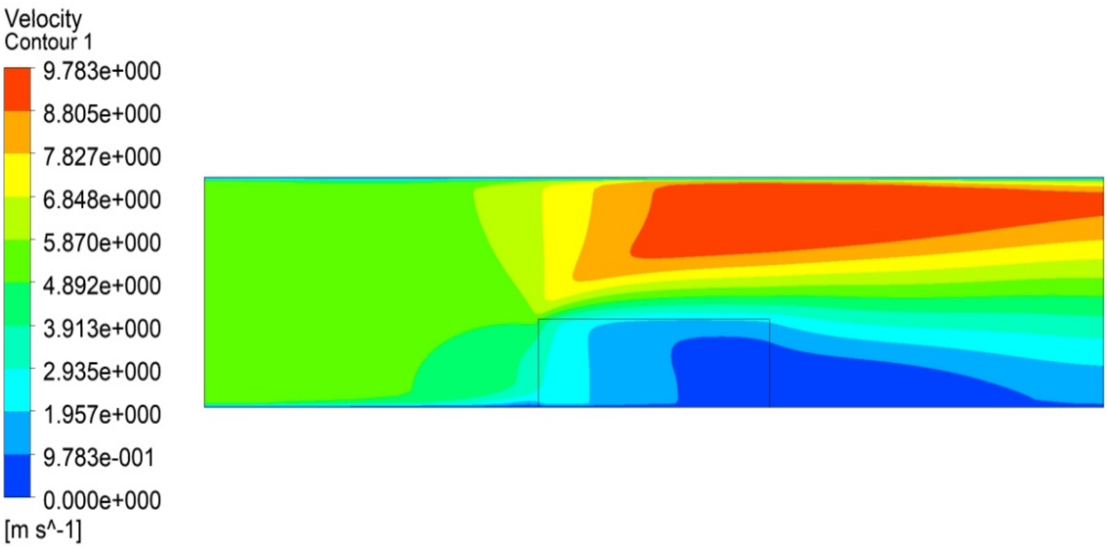

`

(c)

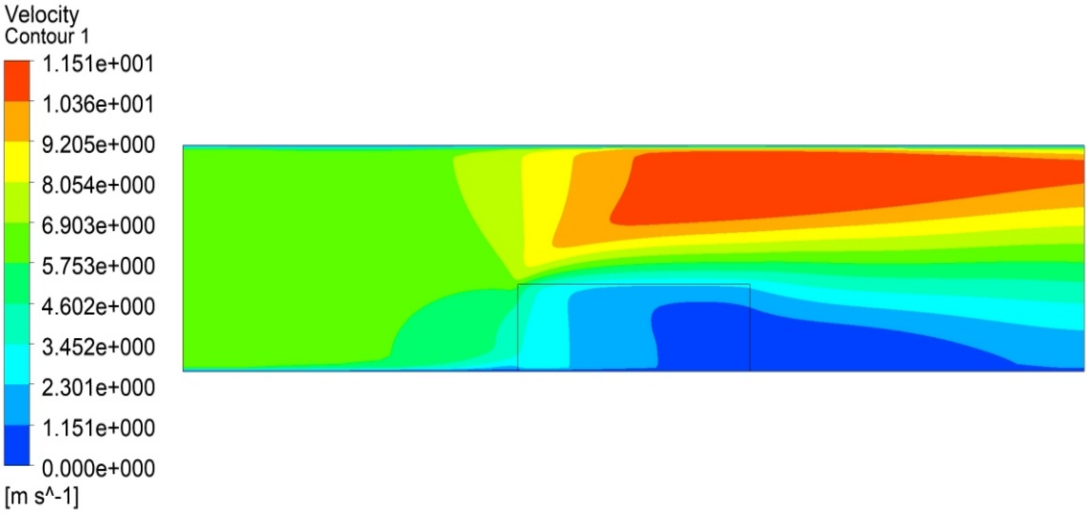

Figure 4.9: Velocity contour of 30 PPI with h/H = 0.39 at different velocities (a) u_{inlet} = 3.9 m/s, (b) u_{inlet} = 5.5 m/s, and (c) u_{inlet} = 6.2 m/s

The blockage ratio, h/H = 0.39 with 30 PPI porous medium proven to have a more significant impact on the velocity distribution across the channel as shown in **Figure 4.9**. For example in **Figure 4.9 (c)**, the velocity contour at the entrance region is in green (v = 6.91 m/s) until almost half (x = 0.11m) of the channel. There are colour transitions from light green (v = 8.05 m/s) to light blue (v = 2.31 m/s) at the entrance of the porous medium implying the reduction in velocity profile before it enters the porous medium. As the blockage ratio and pore density increases, the fluid enters the porous medium has higher resistance due to the inertial resistance parameter set. There is a boundary layer formed on the interface of the porous medium in this channel configuration. Then in the porous medium, light blue changes to dark blue which means the velocity profile in the porous medium is reducing to the lowest until the end of the porous medium.

`

4.2.5 Comparison between experimental and simulation data

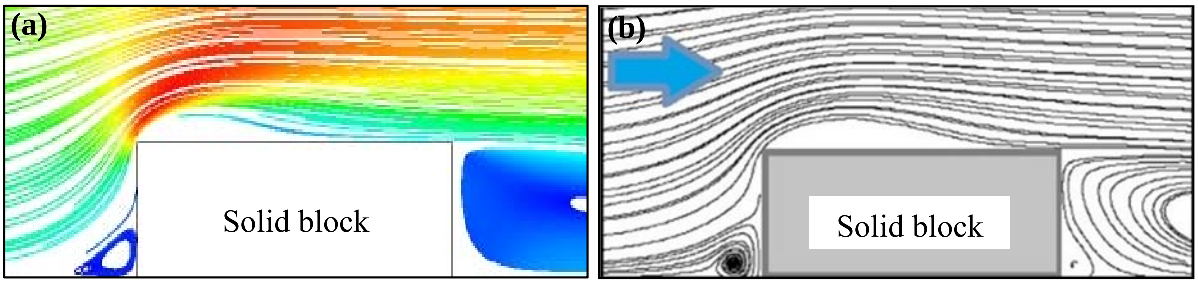

Figure 4.10: Streamline over a solid block with h/H = 0.39 at u_{inlet} = 6.2 m/s
(a) simulation and (b) experimental data [12]

Streamline across a channel partially filled with a solid block (blockage ratio (h/H) = 0.39) is shown in **Figure 4.10**. From both methods (experimental/simulation), there is a formation of the vortex at the front of the solid block. A large flow separation also formed at the back of the solid block in the downstream region. At the front region, near the block interface, vena-contract was formed. The fluid streamline cannot follow the abrupt changes of direction due to the existence of a solid block at the centre of the channel. The streamlines are unable to closely follow the sharp angles of the block. As the results from Figure 4.10 (a) and (b) are in agreement. It shows that the simulation and parameter settings used in this study are acceptable for further analysis with the porous medium. However, Ergun-Forcheimmer's equation is added to take into account the inertial and viscous effects for the porous medium.

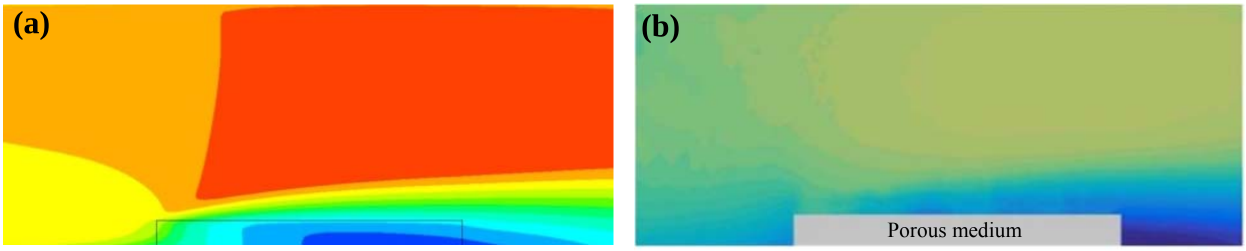

Figure 4.11: Velocity contours of 10 PPI with h/H = 0.13 at u_{inlet} = 6.2 m/s
(a) simulation and (b) experimental data [12]

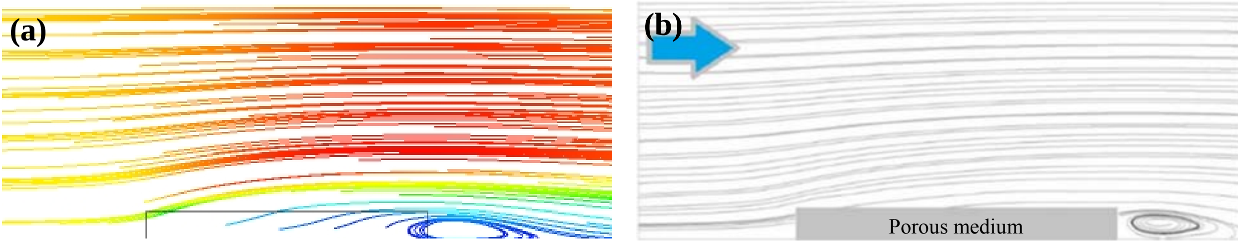

Figure 4.12: Streamline of 10 PPI with h/H = 0.13 at u_{inlet} = 6.2 m/s
(a) simulation and (b) experimental data [12]

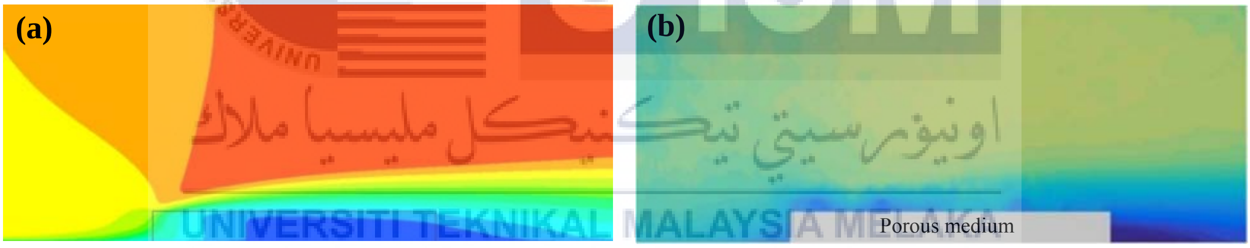

Figure 4.13: Velocity contours of 30 PPI with h/H = 0.13 at u_{inlet} = 6.2 m/s
(a) simulation and (b) experimental data [12]

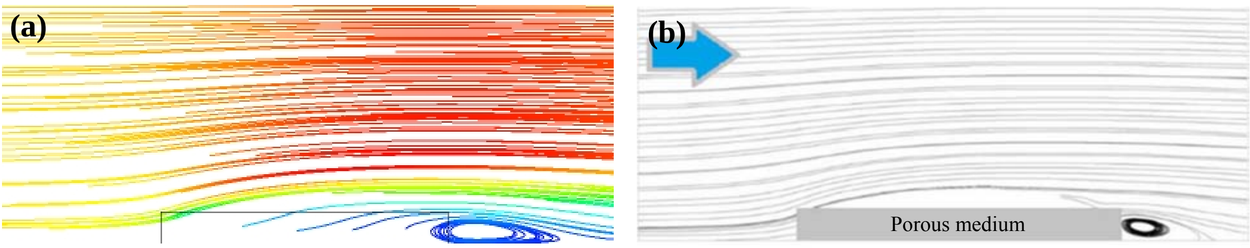

Figure 4.14: Streamlines of 30 PPI with h/H = 0.13 at u_{inlet} = 6.2 m/s
(a) simulation and (b) experimental data [12]

`

The lowest blockage ratio, h/H = 0.05 does not have a significant effect on the fluid flow in the channel. The streamlines from **Figure 4.12** and **4.14** are for the same blockage ratio, h/H = 0.13 but with different PPIs, which is 10 and 30 PPI. There is a recirculation zone exists at the back of the porous medium in the downstream region. The results are interesting, as the flow is expected to pass through the porous region. Due to the limitation of PIV, where the data was taken only in the non-porous region, the previous experimental study [1] [12] expected that the reason for this formation is due to the ligaments and surface roughness of the metal foam. The present simulation can explore further detail on fluid behaviour in the porous region.

From their experimental result as shown in **Figure 4.11 (b**) and **4.13 (b)**, there existed a recirculation zone at the back of 10 PPI and 30 PPI foam block. Meanwhile, the simulation results in **Figure 4.11 (a**) and **4.13 (a**), show the 30 PPI recirculation zone is slightly larger compared to 10 PPIs. This possibly happened because of a lower porosity in the 30 PPI block that increases the inertial effects. Hence, more airflow could not pass the 30 PPI foam block and resulting in a more concentrated recirculation zone to appear at the back of the foam block.

The fluid flow behaviour can be observed better by referring to streamline simulation results, where **Figure 4.12 (a)** and **4.14 (a)** show the recirculation zone in 10 PPI with lower resistance is less concentrated compared to 30 PPI foam. Naturally, the air in the porous region would tend to search a way out or a lower resistance path. However, one must also take note that, the inertial effects in the simulation could be slightly different as compared to the experiments.

`

This is because to simulate the flow behaviours in the partially filled channel, the inertial effects were calculated using on only two parameters: (1) pore diameter and (2) porosity as shown in **Table 3.2**. This might contribute to a slightly different result between these two approaches since the amount of restriction is undefined based on the block results. Nevertheless, the results of simulation and experiment are in agreement that a recirculation zone existed at the back of foam block at u_{inlet} = 6.2 m/s for both 10 and 30 PPI foam with h/H = 0.13. The recirculation zone happened from the detachment of fluid flow when entering the original passage (channel) size and changed into the form of eddy and vortices at further down of the channel. However, there is no flow disturbance in the regions far away from the partially filled section.

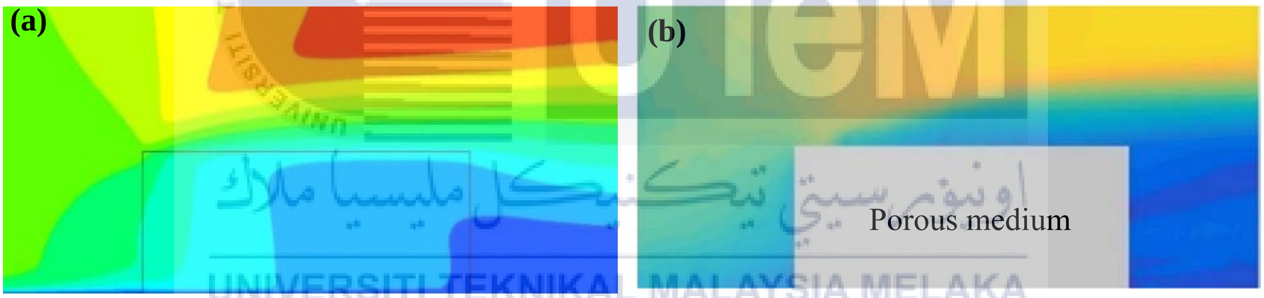

Figure 4.15: Velocity contours of 10 PPI with h/H = 0.39 at u_{inlet} = 6.2 m/s
(a) simulation and (b) experimental data [12]

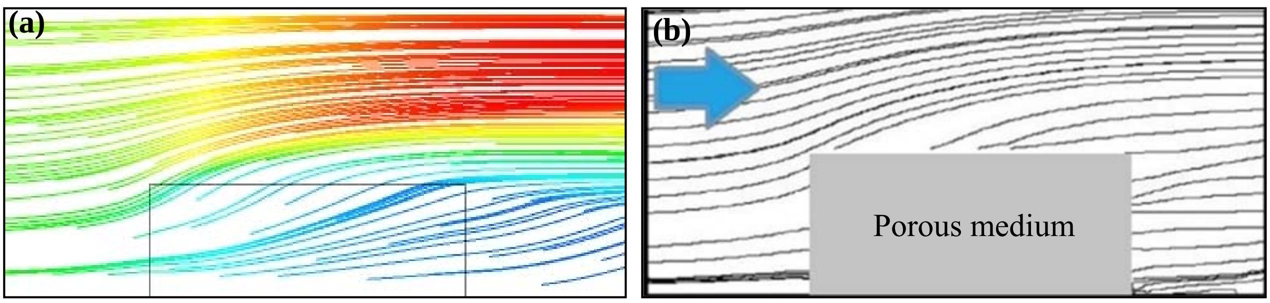

Figure 4.16: Streamline of 10 PPI with h/H = 0.39 at u_{inlet} = 6.2 m/s
(a) simulation and (b) experimental data [12]

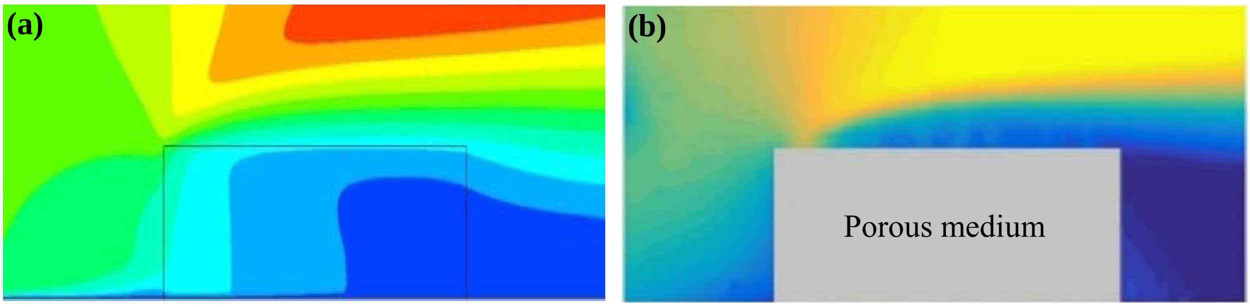

Figure 4.17: Velocity contours of 30 PPI with h/H = 0.39 at u_{inlet} = 6.2 m/s
(a) simulation and (b) experimental data [12]

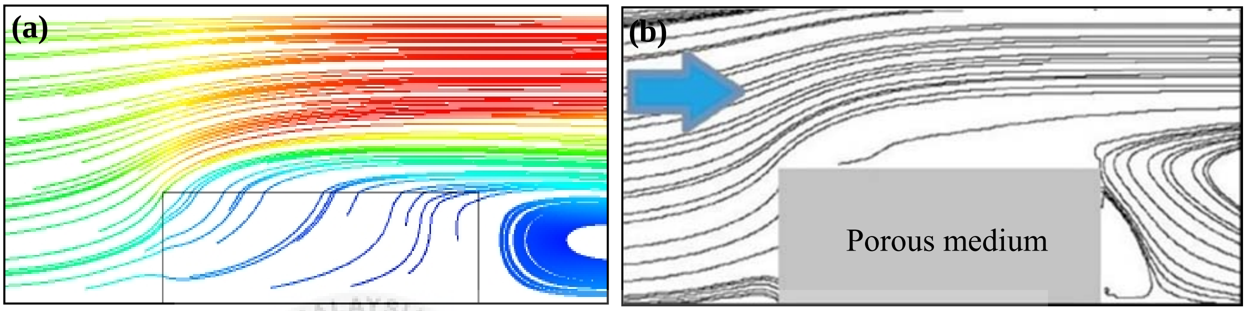

Figure 4.18: Streamline of 30 PPI with h/H = 0.39 at u_{inlet} = 6.2 m/s
(a) simulation and (b) experimental data [12]

For thicker foam h/H=0.39, the recirculation zone is formed at the back of the foam in the downstream region the same as for the thinner foam, h/H = 0.13. Note that, for the experimental data, the inertial resistance could be contributed by the foam thickness or the larger surface area of the ligaments but in the simulation, the inertial resistance is calculated according to the pore densities as 5, 10 and 30 PPI foam with the porosity of 0.92, 0.91 and 0.94 respectively. For 10 PPI, the fluid enters the porous region and flows until the end of the block into the downstream region at lower velocity as compared to non-porous region unlike the flow experiences resistance caused by the complex ligament construction. Unlike the 30 PPI foam, no recirculation zone at the back of 10 PPI block. However, there exists a recirculation zone at the downstream region of 30 PPI when the blockage ratio is significant, for example, h/H =0.39 at u_{inlet} = 3.9 m/s and 6.2 m/s as shown in the **Figure 4.15** and **4.17**. The streamlines in **Figure 4.16** and **4.18** are for the highest blockage ratio, h/H = 0.39 with velocities, u_{inlet} = 3.9 m/s and 6.2 m/s.

4.3 The simulation results of velocity profiles

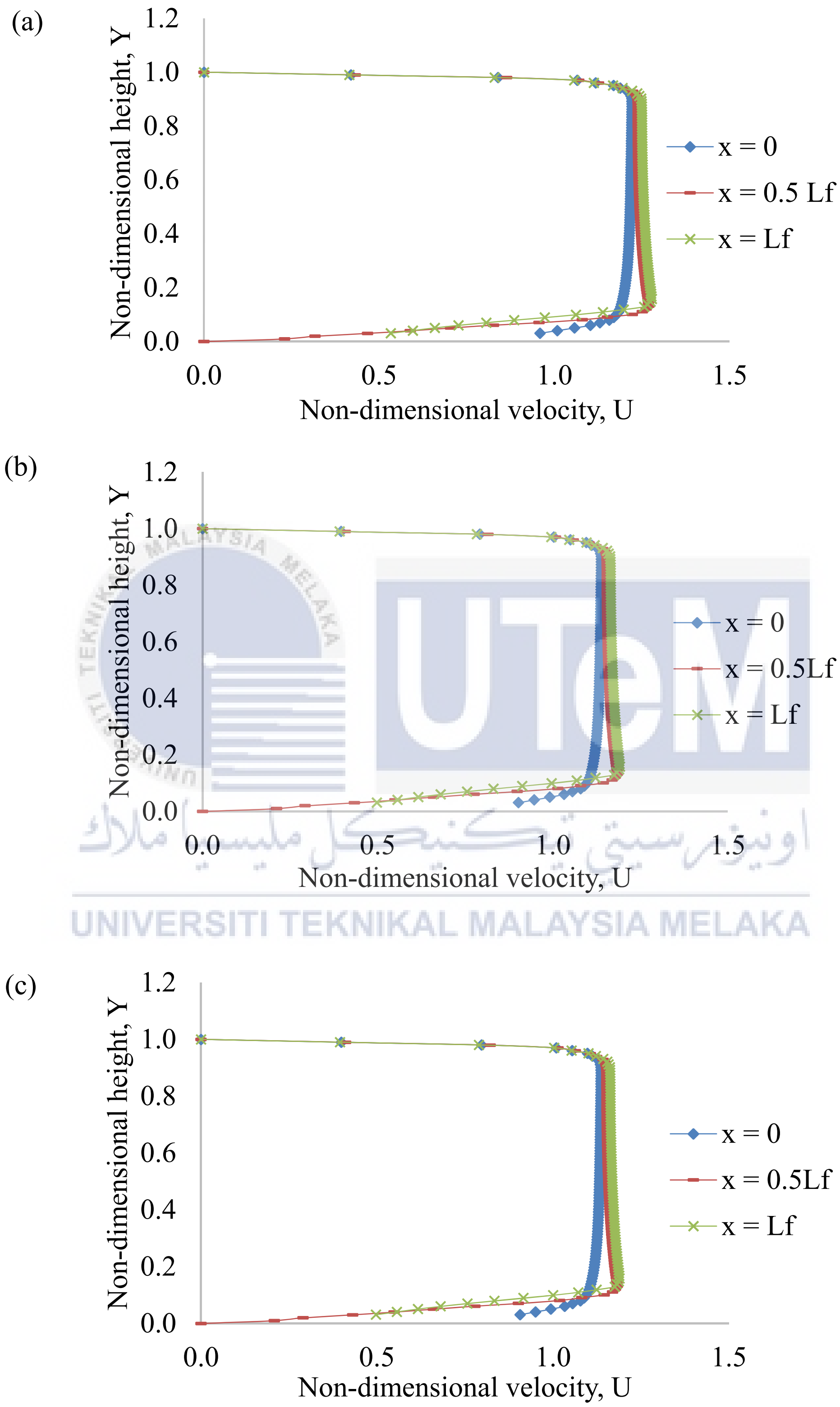

Figure 4.19: Velocity profile of 5 PPI with h/H = 0.03 at different velocities (a) u_{inlet} = 6.5 m/s, (b) u_{inlet} = 9.5 m/s, and (c) u_{inlet} = 12.5 m/s

`

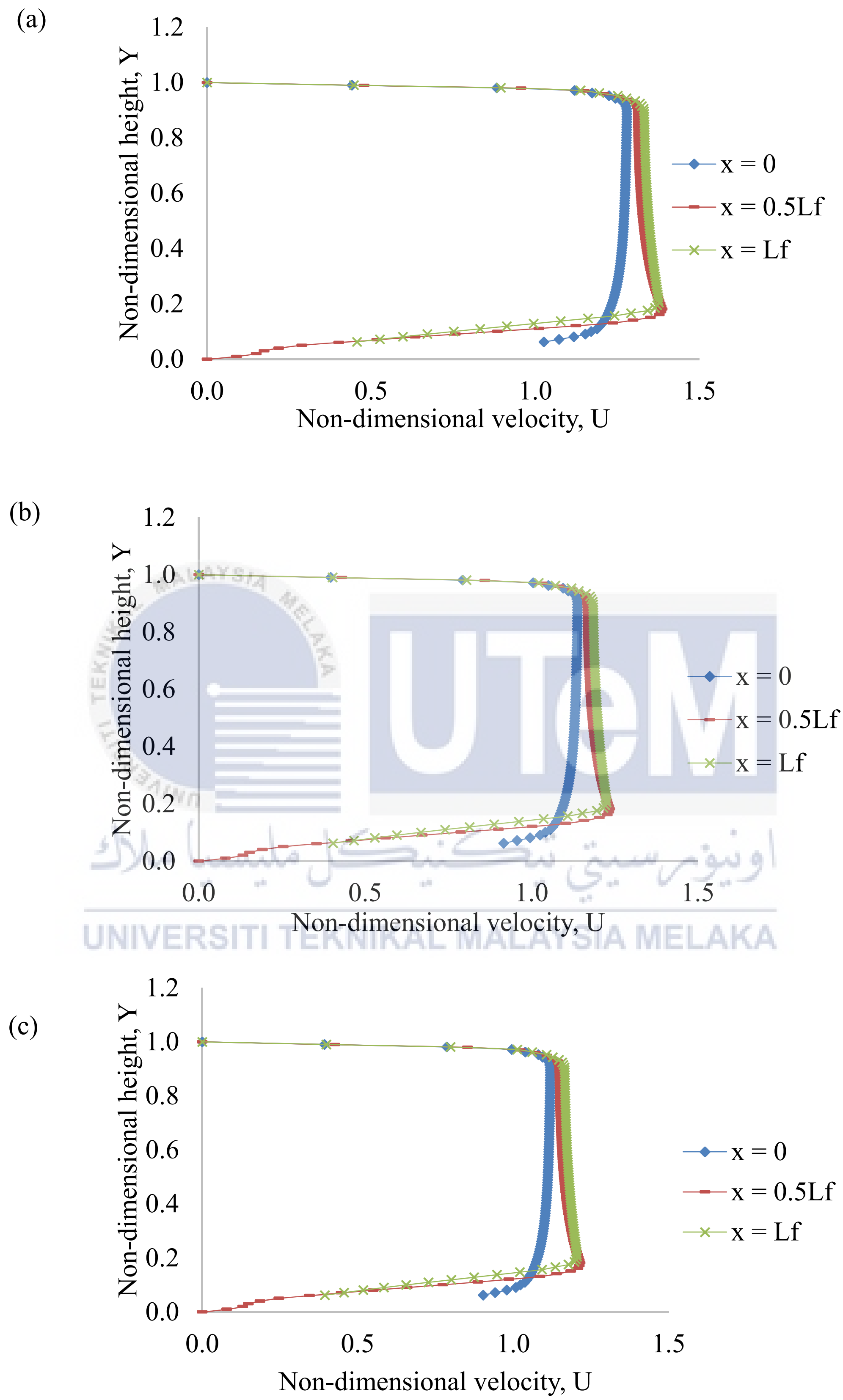

Figure 4.20: Velocity profile of 5 PPI with h/H = 0.06 at different velocities (a) u_{inlet} = 6.5 m/s, (b) u_{inlet} = 9.5 m/s, and (c) u_{inlet} = 12.5 m/s

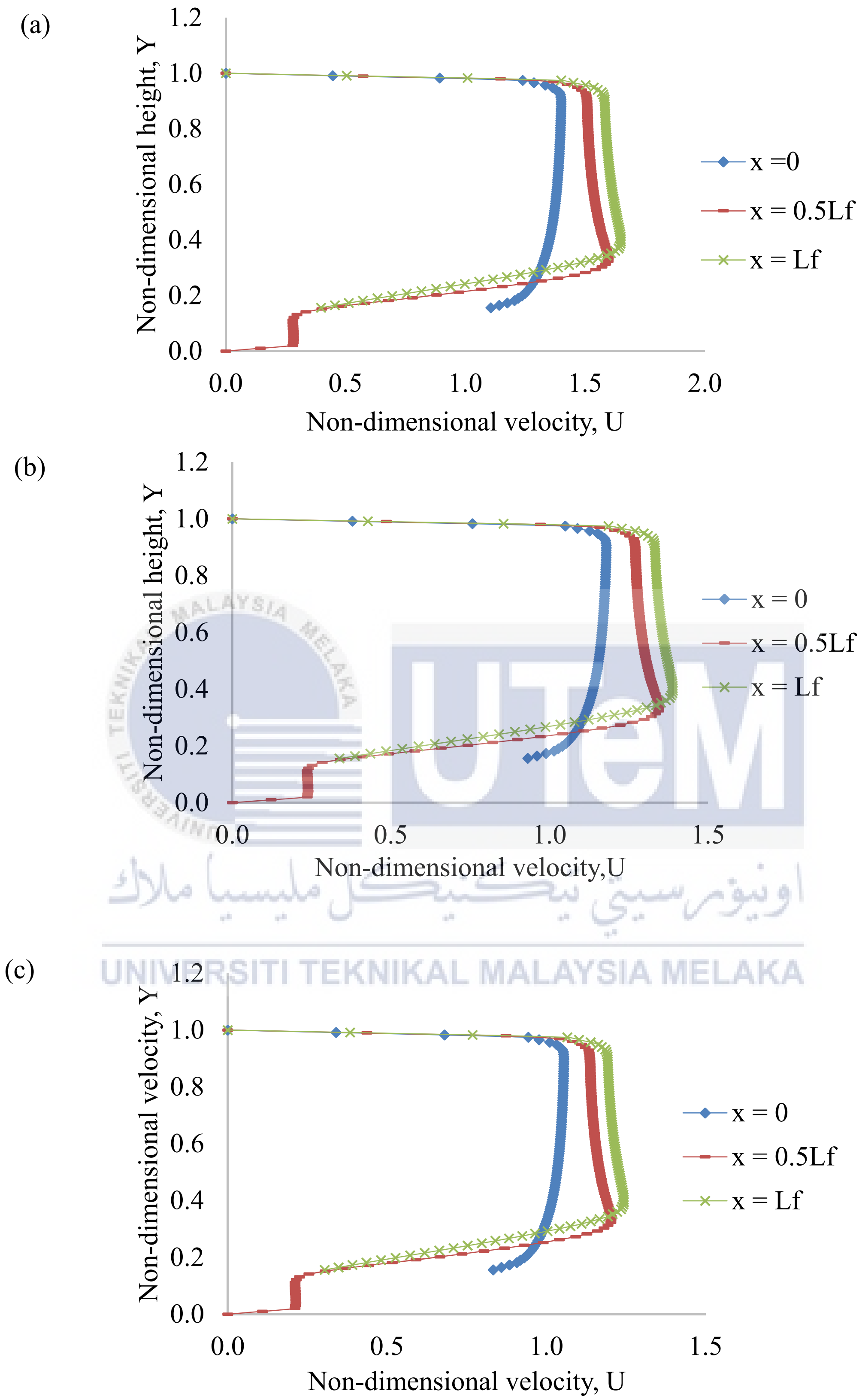

Figure 4.21: Velocity profile of 5 PPI with h/H = 0.16 at different velocities
(a) u_{inlet} = 6.5 m/s, (b) u_{inlet} = 9.5 m/s, and (c) u_{inlet} = 12.5 m/s

`

Figure 4.19, 4.20 and **4.21** represent the velocity profiles of 5 PPI which have different blockage ratios, h/H = 0.03, 0.06 and 0.16. The velocities used for the channels are u_{inlet} = 6.5, 9.5 and 12.5 m/s respectively. The velocity profiles are measured in three different locations of porous medium in the channel as shown in **Figure 3.11,** (1) x = 0, (2) x = 0.5Lf, and (3) x = Lf. Hundred sample data were collected to plot the graph so that the result will be more accurate. A large amount of air enters the 5 PPI foam since it has larger pores as compared to 10 and 30 PPI foams. For 5 PPI foam when h/H = 0.16, which causes the velocity of the freestream region to be more stable when the flow passes across the channel. In **Figure 4.21** it is noticeable that the velocity reduces in the porous medium (x = 0.5Lf) because there is a sudden drop at U =0.25 compared to Figure **4.19** and **4.20**.

(a)

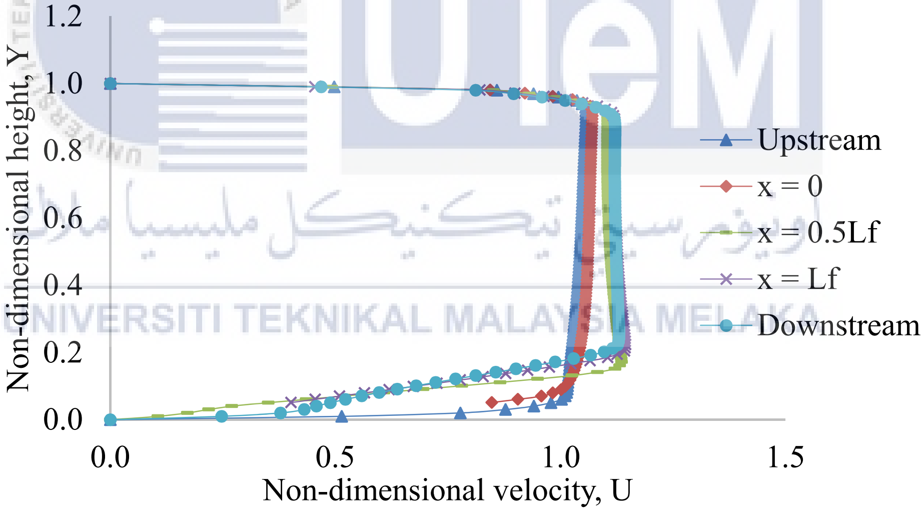

(b)

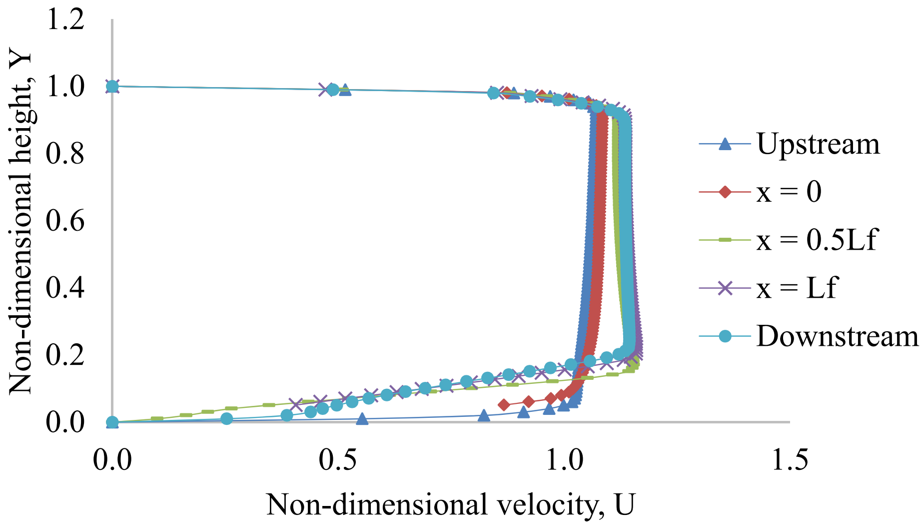

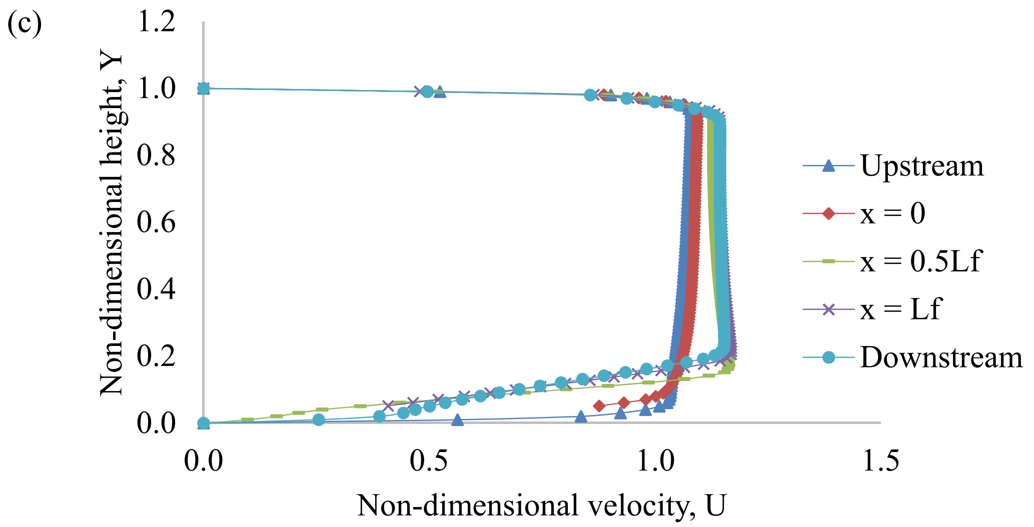

Figure 4.22: Velocity profile of 10 PPI with h/H = 0.05 at different velocities (a) u_{inlet} = 3.9 m/s, (b) u_{inlet} = 5.5 m/s, and (c) u_{inlet} = 6.2 m/s

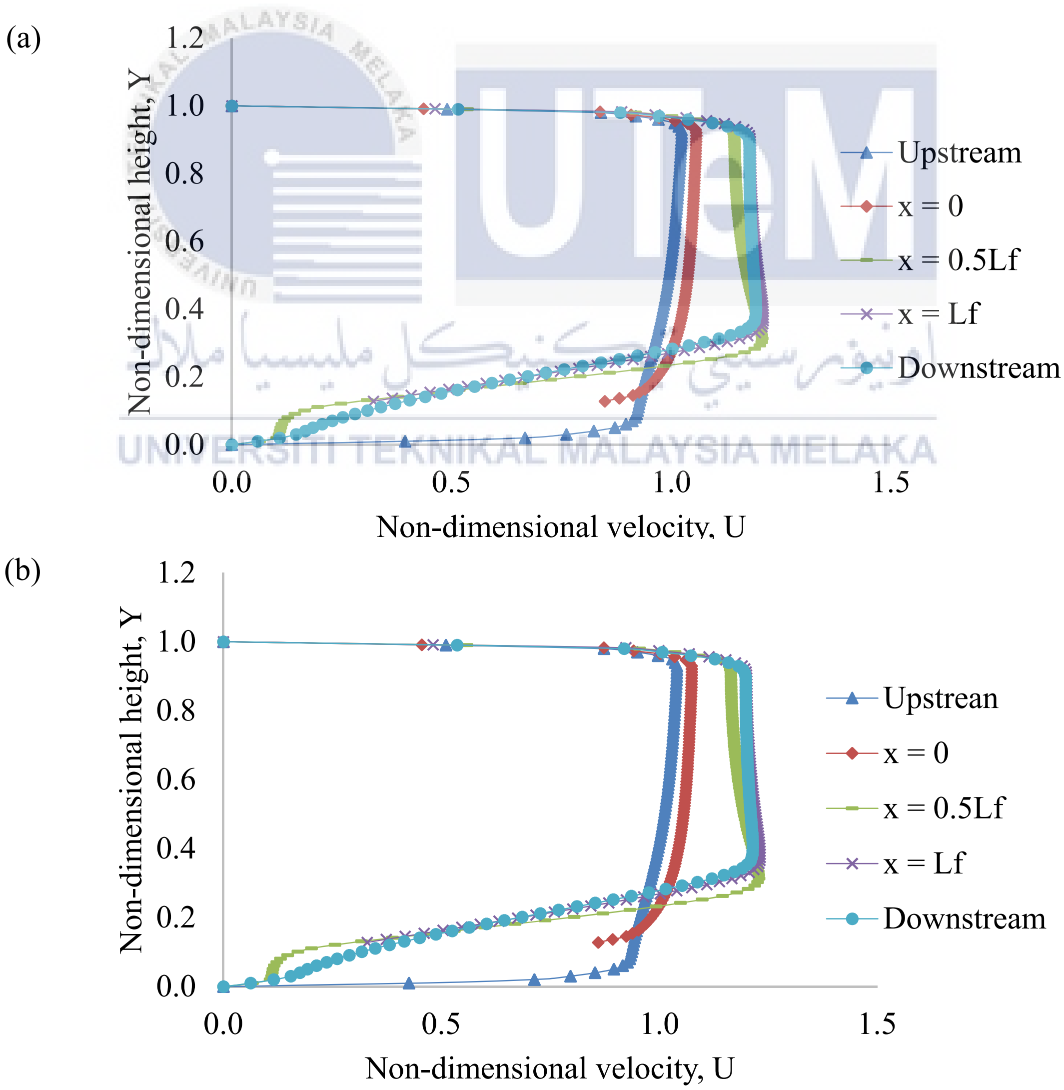

(c)

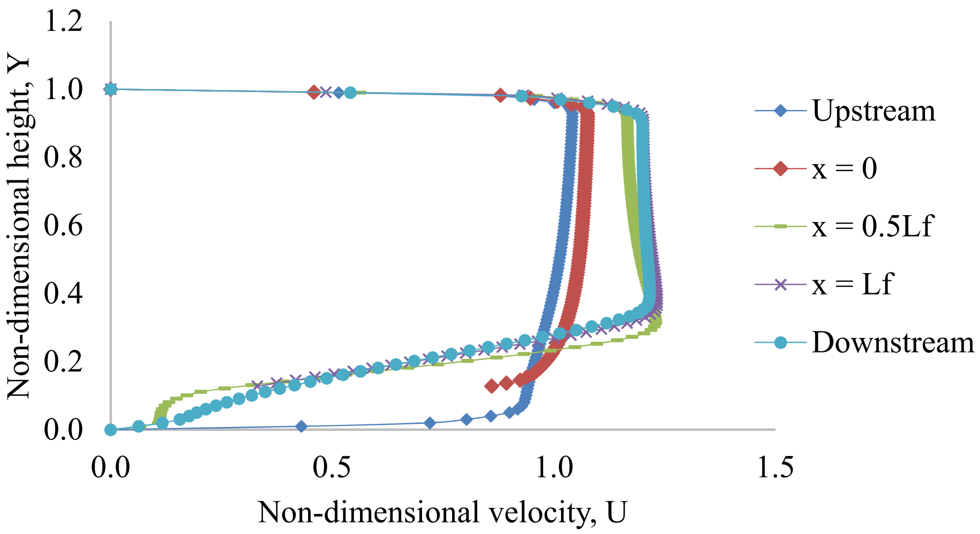

Figure 4.23: Velocity profile of 10 PPI with h/H = 0.13 at different velocities
(a) u_{inlet} = 3.9 m/s, (b) u_{inlet} = 5.5 m/s, and (c) u_{inlet} = 6.2 m/s

(a)

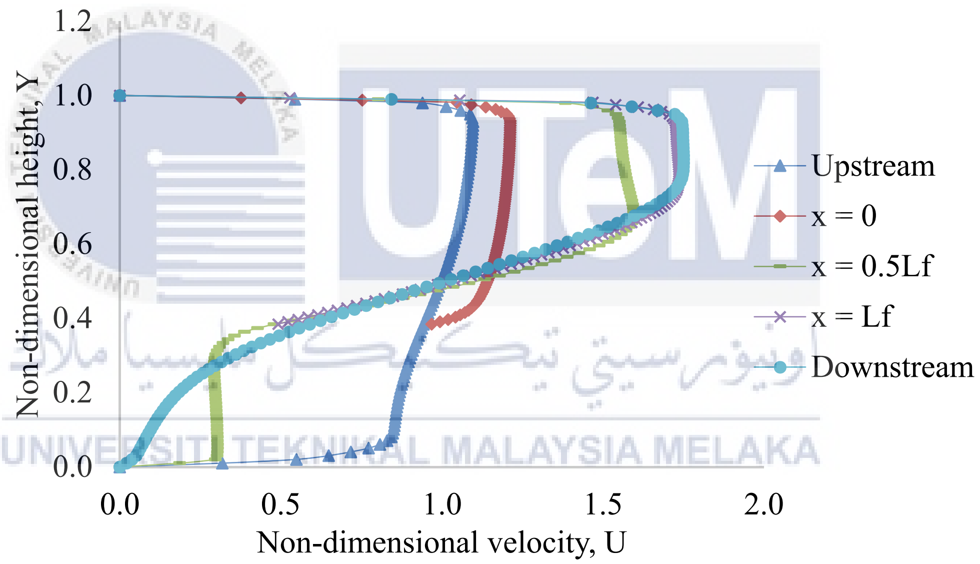

(b)

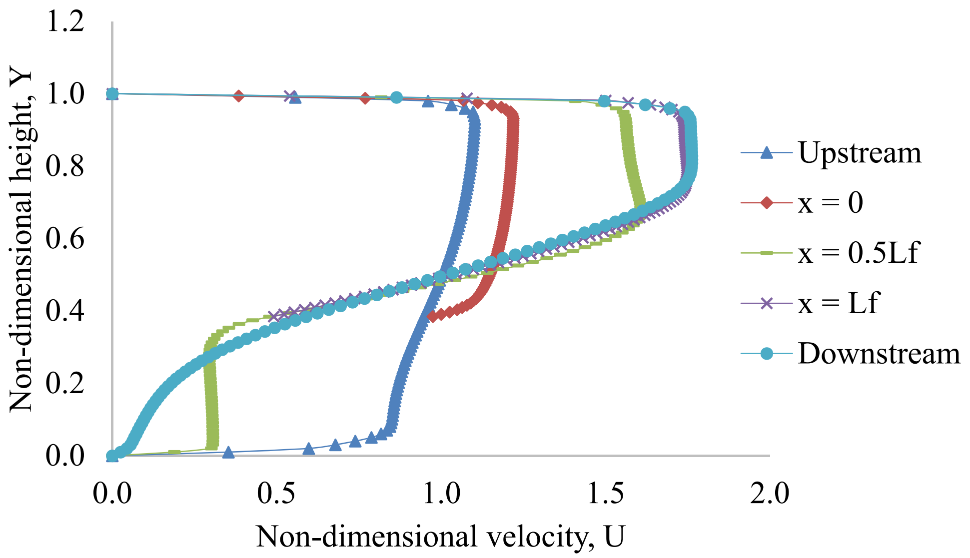

(c)

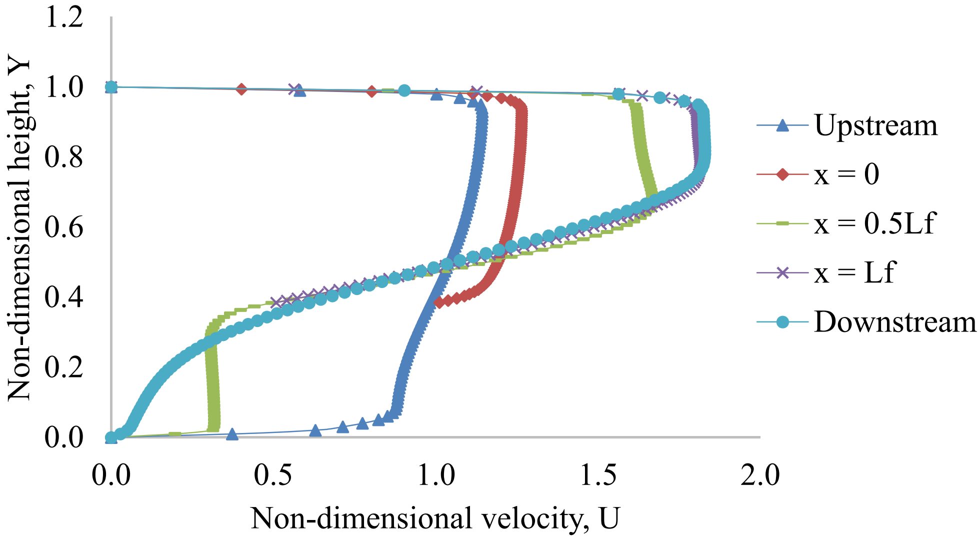

Figure 4.24: Velocity profile of 10 PPI with h/H = 0.39 at different velocities (a) u_{inlet} = 3.9 m/s, (b) u_{inlet} = 5.5 m/s, and (c) u_{inlet} = 6.2 m/s

(a)

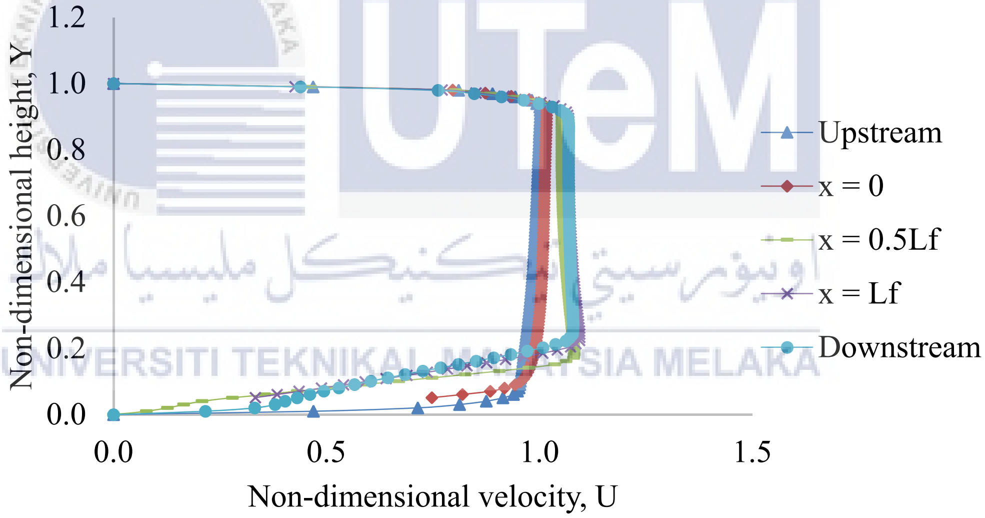

(b)

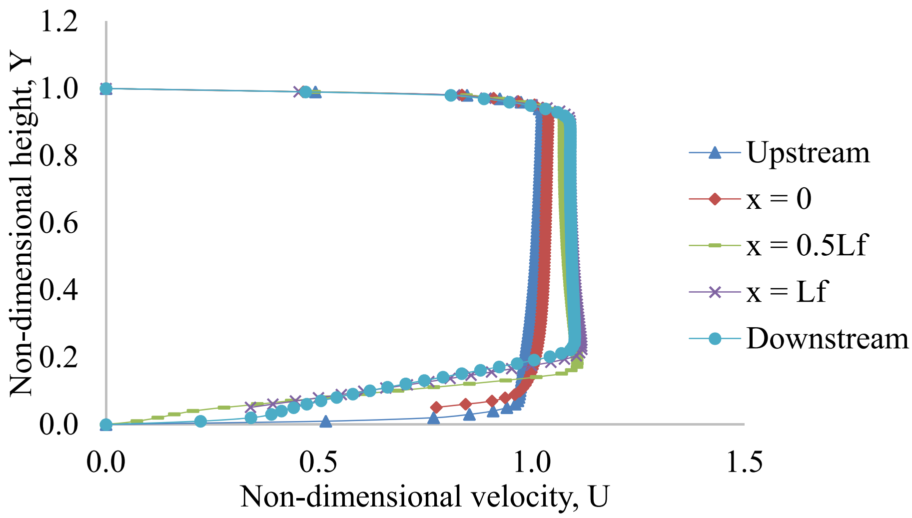

(c)

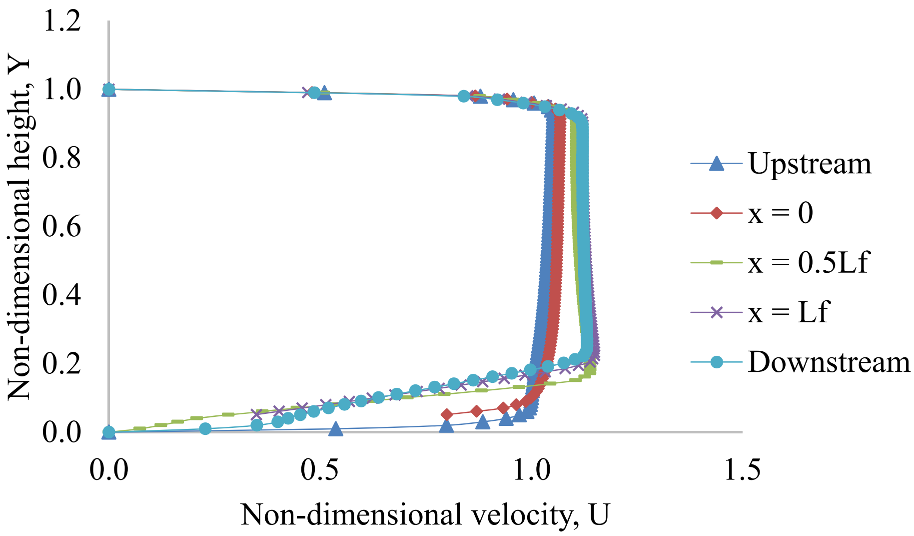

Figure 4.25: Velocity profile of 30 PPI with h/H = 0.05 at different velocities (a) u_{inlet} = 3.9 m/s, (b) u_{inlet} = 5.5 m/s, and (c) u_{inlet} = 6.2 m/s

(a)

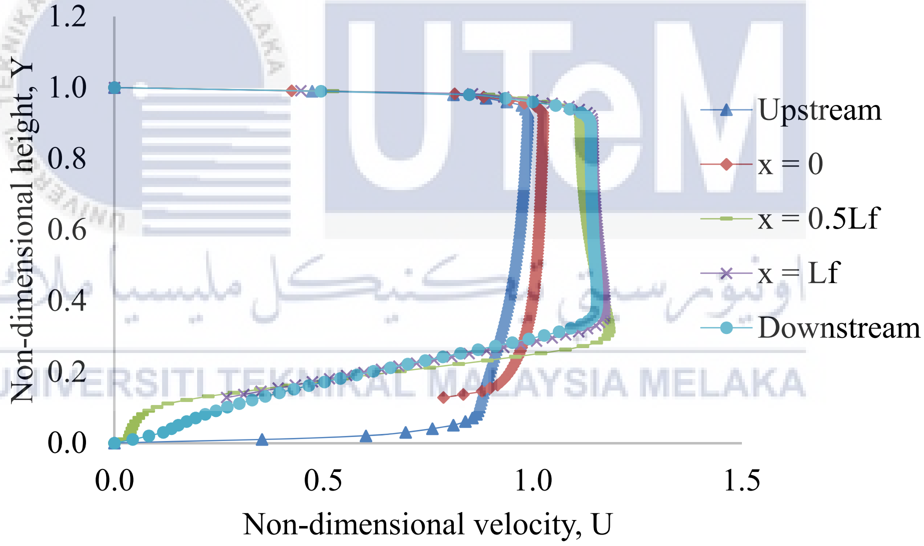

(b)

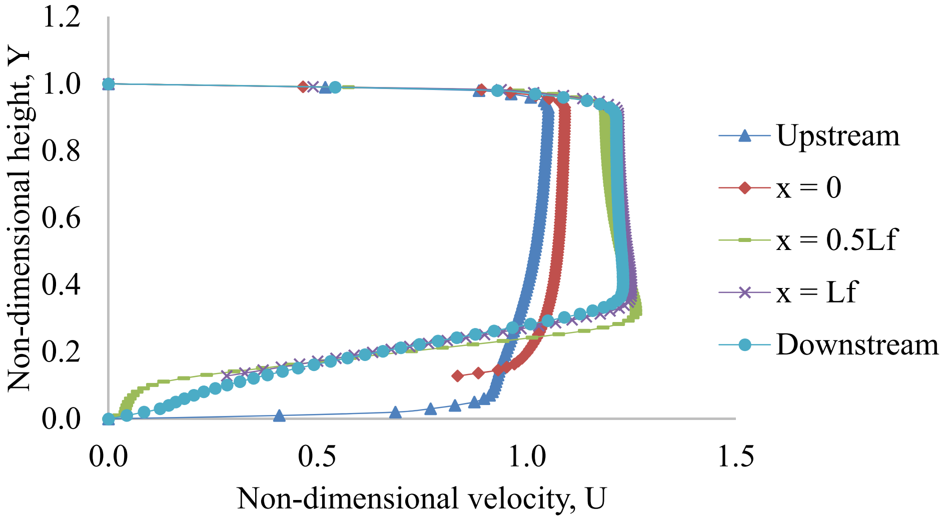

(c)

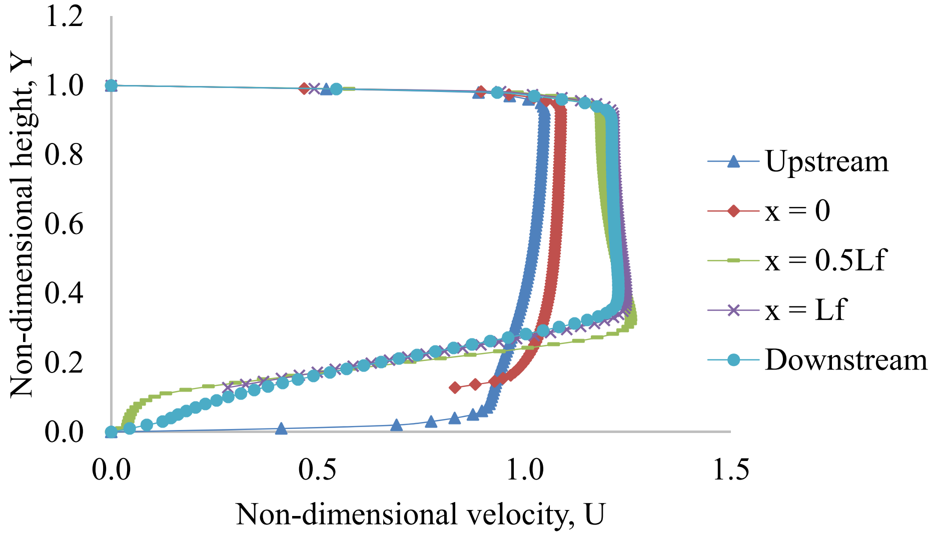

Figure 4.26: Velocity profile of 30 PPI with h/H = 0.13 at different velocities (a) u_{inlet} = 3.9 m/s, (b) u_{inlet} = 5.5 m/s, and (c) u_{inlet} = 6.2 m/s

(a)

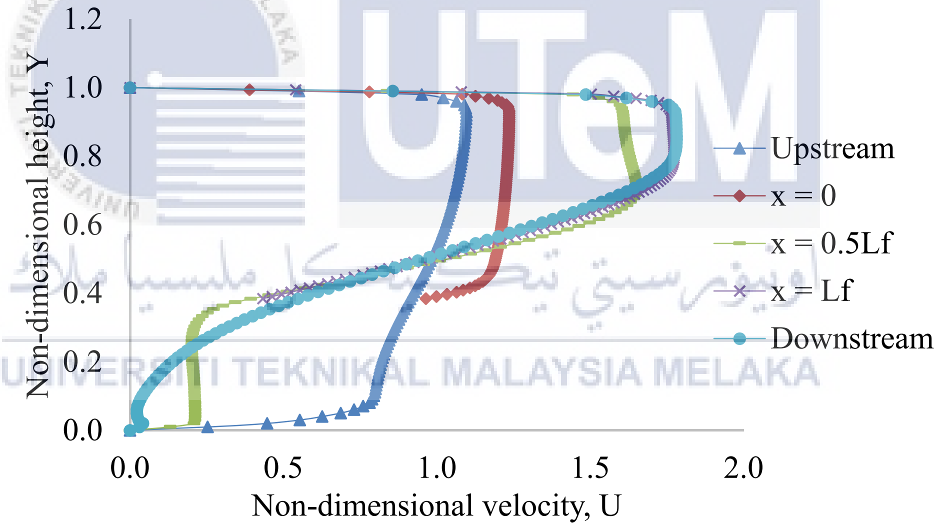

(b)

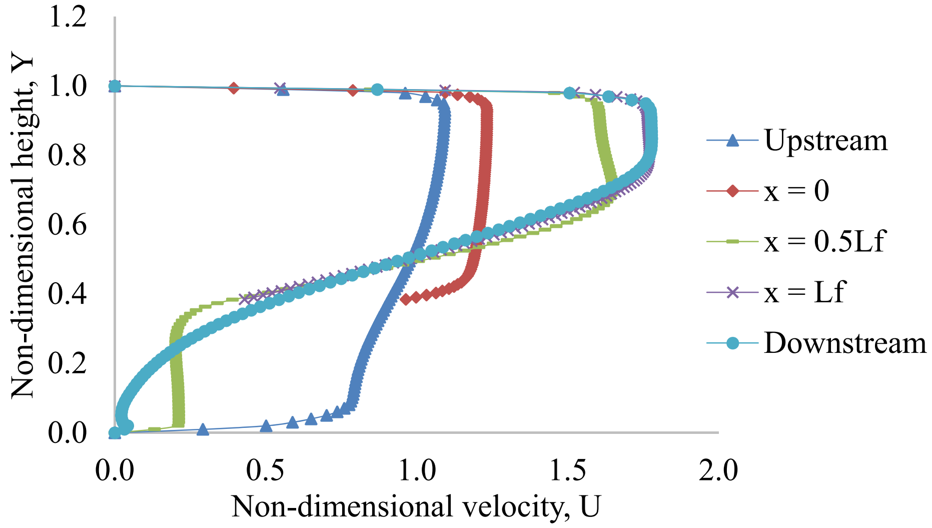

`

(c)

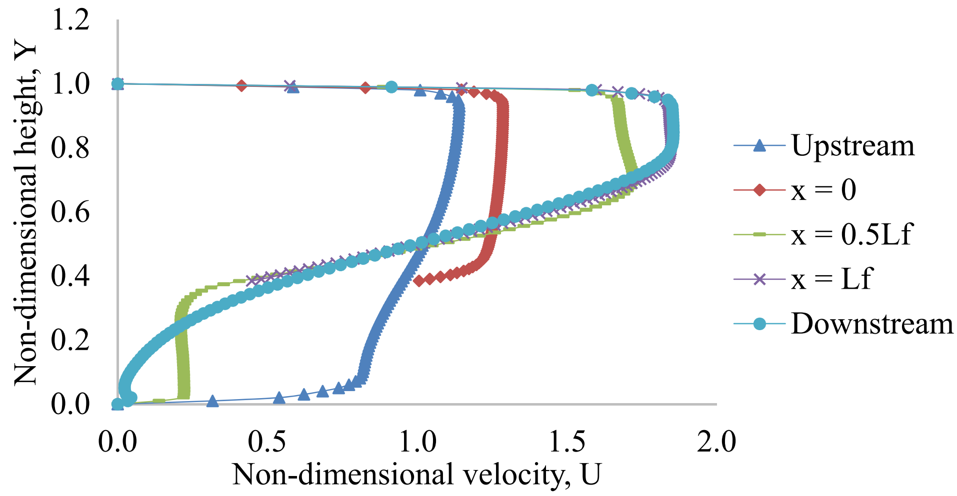

Figure 4.27: Velocity profile of 30 PPI with h/H = 0.39 at different velocities (a) u_{inlet} = 3.9 m/s, (b) u_{inlet} = 5.5 m/s, and (c) u_{inlet} = 6.2 m/s

Figure 4.22 - 4.27 represents the velocity profiles of 10 and 30 PPI which have different blockage ratios, h/H = 0.05, 0.13 and 0.39. The velocity used for the channels is 3.9, 5.5 and 6.2 m/s respectively. The velocity profiles is measured at 5 different locations in the channel as shown in **Figure 3.12**, (1) Upstream, (2) x = 0, (3) x = 0.5Lf, (4) x = Lf and (5) Downstream. Hundred sample data are collected to plot the graph so that the results are more accurate. The highest velocity is mostly obtained at the freestream region except for the blockage ratio of 0.39 and 0.13 with a speed of 3.9 m/s and 5.5 m/s.

The blockage ratio, h/H = 0.05 shows no significant difference in the velocity inside the porous medium. A significant change with the presence of a porous medium can be noticed only with blockage ratio, h/H =0.13. In the blockage ratio, h/H = 0.13 and 0.39, there is also a formation of recirculation zone behind the porous medium in the downstream region. The recirculation zone represents the low – velocity area in the channel.

`

The fluid flow velocity is higher at the free stream region compared to the upstream region, but it changes with an increase in blockage ratio, h/H. The smaller the height of the free-stream region, example; h/H = 0.39, the higher the velocity of the fluid flow in the free-stream region. The porous medium of 30 PPI with the highest blockage ratio, h/H = 0.39 has a larger flow separation at the back of the foam compared to other configurations. The freestream velocities of 10 PPI are lower compared to the 30 PPI cases. Complex and smaller pores of 30 PPI metal foam causes an increase in fluid flow resistance [1]. This makes the air move away and avoid the higher PPI foam.

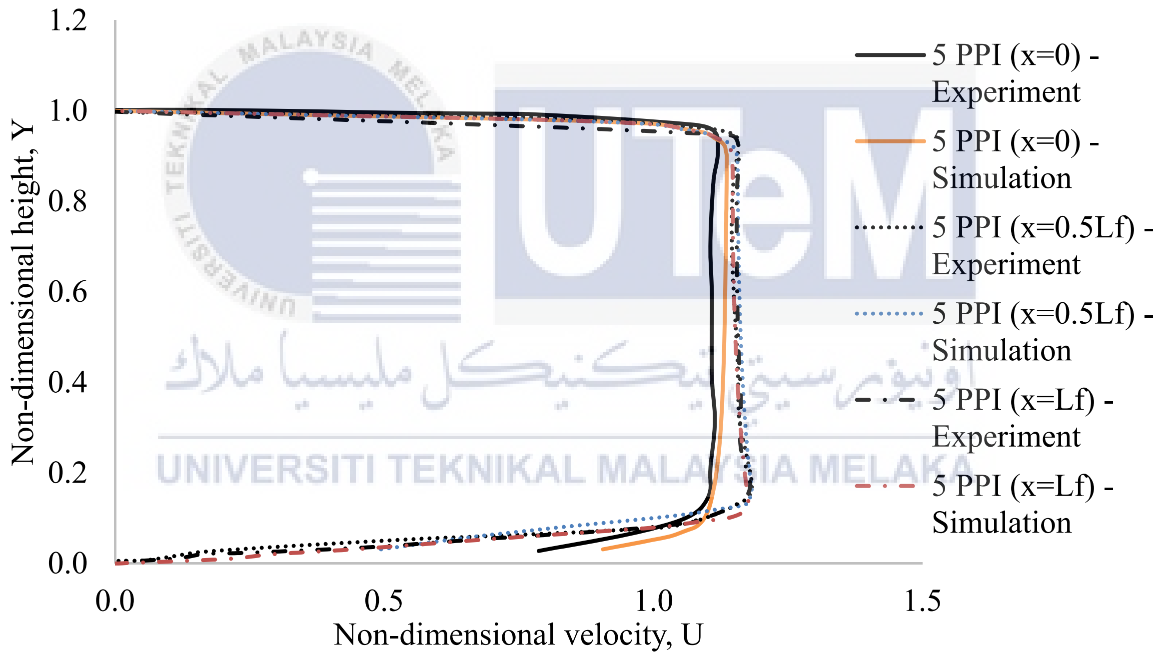

Figure 4.28: Experimental [1] and simulation velocity profile comparison between 5 PPI of h/H = 0.03 at u_{inlet} = 12.5 m/s

`

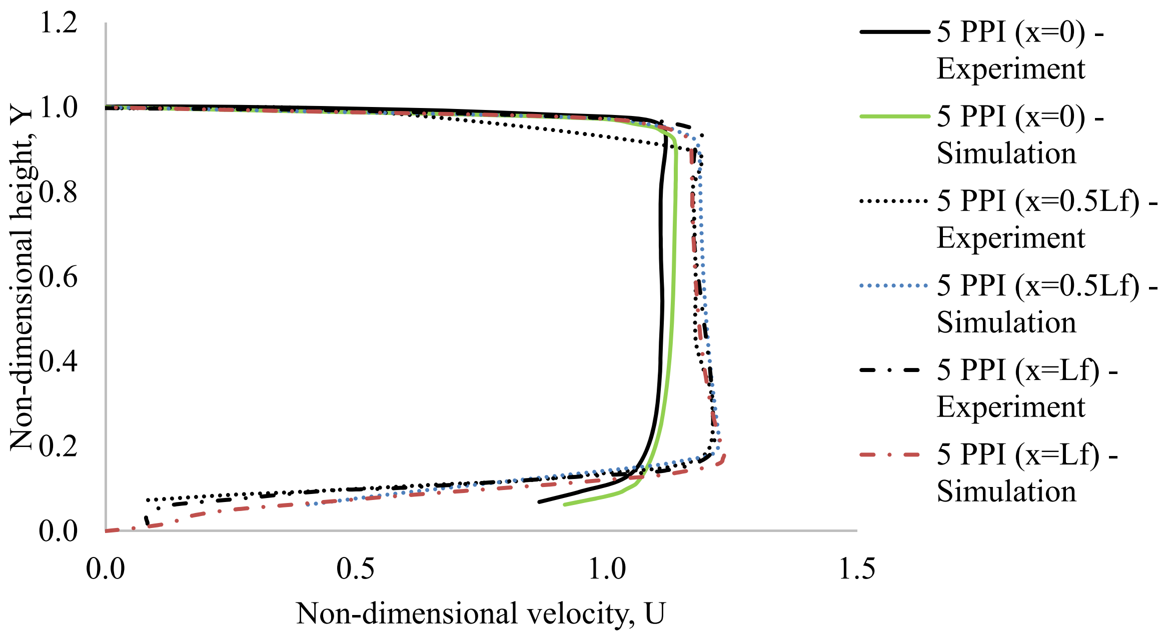

Figure 4.29: Experimental [1] and simulation velocity profile comparison between 5 PPI of h/H = 0.06 at u_{inlet} = 12.5 m/s

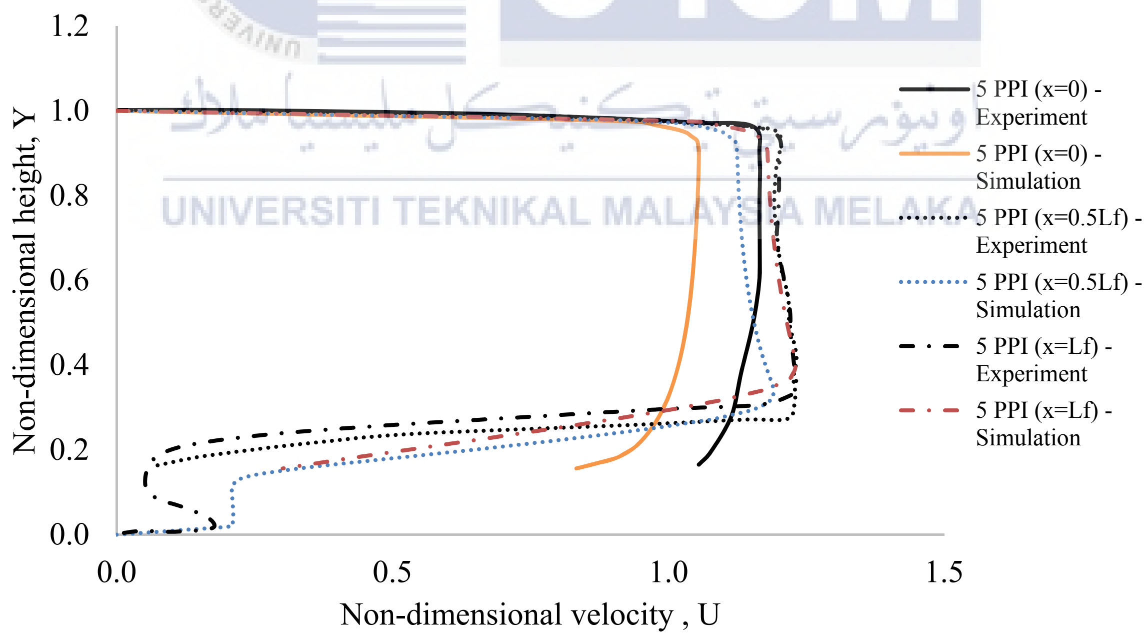

Figure 4.30: Experimental [1] and simulation velocity profile comparison between 5 PPI of h/H = 0.16 at u_{inlet} = 12.5 m/s

`

Figure 4.28, 4.29 and **4.30** represents the comparison of velocity profiles between simulation data of experimental data of 5PPI foam. The comparisons is only for the highest velocity, at u_{inlet} = 12.5 m/s for each blockage ratio, h/H = 0.05, 0.13, and 0.16. **Figure 4.31** shows that the presence of a porous medium does not affect the velocity in the channel. These data are chosen as the inertial and viscous effects in a porous medium are mainly crucial at the highest velocity [1]. In **Figure 4.28** and **4.29**, the velocity profile graph is very identical to the experimental data for all three locations (x=0, x=0.5Lf and x = Lf) observed. Other than that, for **Figure 4.30** the free stream region have a slight difference but for the results obtained are in good agreement with experimental data.

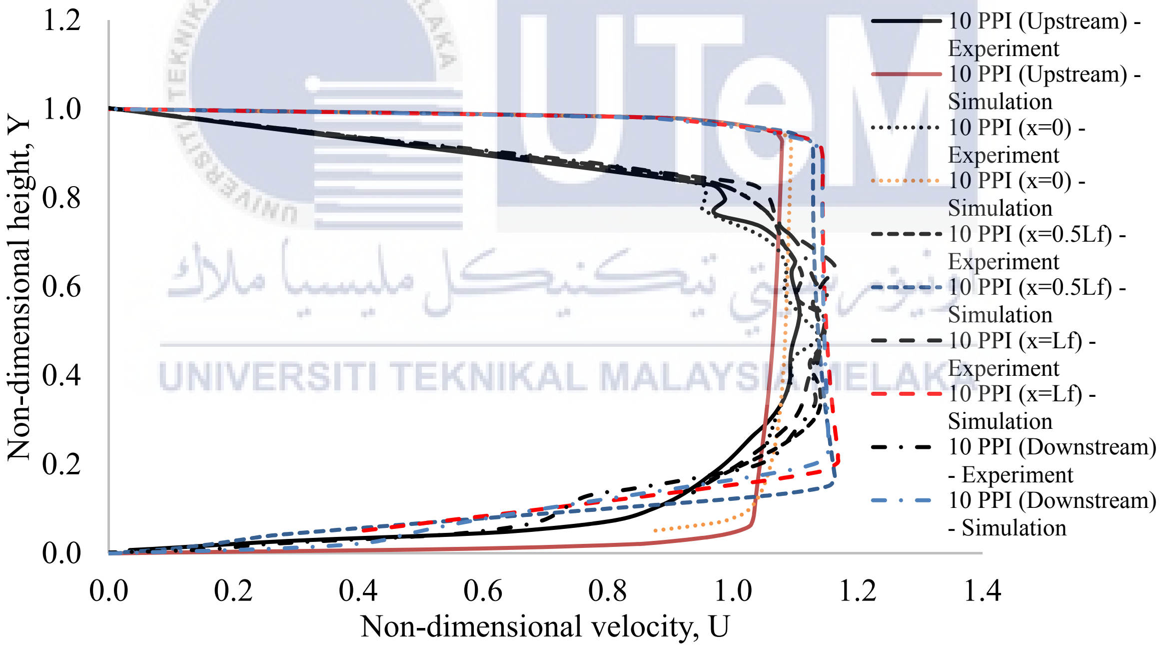

Figure 4.31: Experimental [1] and simulation velocity profile comparison between 10 PPI of h/H = 0.05 at u_{inlet} = 6.2 m/s

`

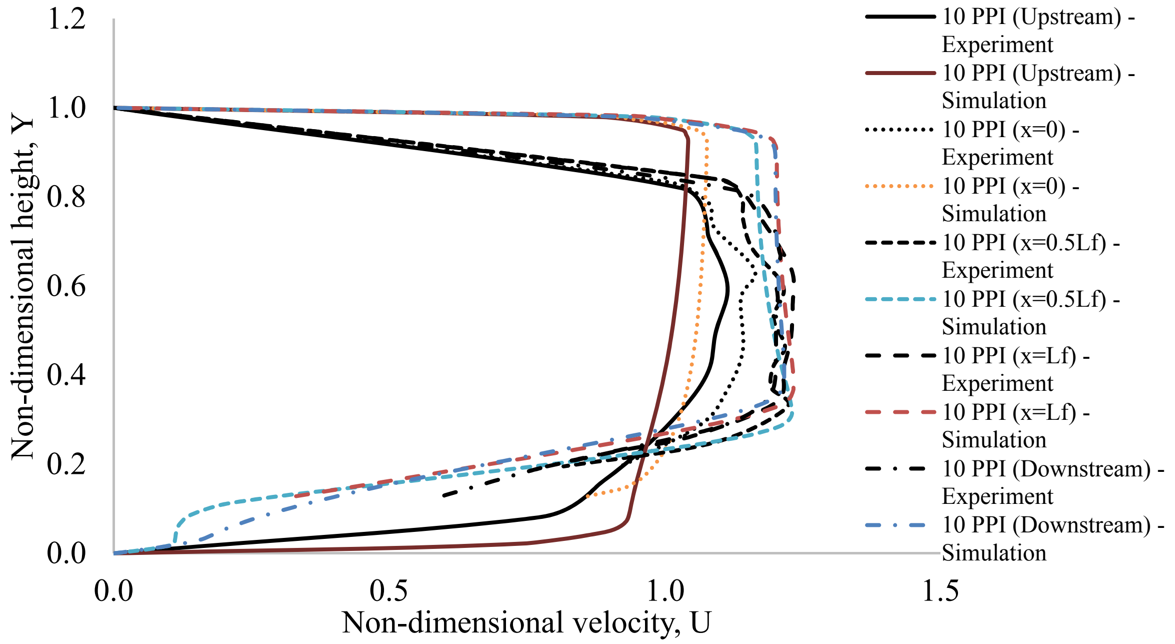

Figure 4.32: Experimental [1] and simulation velocity profile comparison between 10 PPI of h/H = 0.13 at u_{inlet} = 6.2 m/s

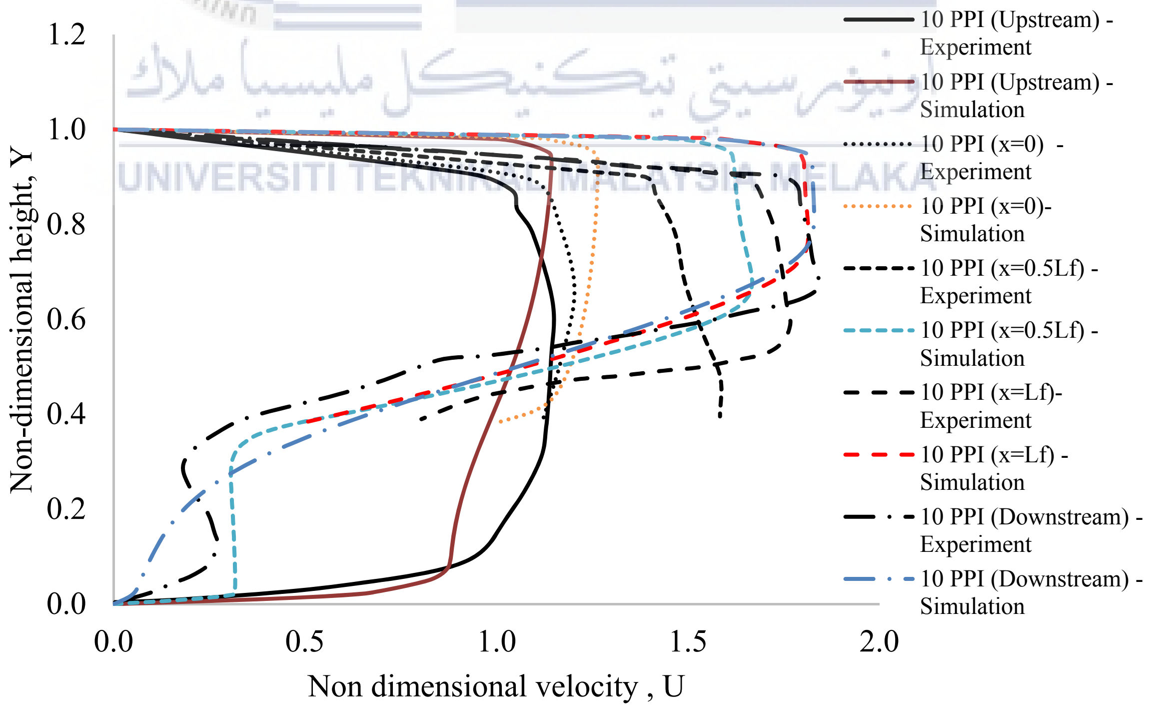

Figure 4.33: Experimental [1] and simulation velocity profile comparison between 10 PPI of h/H = 0.39 at u_{inlet} = 6.2 m/s

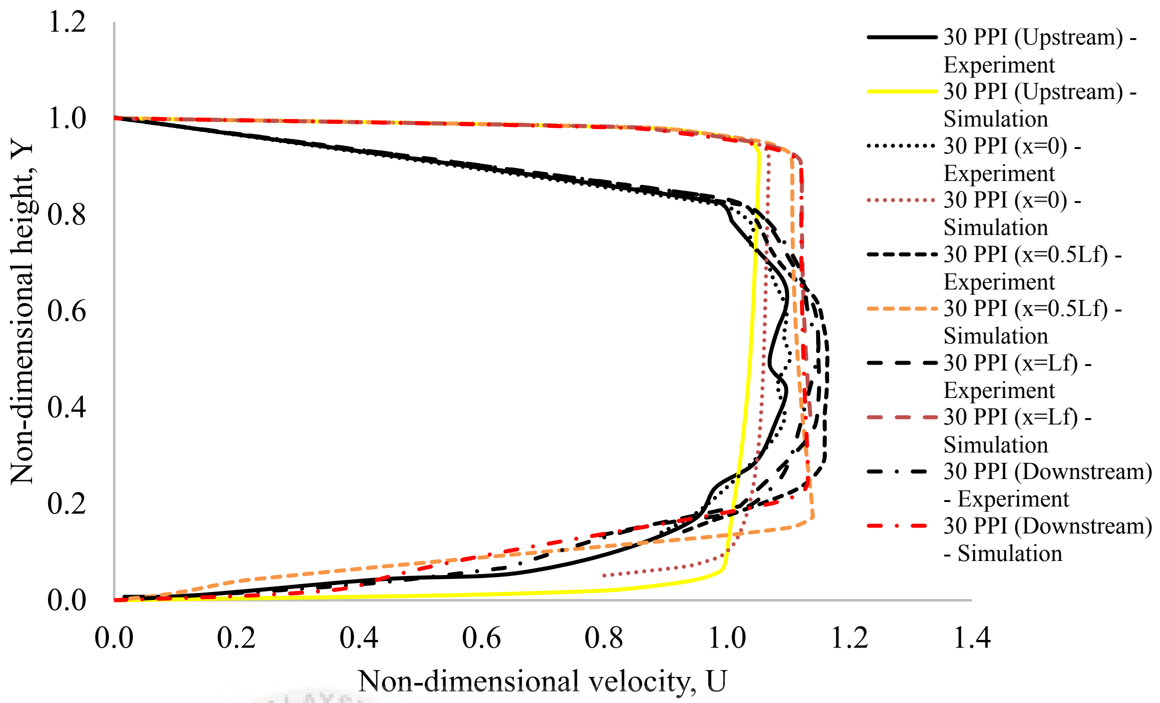

Figure 4.34: Experimental [1] and simulation velocity profile comparison between 30 PPI of h/H = 0.05 at u_{inlet} = 6.2 m/s

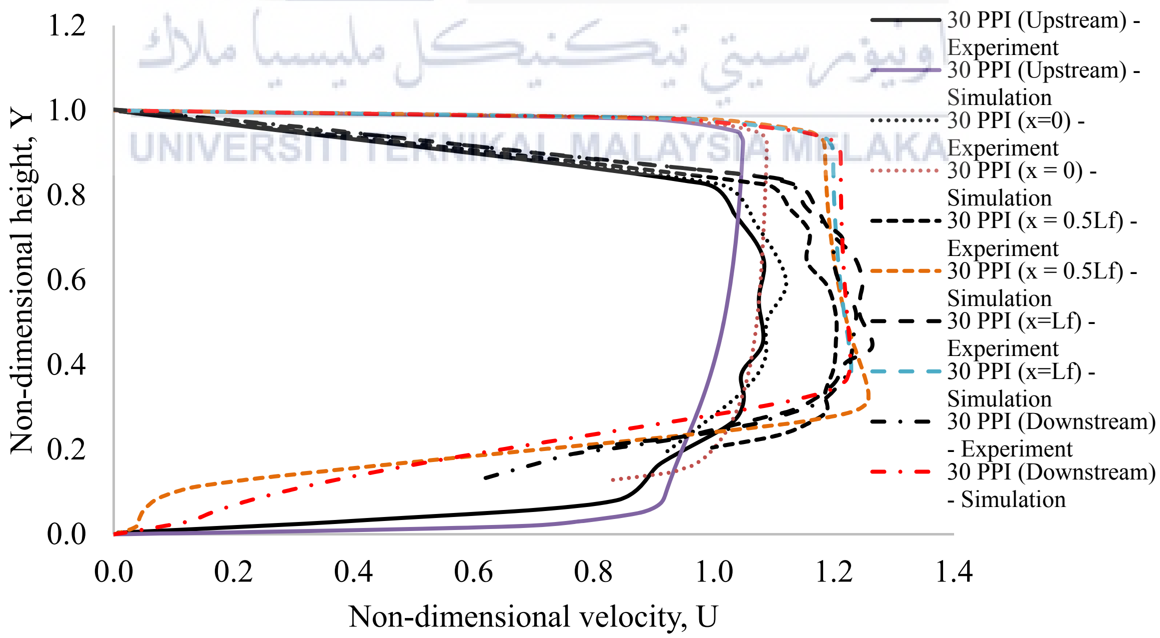

Figure 4.35: Experimental [1] and simulation velocity profile comparison between 30 PPI of h/H = 0.13 at u_{inlet} = 6.2 m/s

`

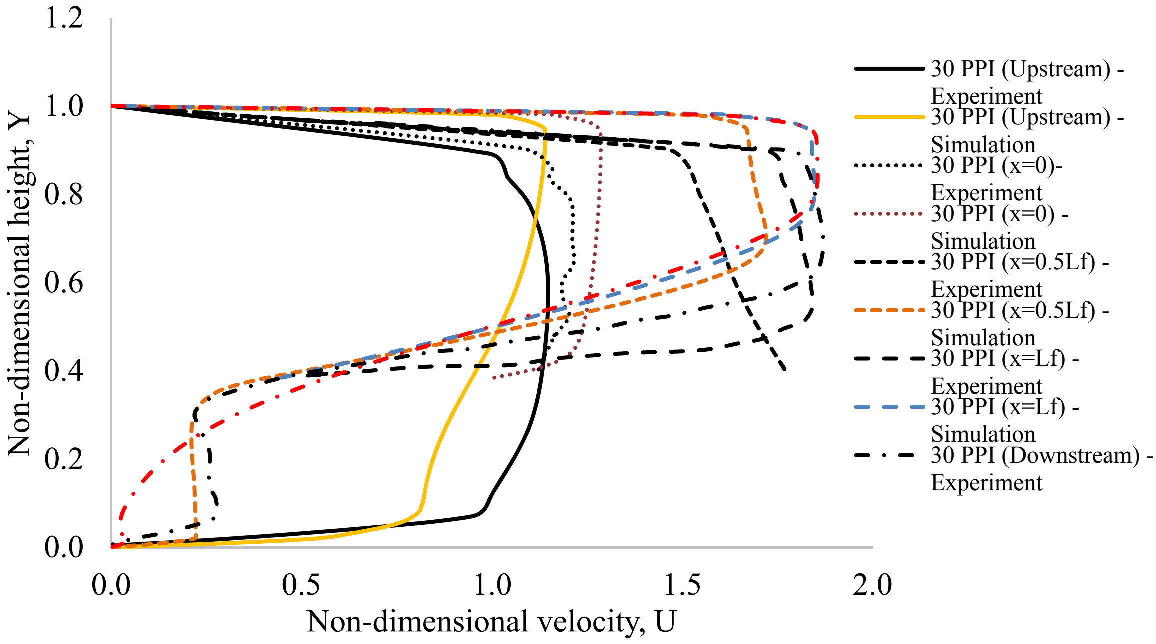

Figure 4.36: Experimental [1] and simulation velocity profile comparison between 30 PPI of h/H = 0.39 at u_{inlet} = 6.2 m/s

Figure 4.31, 4.32 and **4.33** represent the comparison of velocity profiles between simulation data of experimental data of 10 PPI foam. **Figure 4.34, 4.35** and **4.36** represent the comparison of velocity profiles between simulation data of experimental data of 30 PPI foam. Similarly, the comparisons is only for the highest velocity, u_{inlet} = 6.2 m/s for each blockage ratio, h/H = 0.06, 0.13, and 0.39 in the similar channel.

However, in the simulation data obtained, there are some missing data at the walls of the channel as shown for the simulation results. The missing data in the simulation are maybe caused by (1) meshing, (2) chosen model setup such as SST k-ε or true k-ε, and (3) solution method applied. The results from simulation data are nearer to the walls compared to the experimental data. However, the highest velocity obtained from both methods is almost the same. The results observed at five locations are in good agreement with the experimental data.

4.4 Simulation data on the pressure drop across the channel

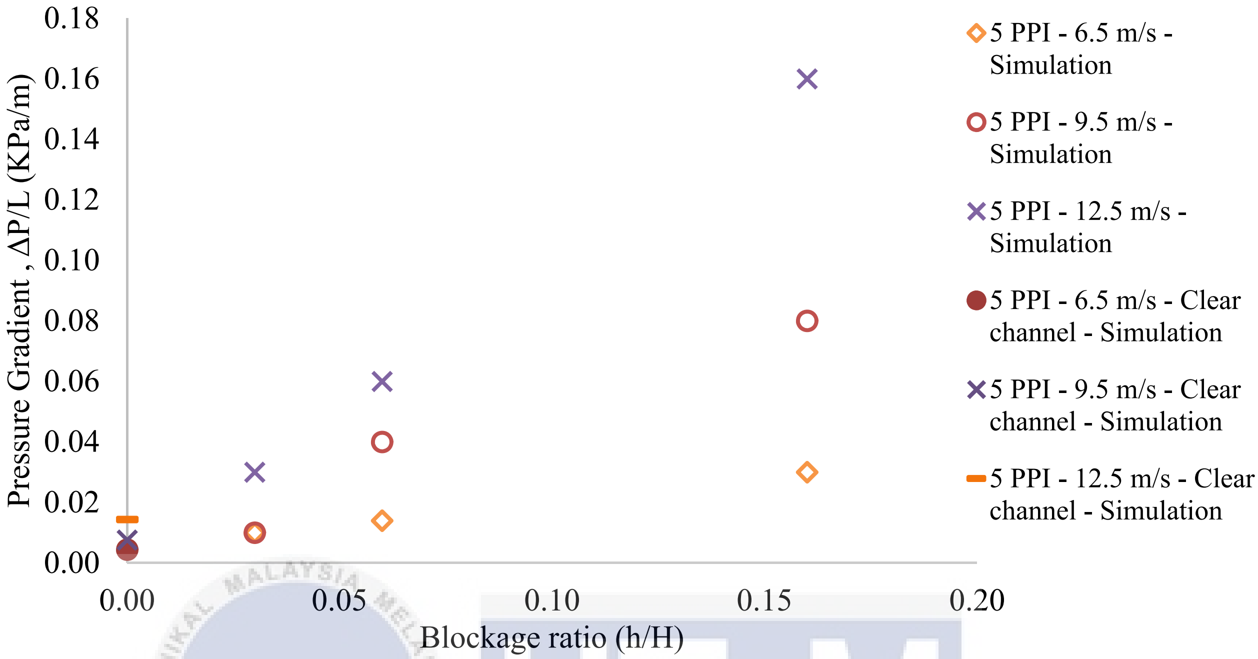

Figure 4.37: Simulation graph of pressure gradient vs blockage ratio - 5 PPI

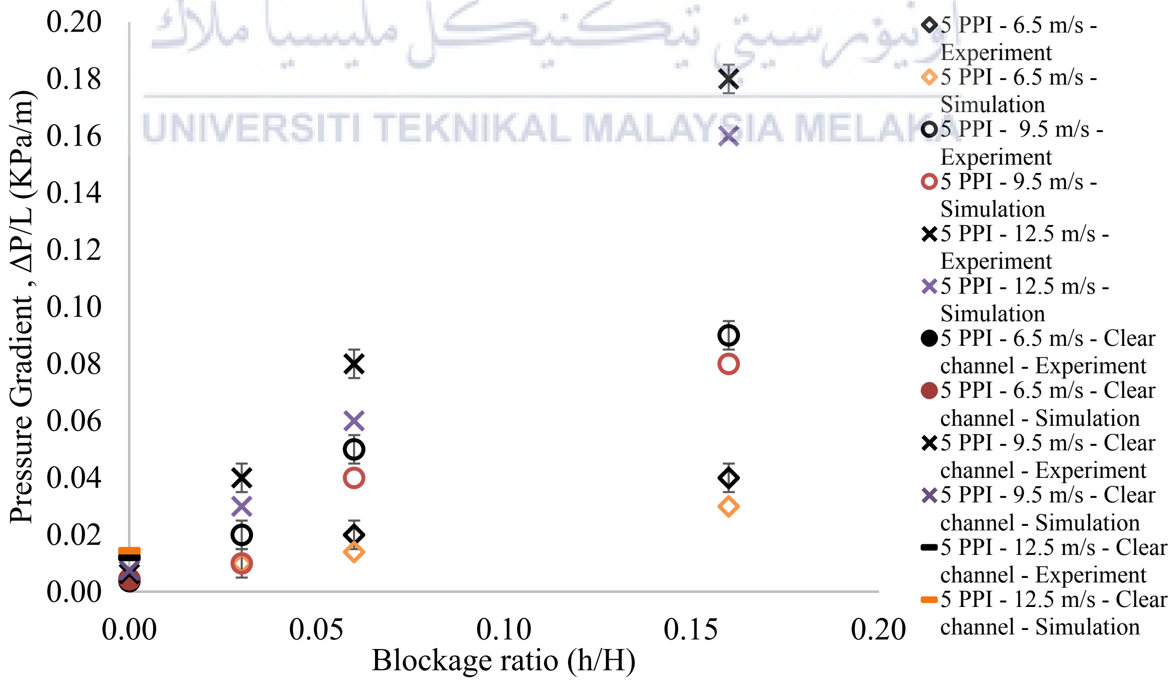

Figure 4.38: Comparison of simulation and experimental [12] graph of pressure gradient vs blockage ratio - 5 PPI

`

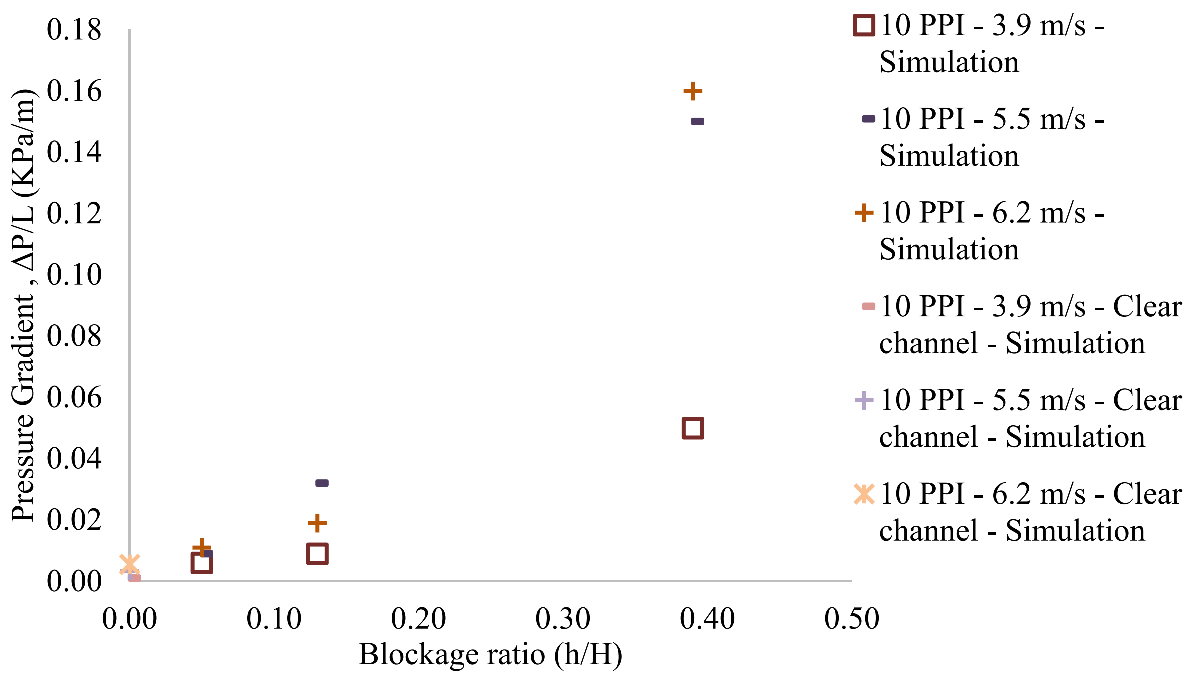

Figure 4.39: Simulation graph of pressure gradient vs blockage ratio - 10 PPI

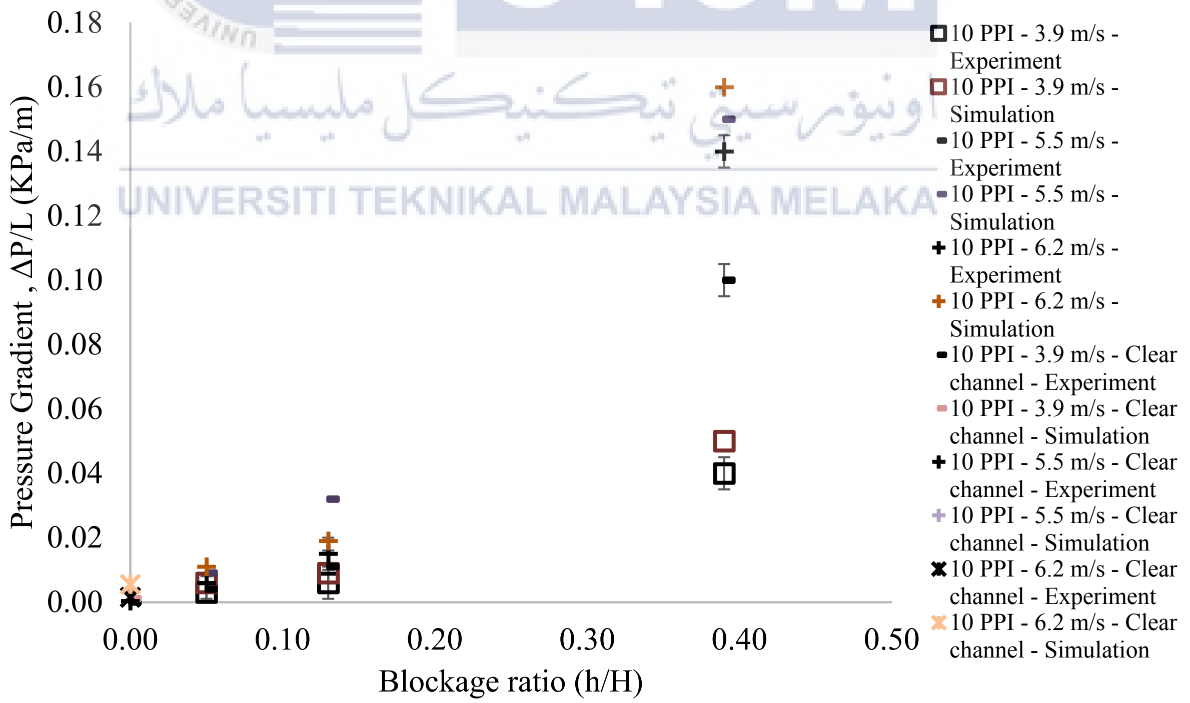

Figure 4.40: Comparison of simulation and experimental [12] graph of pressure gradient vs blockage ratio - 10 PPI

`

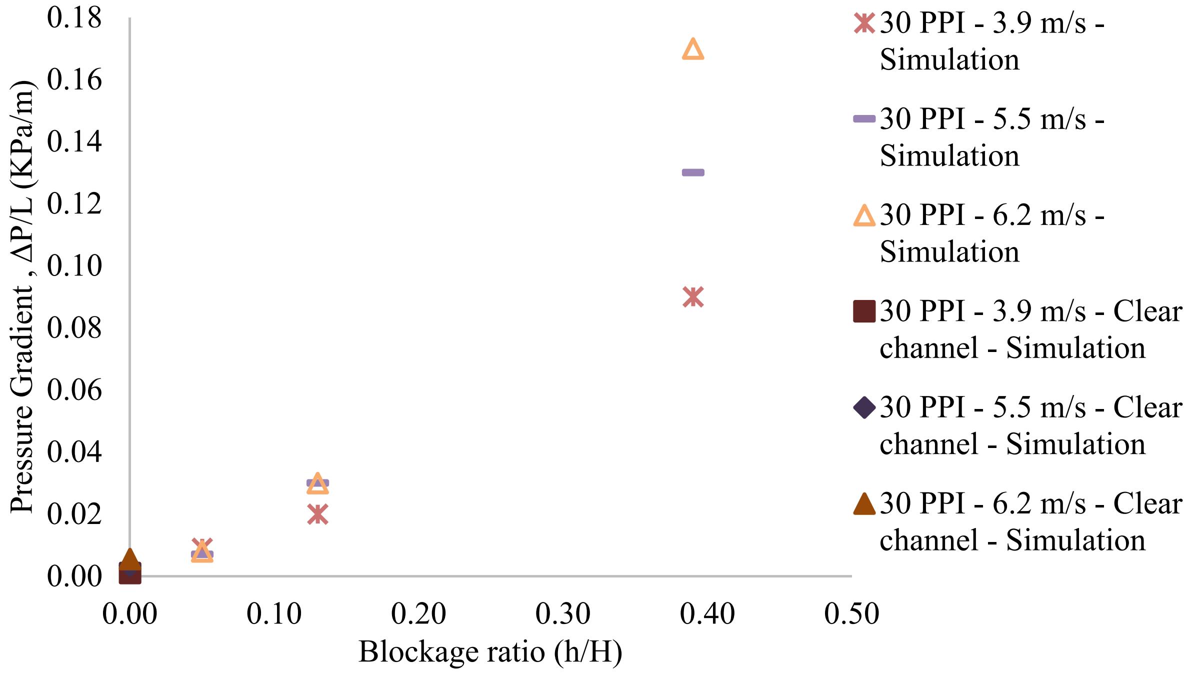

Figure 4.41: Simulation graph of pressure gradient vs blockage ratio - 30 PPI

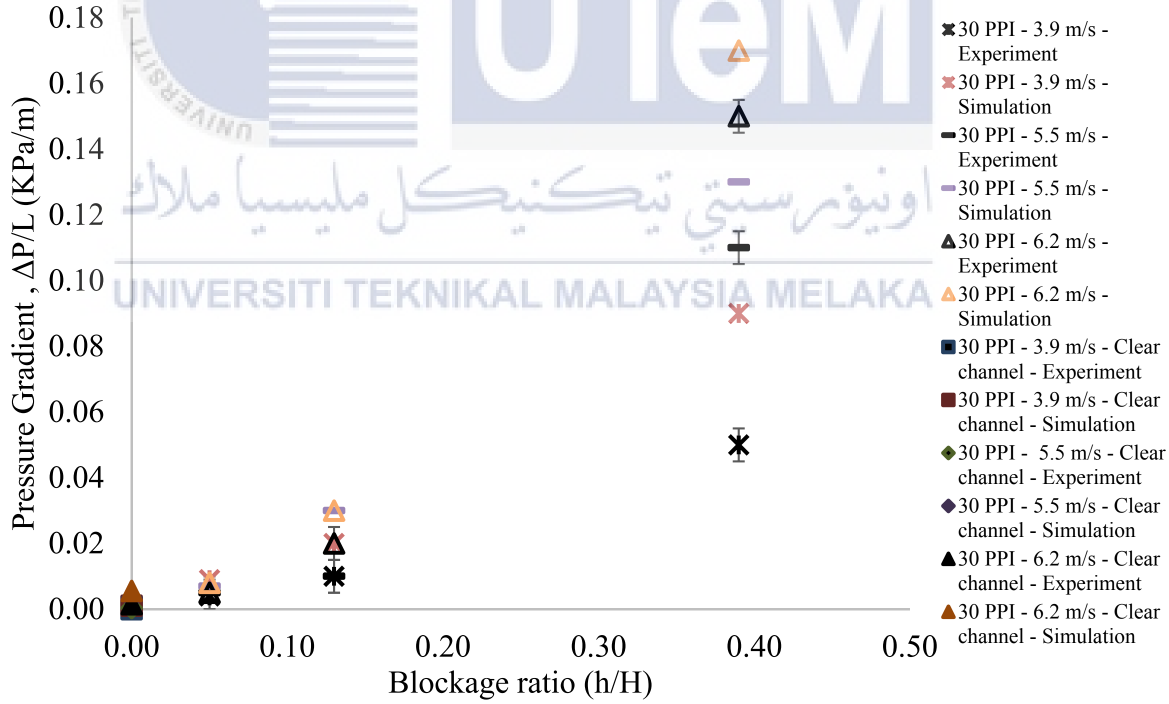

\

Figure 4.42: Comparison of simulation and experimental [12] graph of pressure gradient vs blockage ratio - 30 PPI

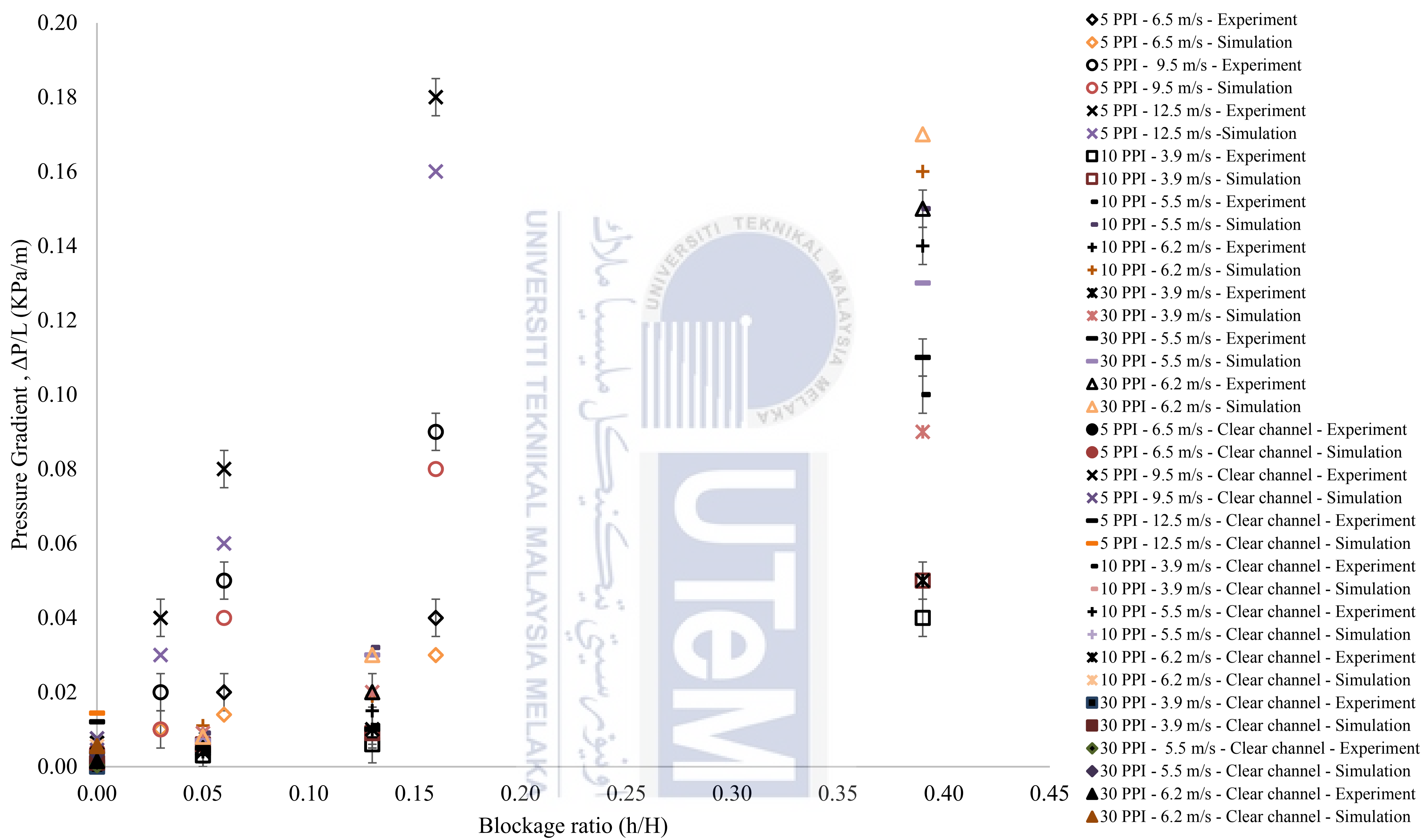

Figure 4.43: Comparison of simulation and experimental [12] graph of pressure gradient vs blockage ratio

`

Figure 4.37, 4.39 and **4.41 s**how the simulation data of pressure gradient vs blockage ratio (h/H) for 5, 10 and 30 PPI respectively. **Figure 4.37** represents 5 PPI with h/H = 0.05 to 0.16 as well for 10 and 30 PPI with h/H = 0.05 to 0.39 in **Figure 4.39** and **4.41**. In **Figure 4.38, 4.40** and **4.42**, the results were compared with the experimental data from previous literature [1] [12]. It is noticeable that pressure drop increases together with the blockage ratio. The pressure drop of 30 PPI is higher than 10 PPI of the inlet velocity, u_{inlet} = 6.2 m/s. When it comes to 5 PPI metal foam with h/H = 0.06 and velocity, u_{inlet} = 12.5 m/s, shows the highest pressure drop compared to the other configurations, due to its largest velocity,v_o.

The 10 and 30 PPI metal foams have higher pressure drops compared to a solid block. We can see that the pressure drop for 30 PPI at u_{inlet} = 6.2 m/s with h/H = 0.39 are quite high. However, the pressure drop in an identical solid block with u_{inlet} = 6.2 m/s is still lower compared to 10 and 30 PPI metal foam with the lower velocity of u_{inlet} = 5.5 m/s as shown in **Figure 4.43**. There are three main reasons of blockage effect on pressure drop; (1) flow restrictions due to sudden change in channel size, (2) complex structure of metal foam, and (3) large wakes at the downstream region.

For the high PPI foams, the wake formed is large enough to cause airflow resistance but pore density or blockage does not affect the pressure drop through the channel as can be observed in **Figure 4.43**. Validation journal [30] insisted that higher pressure drop depends on the higher PPI used also. The pressure drop normally occurs if there is any restrictions or roughness which restricts the fluid flow path throughout the channel. Moreover, the narrower the clear region, the higher the velocity and the greater the pressure drop will be. Due to the turbulent flow regime in this simulation and experimental study, the pressure drop is higher. Based on the graph of overall comparison on the pressure gradient vs blockage ratio in **Figure 4.43**, the simulation data is in good agreement with experimental data from previous experimental data.

4.5 RESULTS SUMMARY

All the results from this study are tabulated in Table 4.1 to classify the effects of h/H and pore density on the pressure drop, velocity profiles and velocity contours in brief.

Table 4.1: Summary on 5, 10 and 30 PPI

Pore density (PPI)	Inlet velocity, u_{inlet} (m/s)	Blockage ratio, h/H	Range of pore velocity, u_{pore} (m/s)	Recirculation zone at downstream	Maximum velocity, u_{max} (m/s)	Pressure drop, ΔP (a reference to solid block)
5	6.5	0.03	0 – 4.16 Decreasing at the entrance to the end of the porous block	No	8.32	Increases by 26 %
		0.06	0 – 4.52 Decreasing at the entrance to the end of the porous block	No	9.04	
		0.16	0 – 5.36 Decreasing at the entrance to the end of the porous block	The presence of foam significant here	10.73	
	9.5	0.03	0 – 5.67 Decreasing at the entrance to the end of the porous block	No	11.33	Increases by 34 %
		0.06	0 – 5.88 Decreasing at the entrance to the end of the porous block	No	11.77	
		0.16	0 – 6.60 Decreasing at the entrance to the end of the porous block	The presence of foam significant here	13.20	

	12.5	0.03	0 – 5.95 Decreasing at the entrance to the end of the porous block	No	14.88	Increases by 52 %
		0.06	0 – 7.62 Decreasing at the entrance to the end of the porous block	No	15.23	
		0.16	0 – 7.76 Decreasing at the entrance to the end of the porous block	The presence of foam significant here	15.55	
10	3.9	0.05	0 – 2.23 Decreasing at the entrance to the end of the porous block	No	4.47	Increases by 45 %
		0.13	0 – 2.37 Decreasing at the entrance to the end of the porous block	The foam is noticed as a solid block and the flow avoids it	4.74	
		0.39	0 – 2.73 Decreasing at the entrance to the end of the porous block	Foam presence is noticed	6.83	
	5.5	0.05	0 – 2.55 Decreasing at the entrance to the end of the porous block	No	6.38	Increases by 68 %
		0.13	0 – 3.40 Decreasing at the entrance to the end of the porous block	The presence of foam significant here	6.81	
		0.39	0 – 3.88 Decreasing at the entrance to the end of the porous block	No	9.70	
	6.2	0.05	0 – 2.90 Decreasing at the entrance to the end of the porous block	No	7.25	Increases by 82 %

		0.13	0 – 3.84 Decreasing at the entrance to the end of the porous block	The presence of foam significant here	7.69	
		0.39	0 – 4.54 Decreasing at the entrance to the end of the porous block	No	11.35	
30	3.9	0.05	0 – 2.14 Decreasing at the entrance to the end of the porous block	No	4.27	Increases by 48 %
		0.13	0 – 2.31 Decreasing at the entrance to the end of the porous block	The presence of foam significant here unlike 10 PPI	4.62	
		0.39	0 – 2.78 Decreasing at the entrance to the end of the porous block	The presence of foam significant here	6.95	
	5.5	0.05	0 – 2.46 Decreasing at the entrance to the end of the porous block	No	6.16	Increases by 72 %
		0.13	0 – 2.78 Decreasing at the entrance to the end of the porous block	The presence of foam significant here unlike 10 PPI	6.95	
		0.39	0 – 3.91 Decreasing at the entrance to the end of the porous block	The presence of foam significant here	9.78	
	6.2	0.05	0 – 2.85 Decreasing at the entrance to the end of the porous block	No	7.14	Increases by 85 %
		0.13	0 – 3.14 Decreasing at the entrance to the end of the porous block	The presence of foam significant here unlike 10 PPI	7.82	

		0.39	0 – 4.62 Decreasing at the entrance to the end of the porous block	The presence of foam significant here	11.51	

`

CHAPTER 5

CONCLUSION AND RECOMMENDATION

5.1 CONCLUSION

This project conducted a CFD simulation, where two-dimensional geometry of the partially filled channel with the porous medium was modelled in the ANSYS Geometry and has been analysed using ANSYS FLUENT. The fluid flow behaviour and pressure drop in the partially filled channel with different properties of the porous block were studied. The results show that higher PPI porous medium in combination with blockage ratio (h/H) has significant effects on the fluid flow behaviour and pressure drops across the channel.

For 5 PPI porous block with h/H = 0.03, the fully developed region is achieved throughout the channel. On the other hand, a fully developed region for h/H = 0.06 and 0.16 is achieved in the middle of the channel as the porous medium height was increased. It also can be concluded that the recirculation zone only exists at h/H = 0.16 only. The velocity speed in the porous medium increases accordingly to the inlet velocity, u_{inlet} speed. For example h/H = 0.16, when the u_{inlet} = 6.5 m/s, the range of velocity in the porous medium is about 0 to 5.36 m/s and when the u_{inlet} = 12.5 m/s, the velocity in the porous medium is 0 to 7.76 m/s. The pressure drop, ΔP across the channel also increases together with the inlet velocity, u_{inlet}, and the h/H configurations.

`

For 10 PPI with h/H = 0.05, a fully developed region was formed at the quarter of the channel similar to the 30 PPI channel with the same configurations. Regardless h/H = 0.13 and 0.39 for both 10 and 30 PPI, the highest velocity was achieved in the middle of the channel in the free-stream region. Both 10 and 30 PPI with h/H = 0.16 have recirculation zone at the exit of porous block. One will say that both of the porous blocks with h/H = 0.39 will have recirculation zone at the back of the porous medium but interesting for 10 PPI porous block, there is no recirculation zone, unlike the 30 PPI porous block. Even though the inlet velocity for both porous blocks is the same, however pore velocity in the 30 PPI is slightly lower compared to 10 PPI at h/H = 0.16. The pressure drop of the porous medium increases as the blockage ratios also increase. In a nutshell, the fluid flow behaviour in the partially filled channel with the porous medium is affected by the foam's PPI and blockage ratio (h/H).

5.2 RECOMMENDATIONS

As a recommendation, future research should focus on the interface of the porous and non-porous regions. The equation to define the porous medium should be revised to get a better or accurate result in ANSYS CFD fluent. The existing are now are not capable to get a very accurate answer. The results obtained using the existing equation gives in agreement results with the experimental but to the exact results. This why the future researcher has to derive a new equation on the porous medium flow. Other than that, the CFD simulation geometry is suggested to be made in three-dimensional (3D) to validate the results between the 2D and 3D model due to the randomness of the pore-ligament of a porous media.

`

REFERENCES

[1] F. Shikh Anuar, I. Ashtiani Abdi, M. Odabaee, and K. Hooman, “Experimental study of fluid flow behaviour and pressure drop in channels partially filled with metal foams,” *Exp. Therm. Fluid Sci.*, vol. 99, no. May, pp. 117–128, 2018.

[2] E. UÇAR, “Heat and fluid flow analysis in a channel partially filled with permeable isotropic porous layer by,” *Thesis*, no. December 2012.

[3] C. G. Aguilar-Madera, F. J. Valdés-Parada, B. Goyeau, and J. A. Ochoa-Tapia, “Convective heat transfer in a channel partially filled with a porous medium,” *Int. J. Therm. Sci.*, vol. 50, no. 8, pp. 1355–1368, 2011.

[4] A. G. Krishnanunni and F. Jesuraj, “Gtindia2013-3605 Cfd Simulation of Open-Cell Aluminum Metal,” *Proc. ASME 2013 Gas Turbine India Conf.*, no. 1, pp. 1–8, 2013.

[5] Wisconsin, U. (2019). Understanding porosity and density. Retrieved February 8, 2020, from http://wgnhs.uwex.edu/maps-data/data/rock-properties/understanding-porosity-density/

[6] L. J. Gauckler, M. M. Wae, C. Conti, and M. J. Duliere, “Ceramic Foam for Molten Metal Filtration,” no. September, pp. 47–50, 1985.

[7] T. J. Lu, A. Hess, and M. F. Ashby, “Sound absorption in metallic foams,” no. July 2015, 1999.

`

[8] T. Properties, "Commercial Applications of Metal Foams : Their Properties and Production," pp. 20–24, 2016.

[9] A. M. Ardo BU, "A Novel Approach for Determining Permeability in Porous Media," *J. Pet. Environ. Biotechnol.*, vol. 06, no. 04, 2015.

[10] T. C. Jen and T. Z. Yan, "Developing fluid flow and heat transfer in a channel partially filled with porous medium," *Int. J. Heat Mass Transf.*, vol. 48, no. 19–20, pp. 3995–4009, 2005.

[11] M. Drahansky *et al.*, "High-Porosity Metal Foams: Potentials, Applications, and Formulations," *Porous Mediu.*, vol. i, no. Intech, p. 13, 2016.

[12] F. Shikh Anuar, I. Ashtiani Abdi, and K. Hooman, "Flow visualization study of partially filled channel with aluminium foam block," *Int. J. Heat Mass Transf.*, vol. 127, pp. 1197–1211, 2018.

[13] M. Hriberšek, R. Jecl, and L. Škerget, "Fluid flow in a channel partially filled with porous material," *Adv. Fluid Mech.*, vol. 32, pp. 465–472, 2002.

[14] A. Berg, "Numerical and experimental study of the fluid flow in porous medium in charging process of stratified thermal storage tank," *Master Sci. thesis*, vol. SE-100 44, no. Division of Applied Thermodynamics and Refrigeration, p. 68, 2013.

`

[15] A. Dybbs and R. V. Edwards, "A new look at porous media fluid mechanics - darcy to turbulent," 1984.

[16] Y.-S. Wu, "Flow-Governing Equations and Mathematical Models," *Multiph. Fluid Flow Porous Fract. Reserv.*, pp. 29–47, 2016.

[17] P. Quadbeck, "Open cell metal foams," *Fraunhofer Inst. Manuf. Technol. Adv. Mater. IFAM, Branch lab Dresden*, no, pp. 4–5, 2016.

[18] P. Joo, "Dynamic mechanical properties of metal foams," *Civ. Eng.*, no. January 1998, p. 37, 2005.

[19] Nair, S. (2018, August 02). Metallic foam. Retrieved February 25, 2020, from https://www.slideshare.net/SandeepNair41/metallic-foam

[20] P. Fernández-Morales, C. A. Cano-Montoya, J. A. Pérez-Mesa, and M. Á. Navacerrada, "Propiedades térmicas y de permeabilidad de espumas metálicas base aluminio para aplicaciones funcionales," *Ing. y Univ.*, vol. 21, no. 1, pp. 115–130, 2017.

[21] A. Cengel. 2014, *Fundamentals and Applications*, 5th ed.,.MC Graw Hills.

[22] S. Liu, A. Afacan, and J. Masliyah, "Steady incompressible laminar flow in porous media," *Chem. Eng. Sci.*, vol. 49, no. 21, pp. 3565–3586, 1994.

`

[23] U. M. S. Costa, J. S. Andrade, H. A. Makse, and H. E. Stanley, “Role of inertia on fluid flow through disordered porous media,” *Phys. A Stat. Mech. its Appl.*, vol. 266, no. 1–4, pp. 420–424, 1999.

[24] P. Macini, E. Mesini, and R. Viola, “Laboratory measurements of non-Darcy flow coefficients in natural and artificial unconsolidated porous media,” *J. Pet. Sci. Eng.*, vol. 77, no. 3–4, pp. 365–374, 2011.

[25] M. D. M. Innocentini, V. R. Salvini, A. Macedo, and V. C. Pandolfelli, “Prediction of ceramic foams permeability using Ergun’s equation,” *Mater. Res.*, vol. 2, no. 4, pp. 283–289, 1999.

[26] Y. Mei-juan and Y. Bo-ming, “A Micro-Mechanism Model for Porous Media,” vol. Vol.52, no. Commun. Theor. Phys., pp. 936–940, 2008.

[27] M. Sener, A. Yataganbaba, and I. Kurtbas, “Forchheimer forced convection in a rectangular channel partially filled with aluminum foam,” *Exp. Therm. Fluid Sci.*, vol. 75, pp. 162–172, 2016.

[28] A. Diani, K. K. Bodla, L. Rossetto, and S. V. Garimella, “Numerical analysis of air flow through metal foams,” *Energy Procedia*, vol. 45, pp. 645–652, 2014.

[29] S. Mancin, C. Zilio, A. Diani, and L. Rossetto, “Air forced convection through metal foams: Experimental results and modeling,” *Int. J. Heat Mass Transf.*, vol. 62, no. 1, pp. 112–123, 2013.

[30] E. Sauret, K. Hooman, and S. C. Saha, “CFD Simulations of Flow and Heat Transfer Through the Porous Interface of a Metal Foam Heat Exchanger Power, no. July, 2014.

[31] B. Kotresha and N. Gnanasekaran, *Analysis of forced convection heat transfer through graded PPI metal foams*. Springer Singapore, 2019.

[32] S. Z. Shuja and B. S. Yilbas, “Flow over rectangular porous block in a fixed width channel: Influence of porosity and aspect ratio,” *Int. J. Comut. Fluid Dyn.*, vol. 21, no. 7–8, pp. 297–305, 2007.

[33] V. V. Calmidi and R. L. Mahajan, “Forced convection in high porosity metal foams,” *J. Heat Transfer*, vol. 122, no. 3, pp. 557–565, 2000.

`

APPENDICES

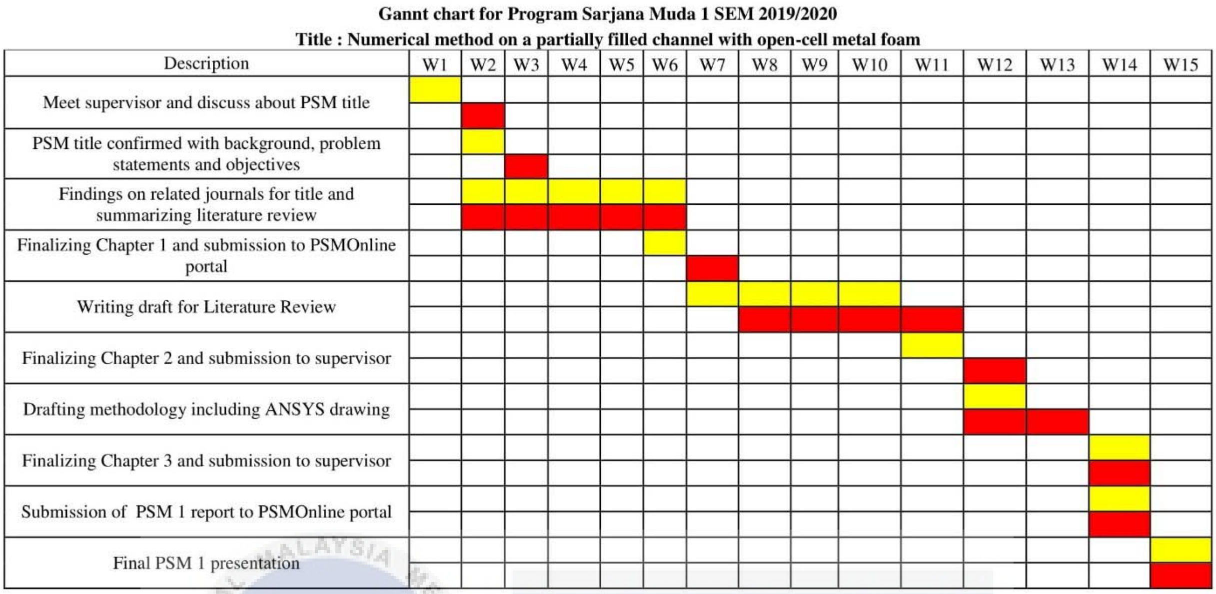

Figure 4.44: PSM I Gantt chart

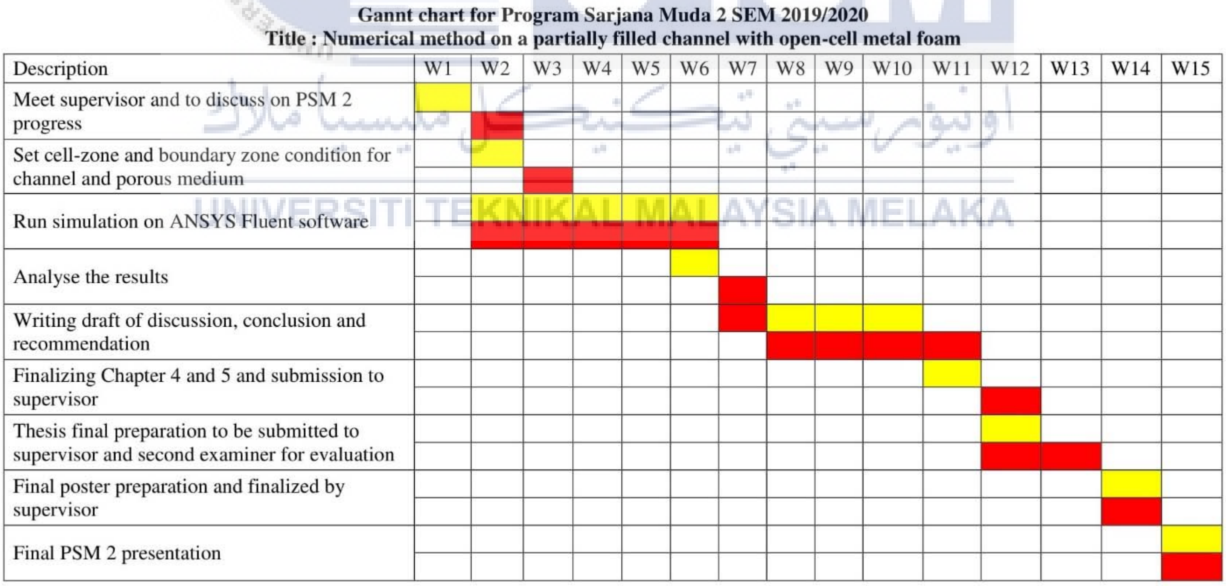

Figure 4.45: PSM II Gantt chart